

Novel Syntheses of *N*-heterocycles From Nitroarenes

BY

RUSSELL FORD

B.Sc., University of Illinois at Chicago, 2014

THESIS

Submitted as partial fulfillment of the requirements
for the degree of Doctor of Philosophy in Chemistry
in the Graduate College of the
University of Illinois at Chicago, 2021

Chicago, Illinois

Defense Committee:

Tom Driver, Chair and Advisor

Laura Anderson

J.T. Mohr

Duncan Wardrop

Ben Stokes, University of California Merced

ACKNOWLEDGEMENTS

There is a quote I've carried with me since I've begun my studies: "If you are the smartest person in the room, then you are in the wrong room". While I do not know to whom it is attributed, I am happy to report that I was never at risk of being the smartest person in SEL 3209C and I have my colleagues past and present to thank for that. The quality of the research they've conducted provided me an intellectual aspiration – a level of excellence that I was not quite able to match.

To my advisor, Tom Driver. I owe you a debt of eternal gratitude. From guidance in the lab to patience while I found my way, thank you for nurturing my scientific curiosity.

Finally, to my partner Stephanie, who I met over a burger and an NHL pre-season game in 2015. My lighthouse beacon, an unwavering source of support. A lifetime of thank-yous would not be enough to express my appreciation, but I will try my best.

Contributions of Authors

Chapter I represents an unpublished review for which I was the sole author under the supervision of my advisor Tom Driver. Chapter II demonstrates a published manuscript (*Org. Lett.* **2019**, *21*, 8827-8831) for which I was the first author with major contribution. My contribution to this project is outlined in tables **2.1**, **2.2**, **2.3** and scheme **2.5**. Chapter III represents unpublished work which will be published soon for which I foresee being a major contributor. Julian Zaleski, an undergraduate student at UIC, assisted in synthesis of some of the starting materials listed in table **3.2**. Chapter IV represents unpublished work for which I was the sole contributor. Figure **4.1** represents a figure reprinted with permission from *Acc. Chem. Res.* **2010**, *43*, 397–408. Copyright 2010 American Chemical Society: <https://pubs.acs.org/doi/10.1021/ar500099z>. Further permissions related to the material excerpted should be directed to the ACS.

TABLE OF CONTENTS

I. ACCESSING NITROSOBENZENE	1
I. INTRODUCTION	1
II. OXIDATION OF ANILINES	3
III. NITROSATION	7
IV. REDUCTION OF NITROARENES	14
V. SUMMARY AND OUTLOOK	27
CITED LITERATURE	29
II. PALLADIUM CATALYZED REDUCTIVE AMINATION OF ENOLIZABLE SP ³ -C-H BONDS	33
EXPERIMENTAL SECTION	46
CITED LITERATURE	101
III. DEVELOPMENT OF IRON-CATALYZED REDUCTIVE NITroso-ENE REACTION TOWARDS SYNTHESIS OF SIX-MEMBERED <i>N</i> -HETEROCYCLES	106
EXPERIMENTAL SECTION	118
CITED LITERATURE	133
IV. SYNTHESIS OF BENZOBISOXAZOLE CRUCIFORM SENSORS	136
EXPERIMENTAL SECTION	148
CITED LITERATURE	157
VITA	159
APPENDIX	160

LIST OF SCHEMES

- Scheme 1.1** Synthetic utility of nitrosobenzene
- Scheme 1.2** Initial synthesis and utility of nitrosobenzene
- Scheme 1.3** Erlich-Sachs synthesis of azomethines
- Scheme 1.4** Overview of nitrosoarene synthesis through an oxidative pathway
- Scheme 1.5** Synthesis of Caro's acid and oxidation of aniline
- Scheme 1.6** Catalytic oxidation of aniline to nitrosobenzene
- Scheme 1.7** Gold-catalyzed oxidation of anilines
- Scheme 1.8** Proposed photocatalytic pathways for synthesis of nitrosoarenes
- Scheme 1.9** Nitrosation via aromatic substitution
- Scheme 1.10** Direct nitrosation of *N*-isopropyl aniline
- Scheme 1.11** Nitrosation of aryl thallium reagents
- Scheme 1.12** Microwave promoted nitrosation of *para*-substituted arenes
- Scheme 1.13** Nitrosation of aryltrifluoroborates
- Scheme 1.14** Mechanism of nitrosation of aryltrifluoroborates
- Scheme 1.15** Zinc mediated reduction of dinitrobenzene
- Scheme 1.16** Zinc / chromium reduction of nitrobenzene
- Scheme 1.17** Reduction of nitrosoarenes by a Grignard reagent
- Scheme 1.18** Synthesis of di-substituted nitrosoarenes
- Scheme 1.19** Mechanism of the Bartoli indole synthesis
- Scheme 1.20** Phosphorus promoted synthesis of carbazoles
- Scheme 1.21** Palladium-catalyzed synthesis of indoles

Scheme 1.22 Mechanism of palladium-catalyzed reduction of nitroarenes

Scheme 1.23 Verification of nitrosoarene intermediate

Scheme 1.24 Iron catalyzed synthesis of di-substituted indoles

Scheme 1.25 Iron-carbonyl catalyzed reduction of nitroarenes

Scheme 1.26 Iron-catalyzed synthesis of indoles

Scheme 2.1 $\text{sp}^3\text{-C-H}$ bond amination

Scheme 2.2 Formation of C–N Bonds from Nitroarenes

Scheme 2.3 Pd(II)-Catalyzed Synthesis of Polysubstituted Indolines from Nitroarenes

Scheme 2.4 Proposed mechanism for Pd-catalyzed $\text{sp}^3\text{-C-N}$ bond formation

Scheme 2.5 Mechanistic probes

Scheme 3.1 Iron-catalyzed reductive cyclization of 2-nitrostilbenes

Scheme 3.2 Intercepting reactive intermediate with nitroso-ene reaction

Scheme 3.3 Various methods to access 6-membered *N*-heterocycles

Scheme 3.4 Sodium hydride promoted synthesis of allyl benzyl ethers from nitrophenols

Scheme 3.5 Synthesis of homoallyl nitrobenzenes from fluoronitrobenzenes

Scheme 3.6 Potential mechanism for the Fe-catalyzed reductive nitroso-ene reaction

Scheme 3.7 Mechanistic probes

Scheme 4.1 Two-step synthesis of cruciform **4.5**

Scheme 4.2 Retrosynthetic analysis of bispyrrolothiophenes

Scheme 4.3 Retrosynthetic approach to form bispyrrolothiophene benzobisoxazole cruciform

Scheme 4.4 Synthesis of pyrrolothiophene functionality

Scheme 4.5 Synthesis of bispyrrolothiophene axis

Scheme 4.6 Revised retrosynthetic scheme to synthesize benzobisoxazole cruciforms

Scheme 4.7 Construction of benzobisoxazole core

Scheme 4.8 Construction of benzobisoxazole cruciform axes

LIST OF FIGURES

Figure 3.1 Naturally occurring 1,4-benzoxazine molecules

Figure 4.1 Frontier molecular orbitals of cruciforms **4.1** and **4.2**

Figure 4.2 Molecule studied for FMO separation

Figure 4.3 Examples of cruciform molecules used as sensors

Figure 4.4 DFT calculations of bispyrrolothiophene benzobisoxazole cruciform

LIST OF TABLES

Table 1.1 Bayer's synthesis of nitrosoarenes

Table 1.2 Nitrosation of arylstannanes

Table 1.3 Direct nitrosation of substituted anisoles

Table 1.4 Nitrosation of electron-rich and electron-neutral arenes

Table 1.5 Nitrosation of electron-poor arenes

Table 1.6 Synthesis of di-substituted nitrosoarenes

Table 1.7 Synthesis of nitrosoaryl heterocycles

Table 1.8 Bartoli's synthesis of substituted indoles

Table 1.9 Synthesis of carbazoles

Table 1.10 Palladium catalyzed synthesis of *N*-heterocycles

Table 1.11 Synthesis of 3*H*-indoles by reductive cyclization

Table 1.12 Limitations of 3*H*-indole synthesis

Table 2.1 Development of optimal conditions

Table 2.2 Scope and limitations of substituted nitroarenes

Table 2.3 Investigation of nucleophile scope

Table 3.1 Development of optimal conditions

Table 3.2 Initial investigation into scope and limitations of nitroso-ene reaction

Table 4.1 Initial spectrophotometric data

LIST OF ABBREVIATIONS

Ac	acetyl
Alk	alkyl
aq	aqueous
Ar	aryl
atm	atmosphere
Bn	benzyl
Boc	<i>tert</i> -butoxycarbonyl
BPhen	bathophenanthroline
BPIn	pinacolborane borate
Bz	benzoyl
<i>n</i> -Bu	butyl
<i>t</i> -Bu	<i>tert</i> -butyl
Calcd	calculated
cat.	catalytic amount
Cbz	carboxybenzyl
COD	1,5-cyclooctadiene
Cy	cyclohexyl
#	chemical shift in parts per million downfield from tetramethylsilane (NMR)
d	doublet
dba	dibenzylidene acetone
DABCO	1,4-diazabicyclo[2.2.2]octane

LIST OF ABBREVIATIONS (continued)

DCM	dichloromethane
DCE	1,2-dichloroethane
DDQ	2,3-dichloro-5,6-dicyanobenzoquinone
DEPT	distortionless enhancement by polarization transfer
DFT	Density Functional Theory
DMA	dimethylacetamide
DMB	2,4-dimethoxybenzyl
DME	1,2-dimethoxyethane
DMF	dimethylformamide
DMSO	dimethylsulfoxide
dppf	1,1'-bis(diphenylphosphino)ferrocene
EI	electron impact ionization – in mass spectrometry
Et	ethyl
equiv.	equivalent
G	group, Gibbs free energy
g	gram
GC	gas chromatography
h, hrs	hour, hours
HR	high resolution – in mass spectrometry
Hz	Hertz
<i>J</i>	spin-spin coupling constant – in NMR

LIST OF ABBREVIATIONS (continued)

L	ligand
LDA	lithium diisopropyl amide
LHMDS	lithium bis(trimethylsilyl)amide
m	multiplet – in NMR
mp	melting point
[M]	metal
MS	mass spectroscopy
MS	molecular sieves
Me	methyl
mg	milligram
min	minute
mL	milliliter
mm	millimeter
mmol	millimole
mol	mole
MHz	megahertz
m/z	mass to charge ratio
NMR	nuclear magnetic resonance
Ph	phenyl
Phen	phenanthroline
Piv	pivalyl

LIST OF ABBREVIATIONS (continued)

PMB	<i>p</i> -methoxybenzyl
ppm	parts per million
Pr	propyl
<i>i</i> -Pr	isopropyl
<i>n</i> -Pr	propyl
Py	pyridine
q	quartet – in NMR
quint	quintet – in NMR
rt	room temperature
s	singlet – in NMR
sept	septet – in NMR
t	triplet – in NMR
TEMPO	(2,2,6,6-Tetramethylpiperidin-1-yl)oxyl
tf	trifluoromethanesulfonyl
TFA	trifluoro acetate
THF	tetrahydrofuran
TIPS	triisopropylsilyl
TLC	thin layer chromatography
TMS	trimethylsilyl
tmphen	tetramethylphenanthroline

SUMMARY

The synthesis of nitrogen containing heterocycles has remained at the forefront of scientific research due to their ubiquity in natural products, pharmaceuticals, and organic materials. The research conducted in the Driver group focuses on harnessing the reactivities of *N*-aryl nitrenes and nitrosoarenes to rapidly construct a vast library of *N*-heterocycles.

The first chapter briefly outlines the century of research in the field of accessing the reactive nitrosoarene functional group. From years of precedent a number of hypotheses presented themselves that I sought to explore over the course of my graduate career.

Construction of new C–N bonds by way of nucleophilic capture of a nitrosoarene intermediate is discussed in the second chapter. The nitrosoarene is synthesized through a reductive pathway and harnessed to construct a series of indolines.

The third chapter outlines the ongoing work I have performed to develop an iron-catalyzed reductive method to rapidly construct 6-membered *N*-heterocycles that builds upon a previous work in the Driver group. This method represents a pathway to synthesize a series of benzoxazoles, benzothiazoles and tetrahydro quinolines by way of a reductive nitroso-ene reaction.

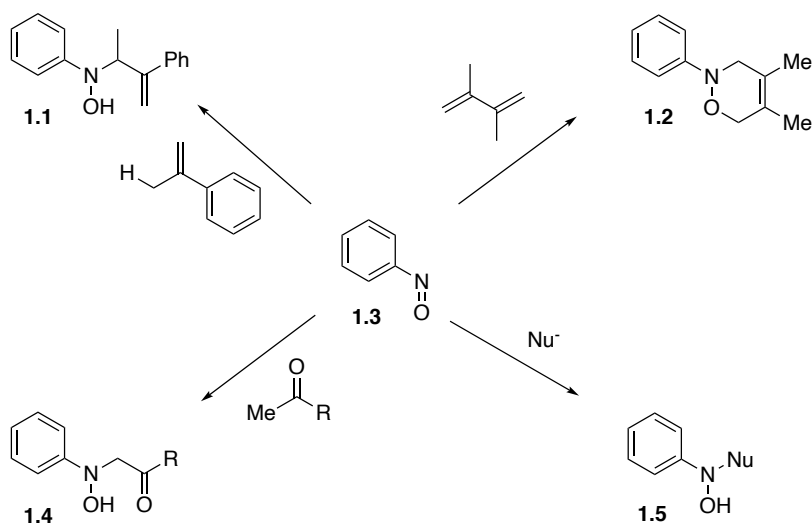
Finally, the fourth chapter outlines my efforts to synthesize a series of benzobisoxazole cruciform molecules. These molecules act as fluorophores and I explored their potential as metal ion sensors.

I. Accessing Nitrosobenzene

I. Introduction

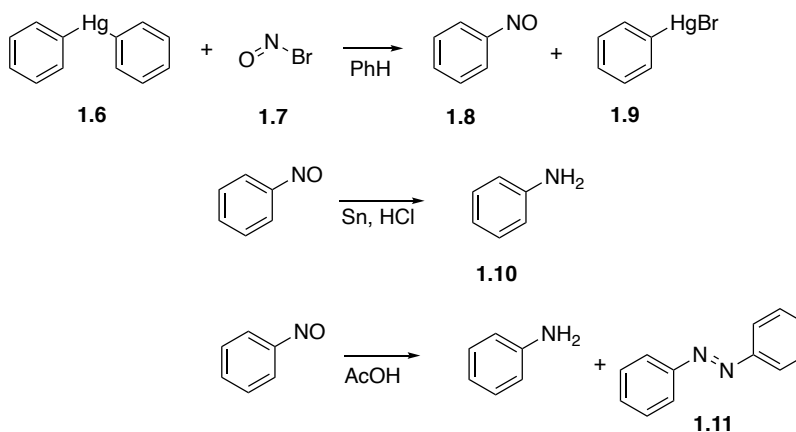
N-heterocycles and other nitrogen containing molecules are intriguing synthetic targets because they exhibit important biological and material properties. Due to these important properties, there exists a significant amount of interest in developing methodologies affording construction of C–N bonds. Generally, C–N bond formation uses nucleophilic sources of nitrogen. The nitroso functionality represents an electrophilic source of nitrogen. Herein, I have documented the advances allowing the access of nitrosoarenes by way of three major pathways: oxidation of anilines, direct nitrosation of substituted benzenes, and reduction of nitroarenes.

Nitrosoarenes are intriguing electrophilic reactive intermediates that facilitate the formation of C–N bonds (Scheme **1.1**). In the presence of an allylic substrate, nitrosoarenes can undergo an electrocyclization reaction to form *N*-hydroxylamine **1.1**.¹ In the presence of a diene, a nitrosoarene can undergo 4+2 cycloaddition and form a new C–N and C–O bond to form oxazine **1.2**.² The nitrosoarene has parallel synthetic utility to the carbonyl moiety as it allows access to C–N bonds by way of a nitroso aldol reaction to form **1.4**.³ Finally, the nitrosoarene can be functionalized by way of nucleophilic addition onto the nitrogen to form **1.5**.⁴ The reactive potential nitrosoarenes **1.3** has made them an intriguing synthetic target since their initial discovery.



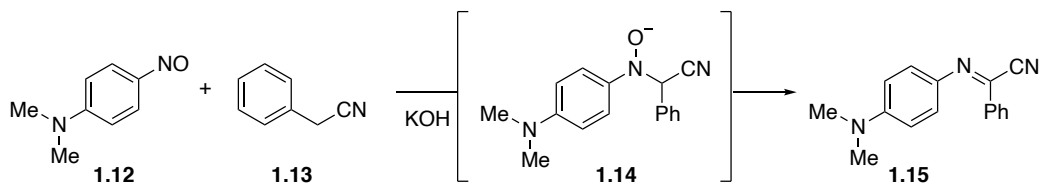
Scheme 1.1 Synthetic utility of nitrosobenzene

In 1874, Baeyer reported the first synthesis of nitrosobenzene through the addition of a solution of nitrosyl bromide **1.7** to a solution of diphenylmercury **1.6**, resulting in a transmetalation reaction to occur, forming nitrosobenzene **1.8** and phenylmercury bromide **1.9** (Scheme **1.2**). The transmetalation This reaction formed a “beautiful green liquid with a colorful odor”.⁵ Further experimentation with this newly formed liquid revealed its potential as a precursor for other nitrogen containing compounds. Addition of tin and hydrochloric acid to nitrosobenzene resulted in the complete reduction into aniline **1.10**. It was also observed that when nitrosobenzene was heated in acetic acid, not only was the nitrosoarene reduced to aniline, but a significant portion of dimerization occurred to form azobenzene **1.11**.



Scheme 1.2 Initial synthesis and utility of nitrosobenzene

At the end of the 19th century, Ehrlich and Sachs outlined a method revealing the potential synthetic utility of nitrosobenzene (Scheme 1.3).⁶ This seminal paper revealed that *p*-nitrosodimethylaniline **1.12** undergoes a condensation reaction with an activated benzyl cyanide **1.13** in the presence of potassium hydroxide to form the azomethine derivative **1.15**. They posited that the reaction proceeded through an *N*-hydroxy anion intermediate. The works by both Baeyer and Erlich and Sachs provided the scientific world brief glimpse into the potential synthetic utility of the nitrosoarene moiety. In the century that followed, scientists have developed a variety of methods to access nitrosoarenes.

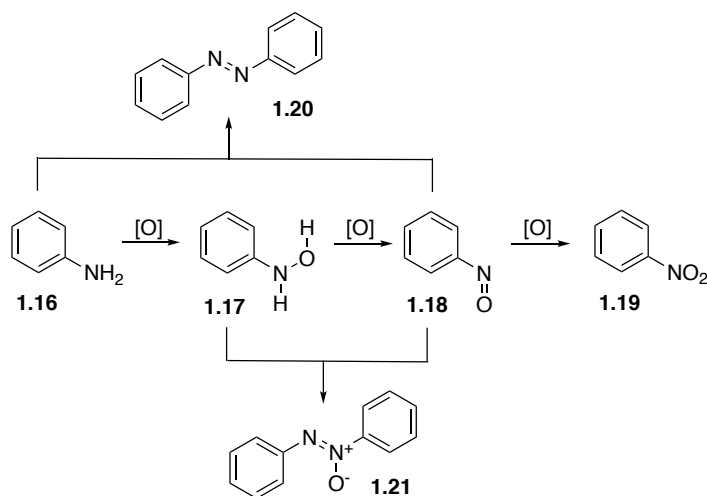


Scheme 1.3 Erlich-Sachs synthesis of azomethines

II. Oxidation of Anilines

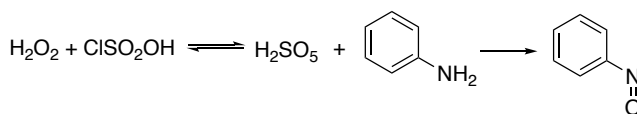
Preparation of nitrosoarenes from anilines is a practical approach, as there have been not only a number of advances in this field but also of the ubiquity and bench-top stability of the aniline precursors. A major difficulty in synthesizing aryl nitroso compounds is that their high

reactivity can lead to undesired side products (Scheme 1.4).⁷ These side reactions include over-oxidation to form nitroarene **1.19**, and the condensation reactions forming azobenzene **1.20** from aniline **1.16** and nitrosoarene **1.18** or azoxybenzene **1.21** from *N*-hydroxaniline **1.17** and nitrosoarene **1.18**.



Scheme 1.4 Overview of nitrosoarene synthesis through an oxidative pathway

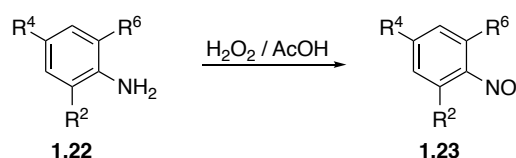
One of the initial reagents used to access nitrosoarenes from anilines was peroxomonosulfuric acid, colloquially referred to as Caro's acid (Scheme 1.5).⁸ While the highly explosive nature of Caro's acid imposes severe limitations on its usage and storage, it did find some synthetic utility towards the synthesis of nitrosoarenes.⁹⁻¹¹



Scheme 1.5 Synthesis of Caro's acid and oxidation of aniline

In the mid-twentieth century, a number of methods emerged to oxidize anilines to nitrosoarenes through the usage of more stable peroxides. In 1960, Bayer and Holmes discovered that a range of aromatic amines **1.22** could be transformed to nitrosoarenes **1.23** through treatment with a mild mixture of hydrogen peroxide in acetic acid (Table 1.1).¹² This method

emerged as one of the first to move away from using Caro's acid and was described as milder than other peroxy-acids which allowed the oxidation to be halted following the formation of the nitrosoarene, preventing over-oxidation to the nitroarene. This method was expanded upon to great effect in the years that followed, allowing access to a broad array of nitrosoarenes.^{13–15}

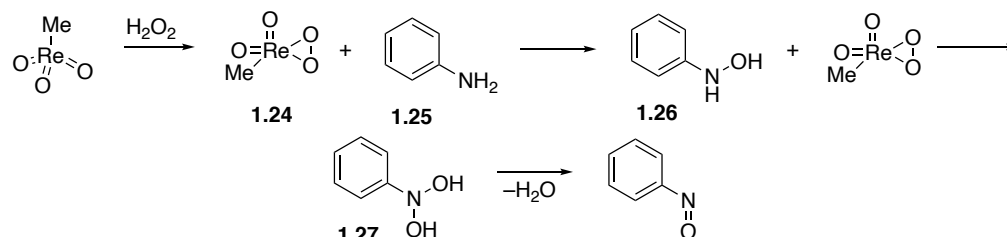


Entry	R ²	R ⁴	R ⁶	yield, %
1	Cl	H	Cl	91
2	Cl	Cl	Cl	74
3	Br	H	Br	26
4	Br	Cl	Br	73
5	Br	CO ₂ Et	Br	38
6	Cl	CO ₂ Et	Cl	39
7	Cl	CN	Cl	77

Table 1.1 Bayer's synthesis of nitrosoarenes

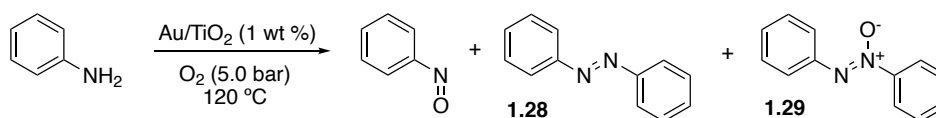
Sole usage of hydrogen peroxide to oxidize anilines is characterized by slow reaction times, indicative of high activation energies.¹⁶ To overcome this limitation, Espenson and co-worker developed a method to oxidize anilines using hydrogen peroxide and a catalytic rhenium salt (Scheme 1.6).¹⁷ Following an exhaustive kinetic mechanism they proposed that the active catalyst is the rhenium peroxide **1.24** that acts as the electrophile for nucleophilic attack by aniline **1.25** to form *N*-hydroxyaniline **1.26**. A second molecule of rhenium peroxide is required to again oxidize the *N*-hydroxyaniline to *N,N*-dihydroxyaniline **1.27**. Finally, dehydration of **1.27** forms the desired nitrosoaren. Catalytic oxidation of anilines to nitrosoarenes is not limited to the usage of rhenium, methods have also been developed employing a catalytic amount of Molybdenum,^{18–20} titanium-supported gold nanoparticles,²¹ selenium,²² or tungsten.²³ In all of these cases, the high activation energies of oxidation of anilines by using hydrogen peroxide is

overcome by first oxidizing the metal center that, in turn, acts as an oxidant for anilines. The usage of potentially explosive hydrogen peroxide has garnered some criticism and spurred scientific exploration into more stable and readily available oxidants.



Scheme 1.6 Catalytic oxidation of aniline to nitrosobenzene

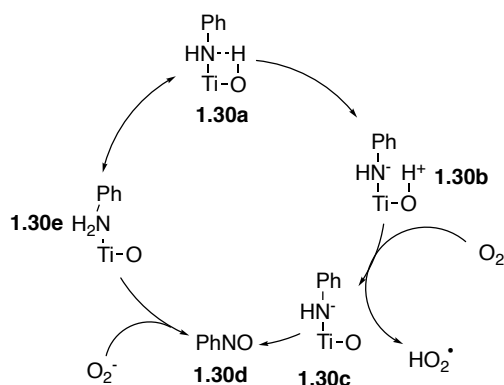
In 2008, García and co-workers discovered that molecular oxygen in combination with a gold / titanium catalyst could oxidize anilines into nitrosoarenes with a significant amount of conversion to azobenzenes **1.28** and **1.29** (Scheme **1.7**).²⁴ While this method did allow for the oxidation of anilines without the usage of hydrogen peroxide, the high temperatures required prevented nitrosobenzene from being isolated in any appreciable yields.



Scheme 1.7 Gold-catalyzed oxidation of anilines

Several reports have emerged recently that have focused upon synthesis of nitrosoarenes by way of a photocatalytic promoted oxidation of anilines over a platinum oxide supported supported on titanium dioxide.²⁵ Exploring this oxidative potential, Wu and co-workers developed a method to oxidize anilines using visible light irradiation and a magnesium oxide / titanium oxide catalyst.²⁶ They proposed two mechanistic pathways (Scheme **1.8**). Aniline is first chemically adsorbed onto the titanium catalyst to form structure **1.30a**. In the first pathway, heterolytic cleavage by the electron-rich catalyst oxygen of the aniline N–H bond forms anilino complex **1.30b**. Visible light irradiation induces a charge transfer into molecular oxygen adsorbed

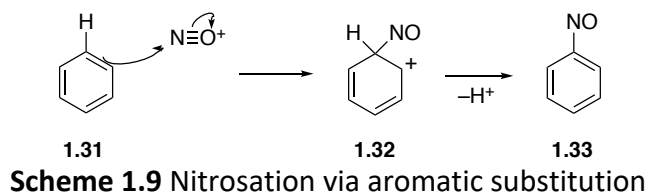
on the catalyst, forming a superoxide radical which abstracts hydrogen to form hydroperoxide and compound **1.30c**. This hydroperoxide reacts with the surface complex to oxidize the anilino compound, liberating nitrosoarene **1.30d** and completing the catalytic cycle. In the second pathway the N–H bond of aniline is not cleaved, but instead complete coordination of the aniline nitrogen onto titanium occurs, forming complex **1.30e**. Through the photoelectric effect, photo-generated electrons are excited on the catalytic surface. Molecular oxygen is reduced to form the superoxide radical that oxidizes the catalytic surface, generating nitrosoarene **1.30d** and completing the catalytic cycle.



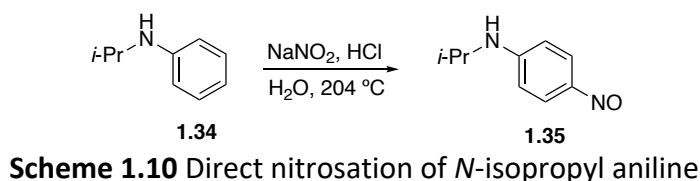
Scheme 1.8 Proposed photocatalytic pathways for synthesis of nitrosoarenes

III. Nitrosation

The initial synthesis of nitrosoarenes by Baeyer proceeded through a transmetallation type substitution reaction of diphenyl mercury and nitrosyl bromide.⁵ Direct substitution reactions also represent an intriguing synthetic pathway towards the formation of nitrosoarenes afforded in part by the relative stability of the nitrosonium ion (Scheme **1.9**).²⁷ The substitution reaction begins with nucleophilic attack of the pi-system of **1.31** to the nitrosonium ion nitrogen, forming the dearomatized nitrosated benzene **1.32**. Deprotonation of the *ipso*-hydrogen restores aromaticity, forming nitrosoarene **1.33**.



In 1955, Willenz reported successful nitrosation of *N*-isopropyl aniline **1.34** through employment of refluxing sodium nitrite and concentrated hydrochloric acid in water to yield the para-nitrosated **1.35** (Scheme **1.10**).²⁸ This method of direct nitrosation is somewhat limited in the form of undesired side products of azobenzenes if the amino functional group was not fully substituted. It could also only yield para-substituted nitrosoarenes.²⁹

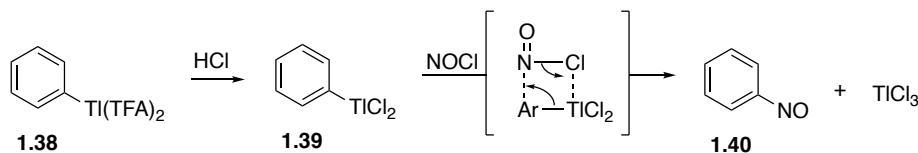


In an effort to overcome this limitation, Walton and co-workers developed a method to prepare nitrosoarenes by way of a substitution reaction between nitrosyl chloride and arylstannanes **1.36** (Table **1.2**).³⁰ This method, while it did require the extra step of synthesizing the arylstannanes from arylmagnesium halides and chlorotrimethylstannane, boasted impressive yields with electronically neutral substituents (Entries 1–4) or electron releasing groups (Entries 5–7) on the ring. In the presence of electron withdrawing groups, however, yields dropped markedly (Entries 8–11).

entry	R ¹	R ²	R ³	yield, %
1	H	H	H	79
2	Me	H	H	64
3	H	Me	H	50
4	H	H	Me	50
5	OMe	H	H	80
6	H	H	OMe	80
7	H	H	SMe	80
8	Cl	H	H	25
9	H	Cl	H	30
10	H	H	Cl	30
11	H	F	H	30

Table 1.2 Nitrosation of arylstannanes

In 1973, Taylor and co-workers developed a method to synthesize nitrosoarenes from aryl thallium reagents (Scheme 1.11).³¹ The reactive aryl thallium chloride **1.39** is prepared by treating aryl thallium trifluoroacetate **1.38** with hydrochloric acid. Nitrosyl chloride is generated *in situ* and first complexes with the aryl thallium chloride to form a four-membered intermediate. Electrophilic substitution forms the nitrosoarene **1.40** and thallium (III) chloride salt. This method proved to be rather limiting in that the nitrosoarene is accessed in three synthetic steps and the number of nitrosoarenes that could be synthesized was small.



Scheme 1.11 Nitrosation of aryl thallium reagents

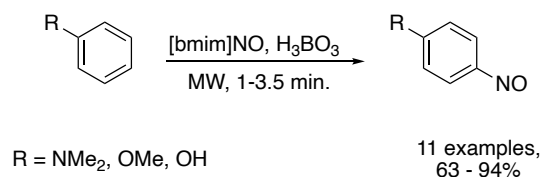
The persistent problem of direct nitrosation methods is overcoming the instability of the nitrosonium ion.²⁷ The Lewis acidity of boron salts can be harnessed to overcome this instability. In 1994, Kochi and Bosch used a nitrosyl tetrafluoroborate salt to achieve the *p*-nitrosation of a

selection of substituted anisoles (Table 1.3).³² This method boasted high yields for mono-methyl-substituted anisoles (Entries 1–3) and di-methyl-substituted anisoles (Entries 5,6). 2-bromoanisole and 3-bromoanisole could also be converted to nitrosoarenes but they observed a much lower conversion rate of 50% (Entries 7,8). With a substituent at the *para*-position there was no nitrosoarene produced. While this method provided a means to use a more stable nitrosonium but was still limited by the fact that substitution could only occur at the *para*-position.

entry	R ²	R ³	R ⁴	R ⁵	R ⁶	yield %
1	H	H	H	H	H	87
2	Me	H	H	H	H	83
3	H	Me	H	H	H	82
4	H	H	Me	H	H	0
5	Me	H	H	H	Me	70
6	H	Me	H	Me	H	84
7	Br	H	H	H	H	50
8	H	Br	H	H	H	50
9	H	H	Me	H	H	0

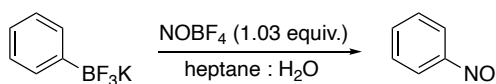
Table 1.3 Direct nitrosation of substituted anisoles

In 2011, Valizadeh and co-worker developed a microwave promoted, solvent-free aromatic nitrosation (Scheme 1.12).³³ This transformation was achieved through the treatment of *N,N*-dimethylaniline with a novel ionic liquid, 1-butyl-3-methylimidazolium nitrite and boric acid. This method boasted a very rapid conversion of arenes to nitrosoarenes but was limited by the required inclusion of an electron releasing group in the form of disubstituted anilines, alkoxyarenes, or phenols.



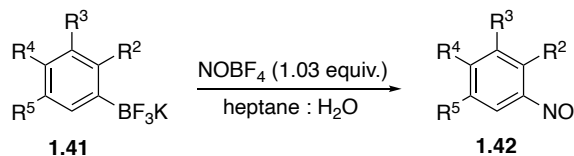
Scheme 1.12 Microwave promoted nitrosation of *para*-substituted arenes

While there have been great advances in the direct nitrosation of arenes, the inability to nitrosate arenes with electron-withdrawing groups installed on them was a problem that seemed insurmountable. Molander's work in 2012 appears to have overcome that limitation (Scheme 1.13).³⁴ Through usage of an aryltrifluoroborate potassium salt and nitrosonium tetrafluoroborates **1.41** in



Scheme 1.13 Nitrosation of aryltrifluoroborates

aqueous conditions, they were able to effectively produce nitrosoarenes **1.42** with high yields (Table 1.4). Unexpectedly, this method produced electron-rich nitrosoarenes in exceptional yields (Entries 1–5). Interestingly, this could also be used to produce nitrosoarenes with electron-neutral substituents such as phenyl, *tert*-butyl, methyl, or isopropyl with no reduction in yield (Entries 6–9).



entry	R ²	R ³	R ⁴	R ⁵	yield %
1	H	H	OMe	H	95
2	H	OMe	H	H	89
3	OMe	H	OMe	H	91
4	H	H	OBn	H	92
5	H	OCH ₂ –	OCH ₂ –	H	91
6	H	H	Ph	H	90
7	H	H	<i>t</i> -Bu	H	93
8	Me	H	H	H	92
9	H	<i>i</i> -Pr	H	<i>i</i> -Pr	88

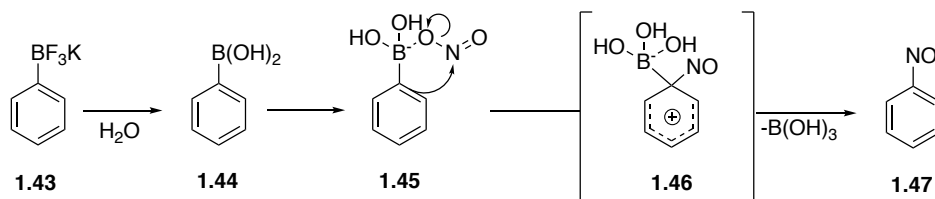
Table 1.4 Nitrosation of electron-rich and electron-neutral arenes

Remarkably, this method could also produce nitrosoarenes with electron-withdrawing substituents (Table 1.5). Aryltrifluoroborates containing ester, ketone or aldehyde groups could be rapidly converted to nitrosoarenes in very high yield (Entries 1–6, 10), in addition to nitriles, amides, nitro, carboxylic acids and trifluoromethane (Entries 7–9, 11). Weakly electron-withdrawing halogens could also be included on the aryltrifluoroborate, affording a synthetic handle for other cross-coupling reactions (Entries 12–15).

entry	R ²	R ³	R ⁴	R ⁵	yield %
1	H	H	CO ₂ Me	H	96
2	H	CO ₂ Me	H	H	95
3	H	COMe	H	H	94
4	H	COH	H	H	91
5	H	H	COH	H	94
6	COH	H	H	H	78
7	H	H	CN	H	89
8	H	MeCONH	H	H	91
9	H	NO ₂	H	CO ₂ H	90
10	H	Me	H	CO ₂ Me	81
11	H	OMe	H	CF ₃	91
12	H	H	I	H	92
13	H	H	Br	H	94
14	H	H	Cl	H	92
15	F	H	H	F	79

Table 1.5 Nitrosation of electron-poor arenes

Molander proposed the following mechanism of nitrosation of aryltrifluoroborates with sodium nitrite (Scheme 1.14). In an aqueous medium, aryl trifluoroborate **1.43** is rapidly converted to boronic acid **1.44**, a phenomenon outlined by Perrin and co-workers.³⁵ Lewis acidic interaction between boron and the nitrite oxygen leads to adduct **1.45**, which undergoes rearrangement to form a new C–N bond at the *ipso*-position, intermediate **1.46**. Aromaticity is restored with the loss of boric acid to form the nitrosoarene **1.47**.

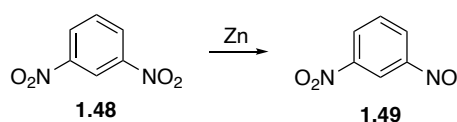


Scheme 1.14 Mechanism of nitrosation of aryltrifluoroborates

IV. Reduction of Nitroarenes

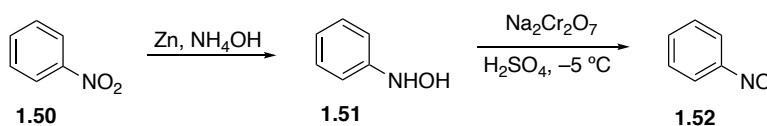
Accessing nitrosoarenes can also be accessed through a reductive pathway starting from nitroarenes.³⁶ Nitroarenes used for reductive nitrosation is a practical approach as a wide array of nitroarenes are commercially available and benchtop stable. An early report was successful in reducing nitrobenzene through the use of a barium oxide salt,³⁷ a promising report that inspired scientists to find methods to access nitrosoarenes from nitroarenes in the century that followed.

Concurrent with the research done by Ostromisslensky and Zerewitinoff, early reports by Always and Gortner revealed that *m*-nitro-nitrosobenzene **1.49** could be produced with the exposure of 1,3-dinitrobenzene **1.48** to zinc powder (Scheme **1.15**).³⁸ Expanding upon this, Stuart and co-workers revealed that nitrosobenzene **1.52** could be accessed by first reducing nitroarene **1.50** into *N*-hydroxyaniline **1.51** (Scheme **1.16**).³⁹ A second reduction step utilizing sodium



Scheme 1.15 Zinc mediated reduction of dinitrobenzene

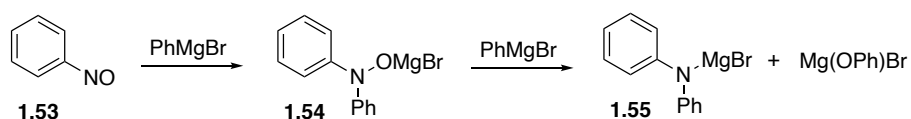
dichromate and concentrated sulfuric acid at decreased temperatures was required to synthesize the desired nitrosoarene. While they claimed that the purity of the nitrosoarene was satisfactory, this method was limited somewhat by the extra synthetic step of *N*-hydroxyaniline reduction resulting in an annunciated yield of about 50%.



Scheme 1.16 Zinc / chromium reduction of nitrobenzene

In 1915, Wieland and Roseau observed the transformation of nitrosobenzene following addition of phenylmagnesium bromide and proposed the reduction was carried out through the

following mechanism (Scheme 1.17),⁴⁰ as visualized by McCracken.⁴¹ Addition of phenylmagnesium bromide to nitrosoarene **1.50** would form the biphenyl magnesium oxide adduct **1.54**. Adding a second equivalent of phenylmagnesium bromide resulted in the deoxygenation of **1.54** into the Lewis adduct **1.55**. While this advancement was not used to synthesize nitrosoarenes, it did provide insight into the potential utility of Grignard



Scheme 1.17 Reduction of nitrosoarenes by a Grignard reagent

reagents as deoxygenation reagents of *N*-oxide amines. While the ability of Grignard reagents to reduce polynitrobenzenes in a conjugate additive fashion was explored in 1963 by Severin,⁴² it was not until Bartoli's work in 1984 was the reduction of 1-nitroarenes to nitrosoarenes explored (Table 1.6).⁴³ Addition of a series of Grignard reagents could successfully reduce

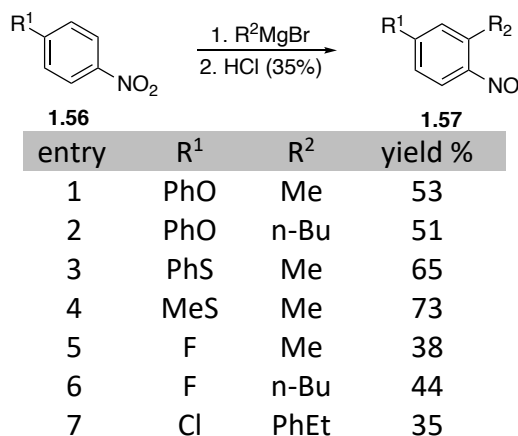
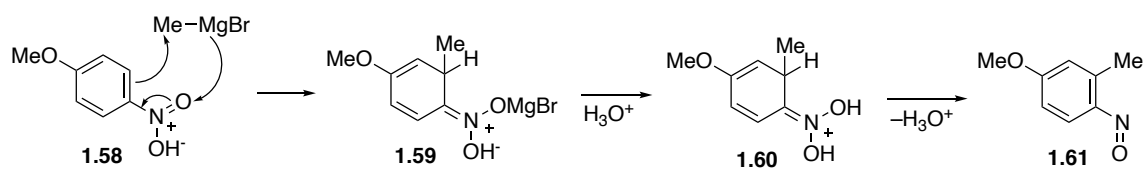


Table 1.6 Synthesis of di-substituted nitrosoarenes

p-substituted nitroarene **1.56**, followed by a wash of concentrated hydrochloric acid to yield di-substituted nitrosoarenes **1.57**. The reaction tolerated a series of alkyl Grignard reagents and produced nitrosoarenes in high yields when the *para*-substituent was an electron-releasing group (Entries 1–4). A decreased yield was observed when the *para*-substituent was a slightly electron

withdrawing halogen, however (Entries –7). Bartoli proposed the mechanism for synthesis of di-substituted nitrosoarenes from nitroarenes in Scheme 1.18. The transformation begins with the conjugate addition of methylmagnesium bromide onto nitroarene **1.58** to form the alkylated, dearomatized **1.59**. Following a wash of concentrated HCl, the magnesium bromide is removed to form *N,N*-dihydroxyaniline **1.60** followed by dehydration to form nitrosoarene **1.61**.



Scheme 1.18 Synthesis of di-substituted nitrosoarenes

Bartoli expanded upon his work towards the synthesis of alkyl-nitroso-substituted bicyclic aromatic systems (Table 1.7).⁴⁴ This method could successfully synthesize di-substituted thiazoles, naphthalenes or benzothiophenes in good yield (Entries 1.64–1.69). The decreased yields observed by both benzoxazoles and quinolines (Entries 1.70–1.73) can be contributed to a competitive addition reaction of the Grignard reagent onto the carbon–nitrogen double bond.

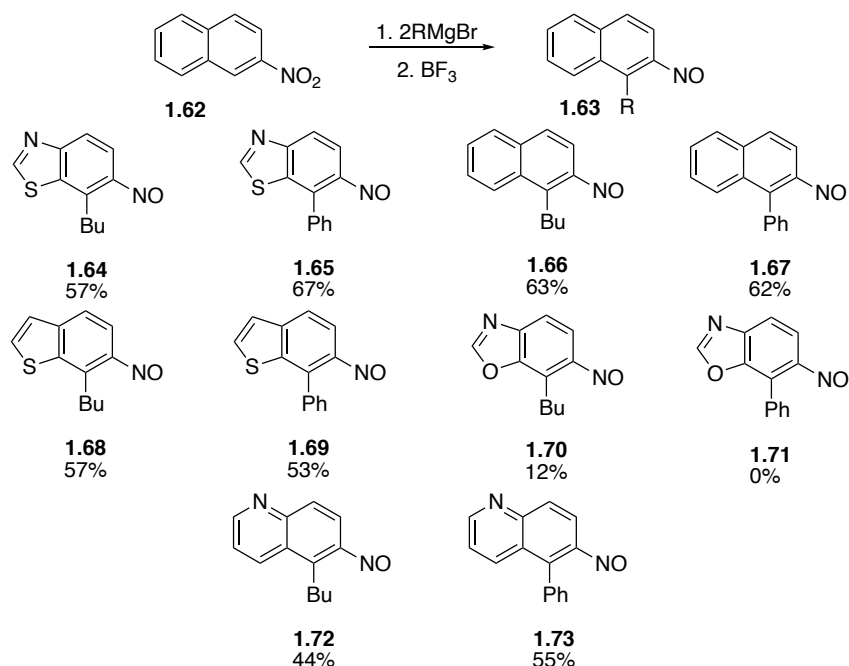


Table 1.7 Synthesis of nitrosoaryl heterocycles

This method developed by Bartoli has proven to be monumentally useful in synthetic organic chemistry, affording the rapid construction of indoles. (Table **1.8**)^{45–47} Bartoli and co-workers observed that, upon careful addition of a Grignard reagent to an *ortho*-substituted nitroarene **1.74**, formation of the substituted indole **1.75** could be observed and isolated following addition of aqueous ammonium hydroxide. The reaction proceeded smoothly when 2-substituted nitroarenes were used (Entries **1.76–1.80**). With no substituent at the 2-position, yield was significantly reduced (Entries **1.82–1.84**) but this method could also synthesize other *N*-heterocycles in poor to moderate yields (Entries **1.85–1.87**).

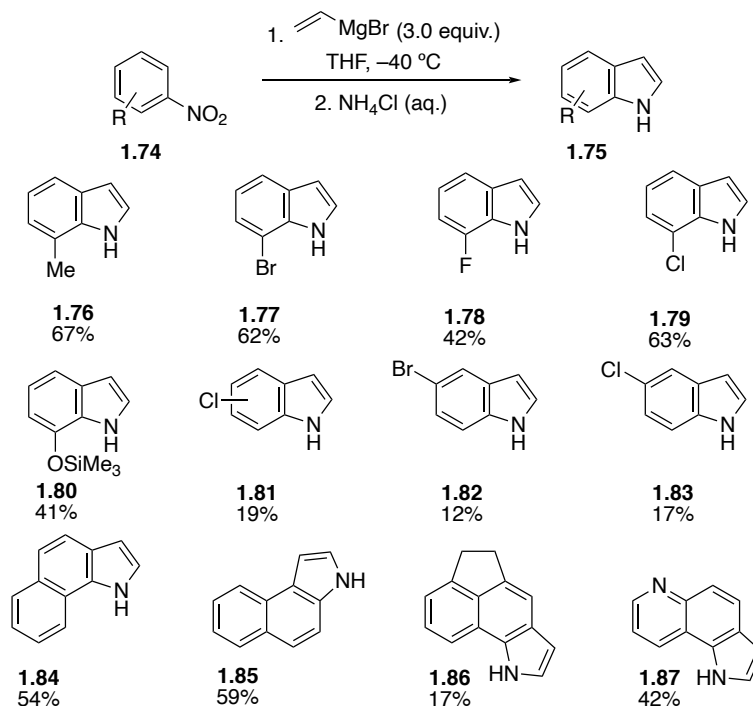
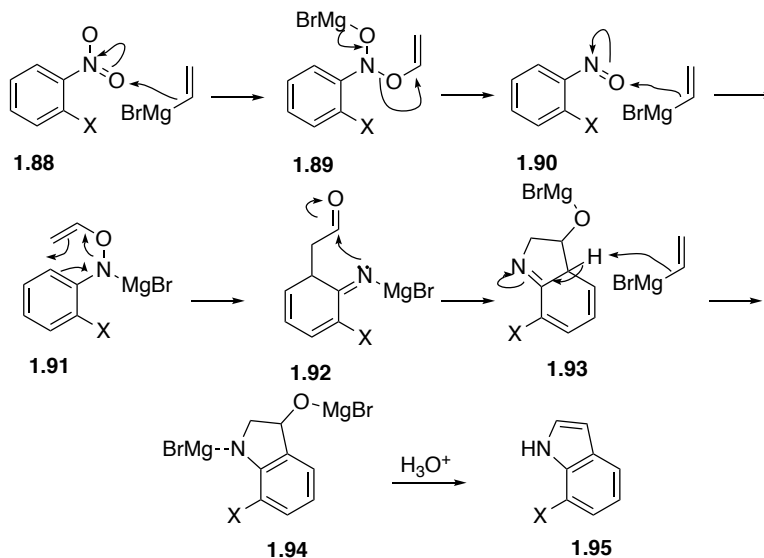


Table 1.8 Bartoli's synthesis of substituted indoles

Though the mechanism of indole synthesis is not quite clear, Bartoli and co-workers proposed the following pathway following mechanistic studies (Scheme **1.19**). First, the Grignard reagent adds to the oxygen atom of the nitro group of **1.88** to form the *O*-allylated **1.89**. Rapid decomposition results in removal of the allylated oxygen leading to formation of nitrosoarene **1.90**. The second equivalent of Grignard reagent adds to the oxygen atom of the nitrosoarene to form *O*-allylated hydroxylamine **1.91**, which undergoes a 3,3 sigmatropic rearrangement, forming the imine **1.92**. The substituent at the 2-position provides the steric hindrance required for this pericyclic step to carry out. Nucleophilic attack of on the carbonyl carbon from the nitrogen forms *N*-heterocycle **1.93**. The hydrogen at the bridgehead position is sufficiently acidic to be removed by the third equivalent of Grignard reagent, restoring aromaticity of the benzene ring and forming indoline **1.94**. Working up the indoline with ammonium chloride yields the indole **1.95**.



In 2001, Kürti and co-workers successfully synthesized a wide array of carbazoles **1.96** from 2-nitrobiphenyls **1.97** (Table **1.9**).⁴⁸ The reaction tolerated both electron-rich and electron-poor substituents (Entries **1.98–1.102**), and only when a strongly electron-withdrawing trifluoromethyl substituent was installed did the reaction yield decrease significantly (Entry **1.103**). Interestingly, the inclusion of an ester or nitrile only saw reduction of the nitro group (Entries **1.104** and **1.105**), leading to the conclusion that rate of nitro group reduction was much higher than the ester or nitrile functionalities. This method also allowed for the rapid synthesis of two biologically active molecules (Entries **1.108** and **1.109**).

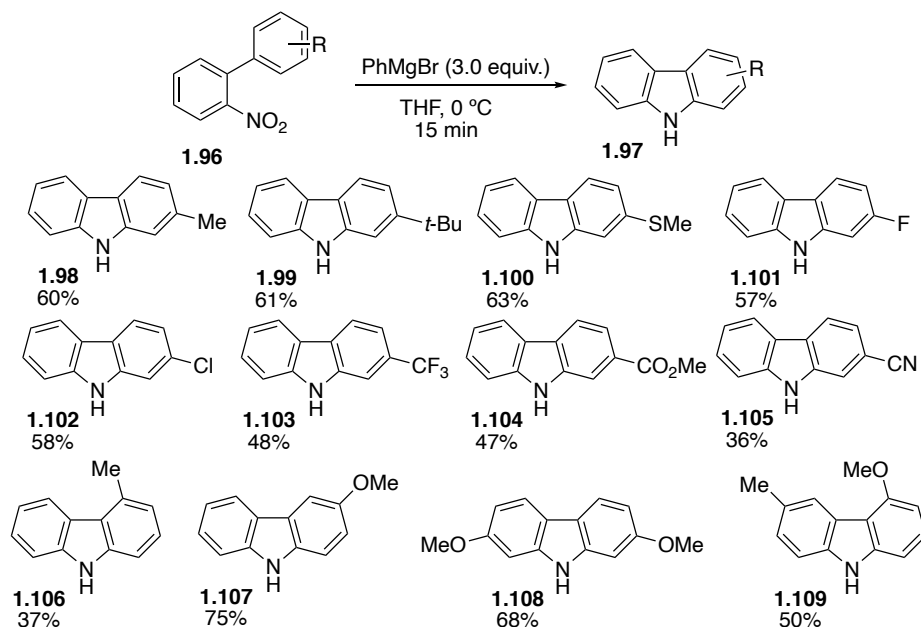
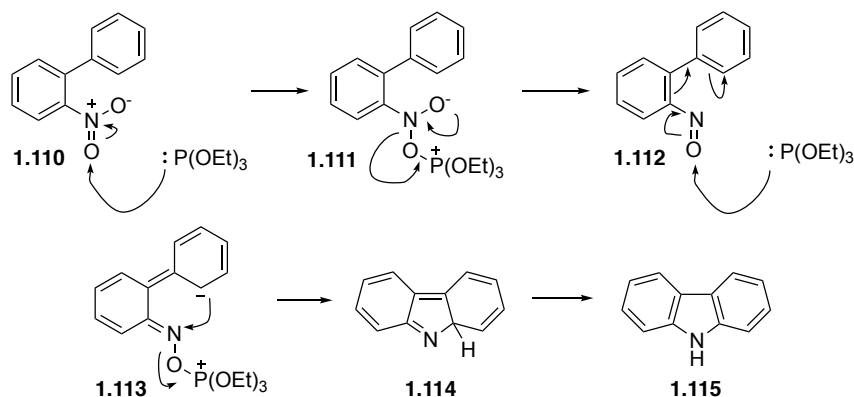


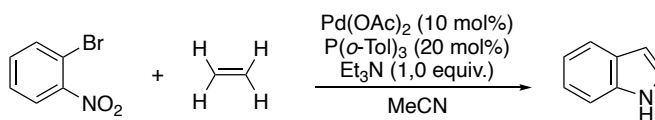
Table 1.9 Synthesis of carbazoles

In 1963, Bunyan and Cadogan revealed that a variety of *N*-heterocycles can be synthesized by a phosphorus promoted reductive cyclization of nitroarenes.⁴⁹ Cadogan and co-workers continued to study this reactivity pattern and proposed the mechanism shown in Scheme **1.20**.⁵⁰ Phosphorus (III) attacks the oxygen of the nitro-group and subsequent deoxygenation forms nitrosoarene **1.112**. A second molecule of triethylphosphite attacks the oxygen of the nitroso-group creates an electrophilic nitrogen which undergoes cyclization to form **1.114**, followed by a hydride shift to establish aromaticity and form carbazole **1.115**. Building upon this work, Sundberg and Kotchmar successfully synthesized 2,3-disubstituted indoles.⁵¹ More recently, Genung and co-workers revealed that 2*H*-indazoles could also be synthesized using the method originally discovered by Cadogan.⁵² While the synthetic utility of this method is undeniable, the nitrosoarene is not the primary reactive intermediate.



Scheme 1.20 Phosphorus promoted synthesis of carbazoles

Researchers have also developed methods to access nitrosoarenes from nitroarenes using a palladium salt catalyst and carbon monoxide as a reductant. In 1989, Kasahara and co-workers revealed the palladium catalyzed reductive cross coupling of 2-bromonitrobenzenes and alkenes to synthesize indoles (Scheme **1.21**).⁵³ During their mechanistic studies they did not mention the existence of a nitrosoarene intermediate. In the years that followed, mechanistic studies revealed the opposite to be true.



Scheme 1.21 Palladium-catalyzed synthesis of indoles

In 1994, Watanabe and co-workers developed a method to generate nitrosoarenes by using a palladium-tin catalytic system (Table **1.10**).⁵⁴ By using substituted nitrostyrenes, they discovered that the nitrosoarene reactive intermediate could be generated *in situ* and then captured in an electrocyclization reaction to form indoles, quinolines, or 2*H*-indazoles. It was observed that the identity of the styryl substituents generally unaffected the reductive cyclization to form indoles **1.116–1.120**. 2-nitrocinnamaldehyde derivatives could also be reduced to the reactive nitrosoarene to form quinolines (Entries **1.121** and **1.122**). It was not stated whether or

not 2-nitrobiphenyl was successfully reduced, or if the intermediate 2-nitrosobiphenyl was unsuccessful in undergoing electrocyclization to form carbazole **1.123**. This method could also smoothly synthesize a series of 2*H*-indazoles (Entries **1.124–1.130**). This work was expanded upon by Söderberg in 1997 and Dong in 2008, building upon the scope of palladium catalyzed reductive annulation to afford indoles.^{55,56}

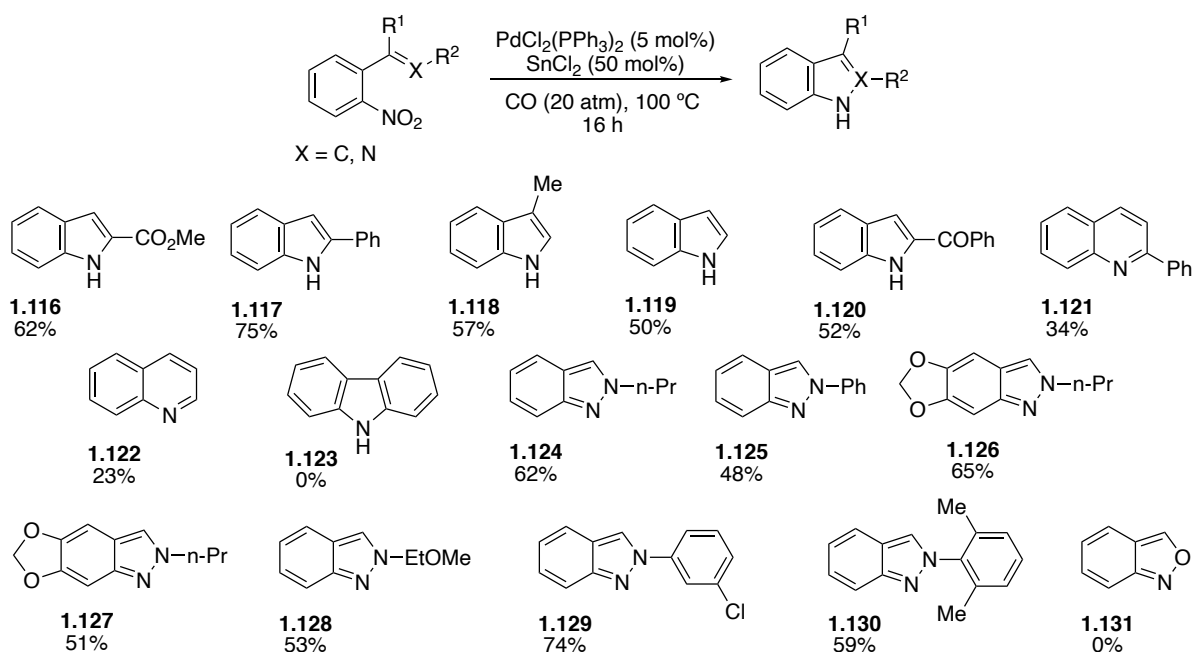
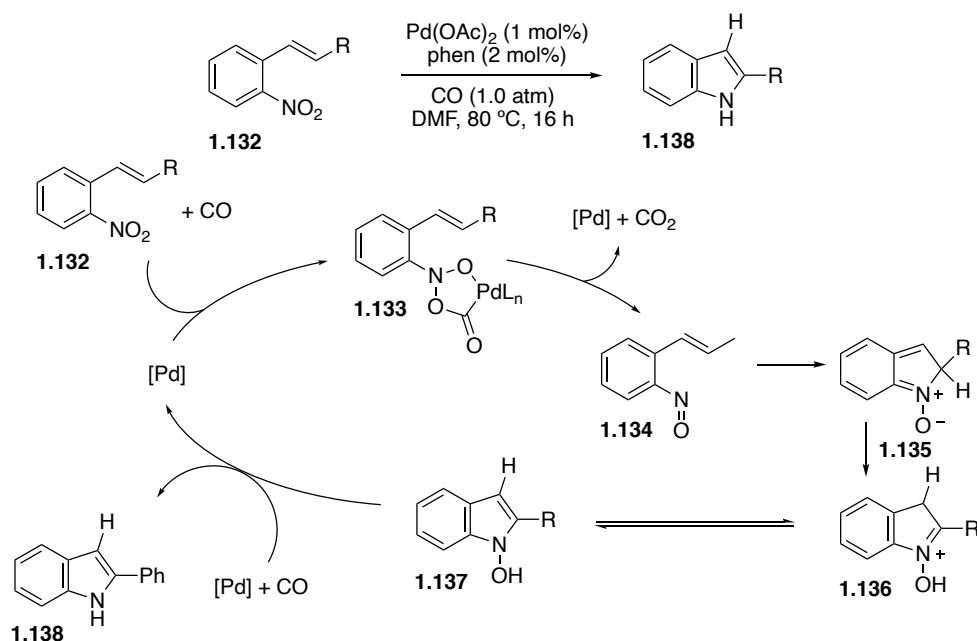


Table 1.10 Palladium catalyzed synthesis of *N*-heterocycles

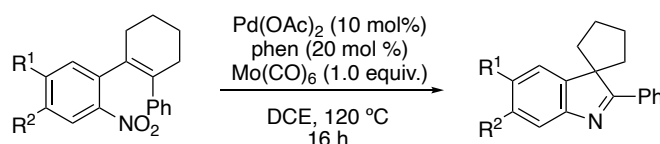
The general mechanism of palladium catalyzed reduction of nitroarenes was studied and outlined by the work by Davies and co-workers in 2005, in which they harnessed the reactivity of the nitrosoarene intermediate to form new C–N bonds (Scheme **1.22**).⁵⁷ 2-nitrostyrene **1.132** oxidatively adds to the palladium catalyst, followed by carbon monoxide insertion into the palladium oxygen bond which forms palladacycle **1.133**, an intermediate initially proposed by Osborn.⁵⁸ Decarboxylation forms nitrosoarene **1.134** which, in the presence of the olefin, undergoes a 6-electron 5-atom electrocyclization to form *N*-heterocycle **1.135**. A 1,5-hydrogen

shift and isomerization forms *N*-hydroxyindole **1.137**. A second molecule of carbon monoxide will cleave the N–O bond to yield the desired indole **1.138**.



Scheme 1.22 Mechanism of palladium-catalyzed reduction of nitroarenes

The Driver group have explored this reactivity pattern extensively in the recent years, by first developing a method allowing the transformation of 2-nitrostyrenes **1.139** into 3*H*-indoles **1.140** in 2015 (Table **1.11**).⁵⁹ Instead of using carbon monoxide gas, Mo(CO)₆ was used as the reductant as CO molecules are liberated when the molybdenum is heated.⁶⁰ They discovered that the inclusion of either electron-withdrawing or electron-releasing groups on the nitroarene had no significant effect on the formation of the desired indole (Entries 1–4, 6–9). Inclusion of a stronger electron-withdrawing trifluoromethyl group did see slight attenuation in yield (Entry 5).



entry	R ¹	R ²	yield %
1	H	H	77
2	MeO	H	60
3	Me	H	64
4	F	H	72
5	F ₃ C	H	54
6	H	MeO	68
7	H	Me	77
8	H	F	88
9	H	CO ₂ Me	75

Table 1.11 Synthesis of 3*H*-indoles by reductive cyclization

This method also allows significant electronic and steric manipulations of the pendant olefin (Table **1.12**). With an electron-rich aryl substituent, yields were increased (Entries **1.141** and **1.142**). It was revealed that phenyl groups have a higher migratory aptitude than lone methyl groups (Entries **1.143** and **1.144**). The reaction could convert substrates with fused rings that could be varied to form 6- 7- or 8- membered cycles (Entries **1.145** – **1.147**). *Ortho*-heterocycle substituents could also be tolerated (Entries **1.148** and **1.149**). The reaction also exhibited a high degree of diastereoselectivity with carefully selected substrates (Entries **1.150** and **1.151**).

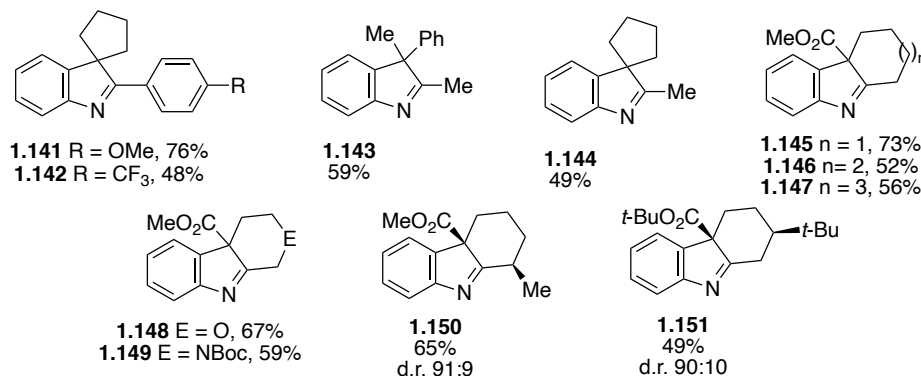
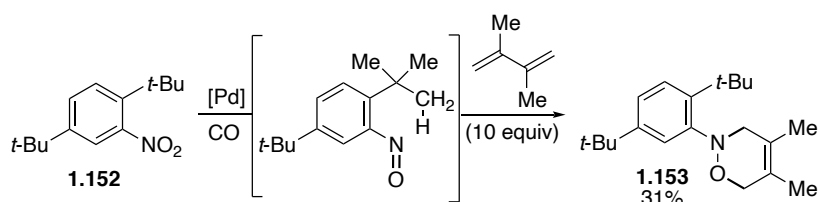


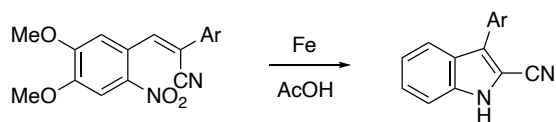
Table 1.12 Limitations of 3*H*-indole synthesis

The reaction was verified to proceed through a reactive nitrosoarene intermediate by submitting 2,5-di-*tert*-butylnitrobenzene to the reductive conditions with an excess of 2,3-dimethylbutadiene (Scheme **1.23**). The nitrosoarene was formed and then captured in a 4+2 cycloaddition to form 1,2-oxazine **1.153**. Interestingly, they did note that in the presence of Mo(CO)_6 the cyclization did not occur and instead had to use pressurized CO gas as the reductant. Following this study, the group continued to explore this reductive pathway as an effective method to synthesize *N*-heterocycles.^{61,62}



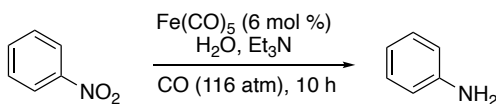
Scheme 1.23 Verification of nitrosoarene intermediate

Studies have shown that iron has the synthetic utility towards reductive transformations, including alkene hydrosilylation,⁶³ transfer hydrogenation of ketones and imines,⁶⁴ hydrosilylation of ketones,⁶⁵ and hydroamination of alkenes using nitroarenes.⁶⁶ The reduction of nitroarenes to anilines was first reported in 1925,⁶⁷ and was expanded upon in 1937 by Lutz and Lytton.⁶⁸ In 1965, Suh and Puma developed an iron-catalyzed method to synthesize 2,3-disubstituted indoles from nitroarenes (Scheme **1.24**).⁶⁹ Interestingly, during their mechanistic studies, they hypothesized that the reactive intermediate was not nitrosobenzene but *N*-hydroxyaniline that acted as a nucleophile in an aza-Wacker type cyclization.



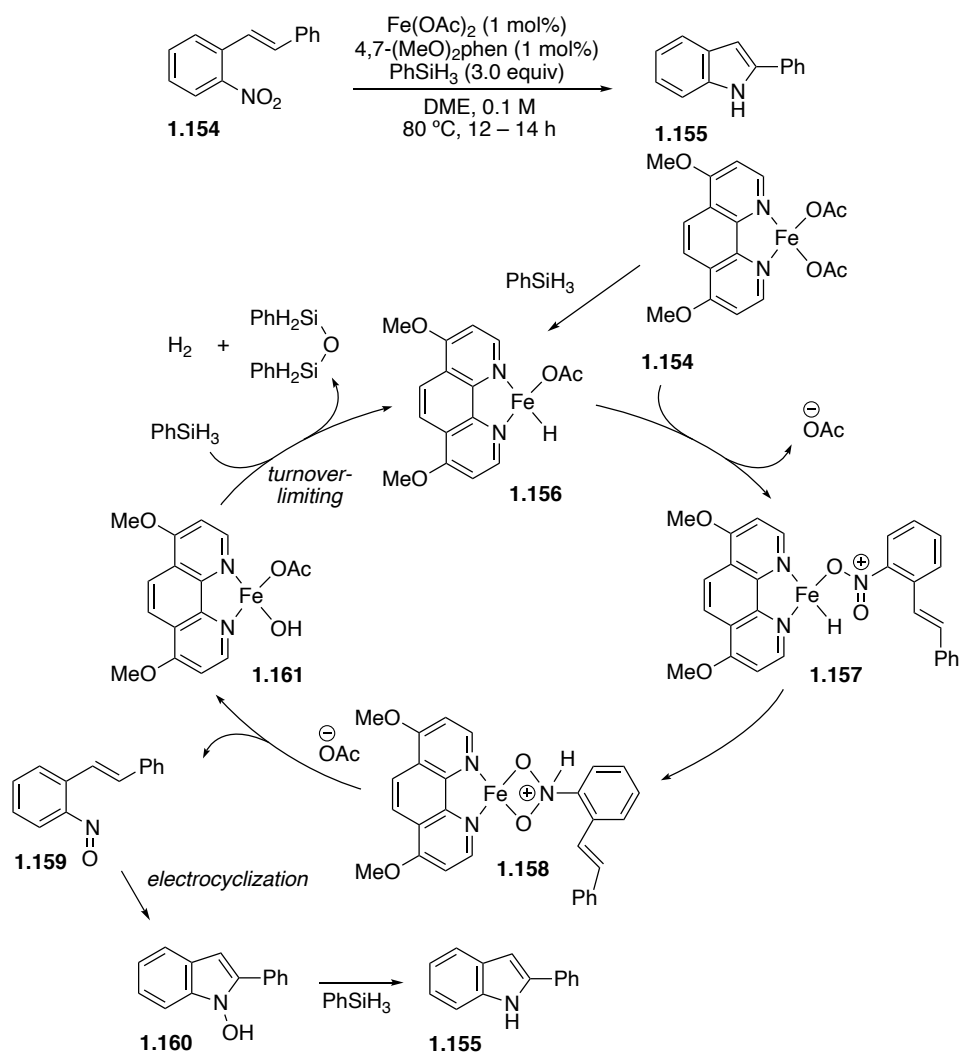
Scheme 1.24 Iron catalyzed synthesis of di-substituted indoles

Des Abbayes and Alper in 1977 studied the reduction of nitroarenes to anilines with iron-carbonyl compounds.⁷⁰ While they too hypothesized that the reaction did not go through a nitrosoarene intermediate, primary deoxygenation occurred by carbonyl insertion onto the nitro group followed by decarboxylation, similar the mechanistic step that was outlined by Davies in 2005. In 1978, Pettit and co-workers discovered that iron-carbonyl compounds readily reduce nitroarenes into anilines (Scheme 1.25).⁷¹ While it required extremely high pressures of carbon monoxide gas, the reduction was carried out quantitatively. In the years that followed, iron was used as a successful catalyst of nitroarenes to synthesize indoles,⁷² carbamates,⁷³ and biphenylenols.⁷⁴



Scheme 1.25 Iron-carbonyl catalyzed reduction of nitroarenes

Recently, the Driver group has attempted to harness this reductive propensity to attempt to synthesize nitrosoarenes *in situ* and capture them in an electrocyclization reaction to form new *N*-heterocycles (Scheme 1.26).⁷⁵ This method utilized an iron hydride species as the active reductant of nitrobenzene and phenylsilane acts as the reductant of the iron catalyst to regenerate the iron hydride. The mechanism begins with the reduction of [4,7-(MeO)₂-phen]Fe(OAc)₂ to the active iron hydride **1.156**. Nitrostyrene **1.154** coordinates with the iron hydride to produce complex **1.157**. The hydride reduces the nitro group to produce ferrocycle **1.158**, which will fragment to produce nitrosostilbene **1.159** and iron hydroxide **1.161**. Reduction of the iron hydroxide with phenylsilane regenerates the active iron hydride catalyst. Electrocyclization of nitrosostilbene forms *N*-hydroxyindole **1.160**, which in turn is reduced by phenylsilane to afford the indole.



Scheme 1.26 Iron-catalyzed synthesis of indoles

V. Summary and Outlook

Nitrosoarenes present intriguing synthetic targets due to their utility in forming new C–N bonds through ene-, nitroso-aldol, and electrocyclization type reactions. This utility has spurred research focused upon synthesizing and utilizing nitrosoarenes for over a century. However, a major difficulty in synthesizing nitrosoarenes is that their high reactivity can lead to undesired side products and are generally not benchtop stable. As such, current methods seek to access nitrosoarene reactive intermediates *in situ* towards the synthesis of increasingly complex molecules. The Driver group has focused on developing methodologies accessing nitrosoarenes

from the reduction of nitroarenes. My contribution to these studies will be outlined in chapters 2 and 3.

CITED LITERATURE

1. Baidya, M.; Yamamoto, H. *Synthesis* **2013**, *45*, 1931–1938.
2. Carosso, S.; Miller, M. *Org. Biomol. Chem.* **2014**, *12*, 7445–7468.
3. Merino, P.; Tejero, T.; Delso, I.; Matute, R. *Synthesis* **2016**, *48*, 653–676.
4. Shah, B.; Zuman, P. *Chem. Rev.* **1994**, *94*, 1621–1641.
5. Baeyer, A. *Chem. Ber.* **1899**, *32*, 1638–1640.
6. Ehrlich P.; Sachs F. *Chem. Ber.* **1899**, *32*, 2341–2346.
7. Priewisch, B., Rück-Braun, K. *J. Org. Chem.* **2005**, *70*, 2350–2352.
8. Caro, H.Z. *Angew. Chem.* **1898**, *11*, 845.
9. Schors, A.; Kraaijeveld, A.; Havinga, E. *Recl. Trav. Chim.* **1955**, *74*, 1243.
10. Holmes, R. R.; Bayer, R. P.; Errede, L. A.; Davis, H. R.; Wiesenfeld, A. W.; Bergman, P. M.; Nicholas, D. L. *J. Org. Chem.* **1965**, *30*, 3837.
11. Bamberger, E. *Ber.* **1910**, *43*, 1842.
12. Holmes, R.; Bayer, R. *J. Am. Chem. Soc.* **1960**, *82*, 3454–3456.
13. Gorrod, J. *Tetrahedron*, **1968**, *59*, 6155–6158.
14. Okazaki, R.; Hosogai, T.; Iwadare, E.; Hasimoto, M.; Inamoto, N. *Bull. Chem. Soc. Jpn.* **1969**, *42*, 3611–3612.
15. Di Nunno, L.; Florio, S.; Todesco, P. *J. Chem. Soc.* **1970**, *10*, 1433–1434.
16. Kahr, K.; Beetha, C. *Chem. Ber.* **1960**, *93*, 132.
17. Zhu, Z.; Espenson, J. *J. Org. Chem.* **1995**, *60*, 1326–1332.
18. Michaela, S.; Porta, F. *J. Chem. Soc., Chem. Commun.* **1993**, *19*, 1510–1511.
19. Prati, L.; Porta, F. *J. Mol. Catal. A* **2000**, *157*, 123–129.
20. Briadar, A.; Kotbagi, T.; Dongare, M.; Umbarkar, S. *Tet. Lett.* **2008**, *49*, 3616–3619.

21. Lykakis, I. et. al. *Adv. Synth. Catal.* **2016**, 358, 1500–1508.
22. Zhao, D.; Johansson, M.; Bäckvall, J. *Eur. J. Org. Chem.* **2007**, 4431–4436.
23. Ghosh, S.; Acharyya, S.; Sasaki, T.; Bal, R. *Green Chem.* **2015**, 17, 1867–1876.
24. Grirrane, A.; García, H. *Science* **2008**, 322, 1661–1664.
25. Shiraishi, Y.; Sakamoto, H.; Fujiwara, K.; Ichikawa, S.; Hirai, T. *ACS Catal.* **2014**, 4, 2418–2425.
26. Chen, J.; Xiong, J.; Song, Y.; Yu, Y.; Wu, L. *Appl. Surf. Sci.* **2018**, 440, 1269–1276.
27. Vančik, H. *Aromatic C-nitroso Compounds* **2013**.
28. Willenz, J. *J. Chem. Soc.* **1955**, 1677–1682.
29. D’Amico, J.; Chen, C.; Walker, L. *J. Am. Chem. Soc.* **1959**, 81, 5957–5963.
30. Bartlett, E.; Eaborn, C.; Walton, D. *J. Org. Chem. Soc. C* **1970**, 12, 1717–1718.
31. McKillop, A.; Danforth, R.; Taylor, E. *J. Org. Chem.* **1973**, 38, 208–209.
32. Bosch, E.; Kochi, J. *J. Org. Chem.* **1994**, 59, 5573–5586.
33. Gholipour, H.; Valizadeh, H. *C. R. Chimie* **2011**, 14, 963–966.
34. Cavalcanti, L.; Molander, G. *J. Org. Chem.* **2012**, 77, 4402–4413.
35. Perrin, D. et. al. *J. Org. Chem.* **2008**, 73, 4662–4670.
36. Gowenlock, B.; Richter-Addo, G. *Chem. Rev.* **2004**, 104, 3315–3340.
37. Zerewitinoff, T.; Ostromisslensky, I. *Ber.* **1911**, 44, 2402.
38. Gortner, R.; Alway, F. *Ber.* **1905**, 38, 1899.
39. Coleman, G.; McCloskey, C.; Stuart, F. *Org. Synth.* **1955**, 3, 711.
40. Wieland, Roseeu, *Ber.* **1915**, 48, 1117.
41. Gilman, H.; McCracken, R. *J. Am. Chem. Soc.* **1927**, 49, 1052–1061.
42. Schnitz, R.; Severin, T. *Chem. Ber.* **1963**, 96, 3081.

43. Bartolli, G. *Acc. Chem. Res.* **1984**, *17*, 109–115.
44. Leardini, R.; Medici, A.; Rosini, G.; Bartoli, G. *J. Chem. Soc. Perkin Trans. 1* **1978**, 692–696.
45. Bartoli, G.; Palmieri, G.; Bosco, M.; Dalpozzo, R. *Tetrahedron Lett.* **1989**, *30*, 2129–2132.
46. Bartoli, G.; Bosco, M.; Dalpozzo, R.; Palmieri, G.; Marcantoni, E. *J. Chem. Soc., Perkin Trans. 1* **1991**, 2757–2761.
47. Dobbs, A. *J. Org. Chem.* **2001**, *66*, 638–641.
48. Gao, H.; Xu, Q.-L.; Yousufuddin, M.; Ess, D. H.; Kürti, L. *Angew. Chem., Int. Ed.* **2014**, *53*, 2701–2705.
49. Bunyan, P. J.; Cadogan, J. I. G. *J.* **1963**, *42*.
50. Searle, R.; Mackie, R.; Cameron-Wood, M.; Cadogan J. I. G. *J. Chem. Soc.* **1965**, 4831–4837.
51. Kotchmar, G.; Sundberg, R. *J. Org. Chem.* **1969**, *34*, 2285–2288.
52. Aspnes, G.; Wei, L.; Genung, N. *Org. Lett.* **2014**, *16*, 3114–3117.
53. Hino, T.; Miyamoto, L.; Murakami, S.; Izumi, T.; Kasahara, A. *J. Heterocycl. Chem.* **1989**, *26*, 1405–1413.
54. Akazome, M.; Kondo, T.; Watanabe Y. *J. Org. Chem.* **1994**, *59*, 3375–3380.
55. Shriver, J.; Söderberg, B. *J. Org. Chem.* **1997**, *62*, 5838–5845.
56. Hsieh, T.; Dong, V. *Tetrahedron* **2008**, *65*, 3062–3068.
57. Davies, I. *et. al. Tetrahedron* **2005**, *61*, 6425–6437.
58. Paul, F.; Fischer, J.; Ochsenbein, P.; Osborn, J. *Organometallics* **1998**, *17*, 2199–2206.
59. Jana, N.; Zhou, F.; Driver, T. *J. Am. Chem. Soc.* **2015**, *137*, 6738–6741.
60. Phillips, J.; Dumestic, J. *Appl. Catal.* **1984**, *9*, 1–30.
61. Zhou, F.; Wang, D.-S.; Driver, T. G. *Adv. Synth. Catal.* **2015**, *357*, 3463–3468.
62. Zhou, F.; Wang, D.-S.; Driver, T. G. *Angew. Chem. Int. Ed.* **2017**, *56*, 4530–4534.

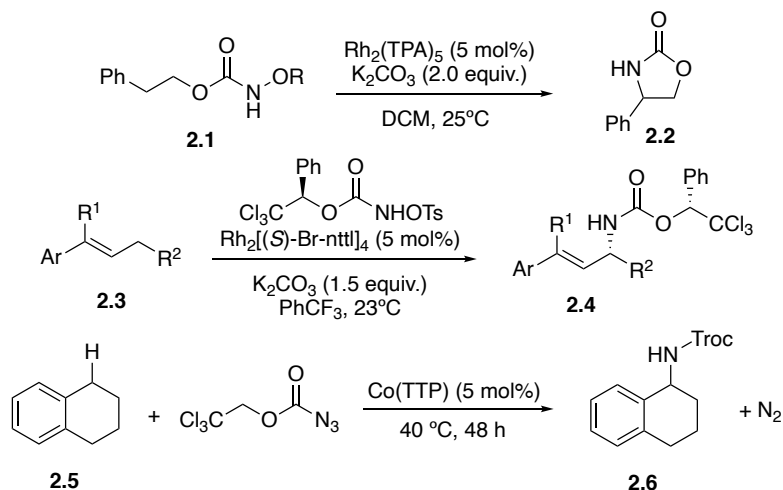
63. Tondreau, A. M.; Atienza, C. C. H.; Weller, K. J.; Nye, S. A.; Lewis, K. M.; Delis, J. G. P.; Chirik, P. J. *Science* **2012**, 335, 567–570.
64. Zuo, W.; Lough, A. J.; Li, Y. F.; Morris, R. H. *Science* **2013**, 342, 1080–1083.
65. Ruddy, A. J.; Kelly, C. M.; Crawford, S. M.; Wheaton, C. A.; Sydora, O. L.; Small, B. L.; Stradiotto, M.; Turculet, L. *Organometallics* **2013**, 32, 5581–5588.
66. Gui, J.; Pan, C.-M.; Jin, Y.; Qin, T.; Lo, J. C.; Lee, B. J.; Spergel, S. H.; Mertzman, M. E.; Pitts, W. J.; La Cruz, T. E.; Schmidt, M. A.; Darvatkar, N.; Natarajan, S. R.; Baran, P. S. *Science* **2015**, 348, 886–891.
67. J. M. Farbenindustrie, H. G. German Patent **1925**, 441, 179.
68. Lutz, R.; Lytton, M. *J. Org. Chem.* **1937**, 2, 68–75.
69. Suh, J.; Puma, B. *J. Org. Chem.* **1965**, 7, 2253–2259.
70. Des Abbayes, H.; Alper, H. *J. Am. Chem. Soc.* **1977**, 99, 98–101.
71. Cann, K.; Cole, T.; Slegeir, W.; Pettit, R. *J. Am. Chem. Soc.* **1978**, 100, 3969.
72. Baldwin, J.; Ponticello, G. *J. Org. Chem.* **1979**, 44, 4403–4405.
73. Alper, H.; Hashem, K. E. *J. Am. Chem. Soc.* **1981**, 103, 6514–6515.
74. Hahn, S.; Miles, D.; Ahn, K.; Hine, J. *J. Am. Chem. Soc.* **1985**, 107, 5092–5096.
75. Shevlin, M.; Guan, X.; Driver, T. *ACS Catal.* **2017**, 7, 5518–5522.

II. Palladium Catalyzed Reductive Amination of Enolizable $\text{sp}^3\text{-C-H}$ Bonds.

(The structure of this chapter followed a published article published by the Driver Group: Pd-Catalyzed Reductive Amination of Enolizable $\text{sp}^3\text{-C-H}$ Bonds. Ford, R.; Alt, I.; Jana, N.; Driver, T.; *Org. Lett.* **2019**, *21*, 8827-8831.)

The development of methods facilitating the amination of $\text{sp}^3\text{-C-H}$ bonds is an intriguing and significant research target as it could streamline the synthesis of important *N*-heterocycles.¹⁻

⁶ While many significant discoveries have been made in this field, $\text{sp}^3\text{-C-N}$ bond formation from $\text{sp}^3\text{-C-H}$ bonds remains limited. This bond formation often requires strong electron-withdrawing substituents on nitrogen used in conjunction with an oxidant. Additionally, activated nitrene-precursors such as oxycarbamates or azides have also seen use (Scheme **2.1**). Lectard and co-workers discovered that treating oxycarbamates **2.1** with a catalytic amount of a rhodium salt in the presence of base facilitates $\text{sp}^3\text{-C-H}$ amination to form oxazolidinones **2.2**.⁷ Lebel and co-workers developed a method accomplishing C-H amination to synthesize allylic amine **2.4** in an intermolecular fashion in 2012 using alkene **2.3**, a rhodium catalyst and chiral *N*-mesyloxycarbamate.⁹ In 2010, Zhang and co-workers discovered that a cobalt porphyrin catalyst could be used with a nitrene precursor to achieve the benzylic C-H amination of arene **2.5** under mild conditions to form Troc-protected amine **2.6**.¹⁰ In the years that followed, a large number of methods enabling $\text{sp}^3\text{-C-H}$ bond amination using azides as nitrene precursors have been developed.¹¹⁻¹⁸ Unfortunately, they all require an extra number of synthetic steps to install the azide functional group. Additionally, azides are a potentially explosive compound.



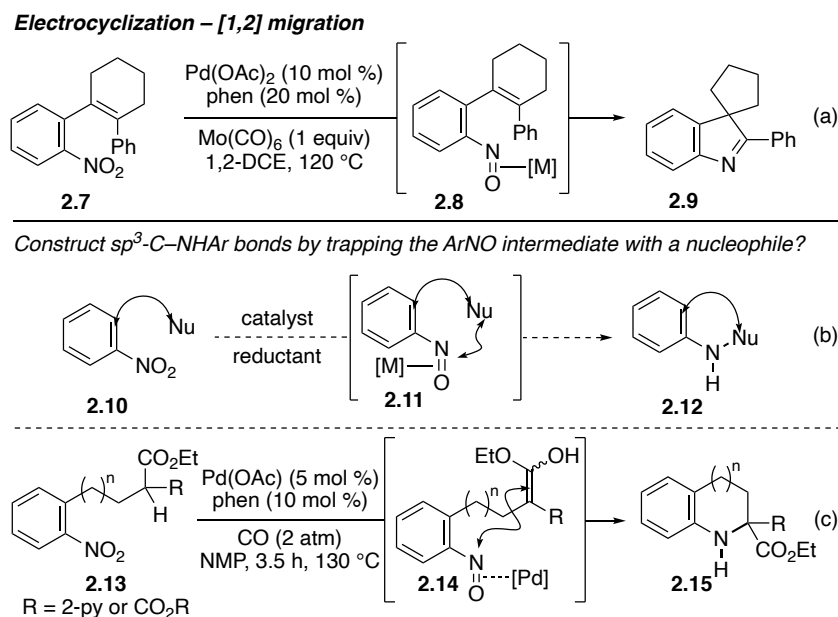
Scheme 2.1 $\text{sp}^3\text{-C-H}$ bond amination

Nitrosoarenes, while synthetically useful as an *N*-atom source for C–N bond formation, particularly through ene-^{19–21} or α -amination reactions^{22,23}, have limited availability due their instability. The nitroso group can be readily reduced to either *N*-hydroxyaniline or aniline.²⁴ There also exists an equilibrium between monomer and dimer nitrosoarene species, and maintaining the equilibrium to favor the monomer is key in accessing it's reactivity.²⁵ This limitation has challenged the exploration of methodologies to form nitrosoarenes *in-situ* from widely available precursors. While accessing nitrosoarenes can be achieved by way of the oxidation of *N*-hydroxyanilines,^{26–31} a vast amount of research has concentrated on accessing them through the reduction of nitroarenes.^{32–36} Using nitroarenes as nitrosoarene precursors is not only synthetically attractive, it is ideal from a practical standpoint. Nitroarene compounds are benchtop stable and a wide array are commercially available.

The Driver group has developed a series of methodologies to promote the formation of N-heterocycles by way of transition metal catalyzed intramolecular C–N bond formation using nitroarenes as the nitrogen source.^{37–39} It has been shown that by trapping nitrosoarenes in an electrocyclization that were generated in situ from either the Pd- or Fe- catalyzed reduction of

nitroarenes **2.7** could form 3*H*-indoles **2.9** (Scheme 2.2a). Building upon these works, I wanted to test the hypothesis that sp^3 -C–N bond formation could be achieved intramolecularly by constructing nitroarenes with a tethered nucleophile that could capture the electrophilic nitrosoarene once generated *in-situ*. (Scheme 2.2b).

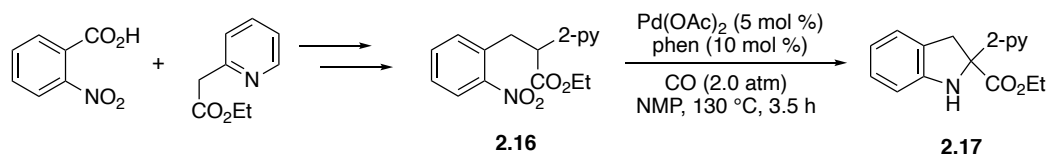
I have developed a method affording partially saturated 5-, 6-, or 7-membered *N*-heterocycles using a palladium(II) catalyzed reductive sp^3 -C–N bond formation from easily synthesized 1,2-disubstituted nitroarenes that uses CO gas as the terminal reductant. This method also allows the electrophilic capture of the nitrosoarene intermediate using a wide selection of nucleophiles to synthesize a broad variety of *N*-heterocycles (Scheme 2.2c).



Scheme 2.2 Formation of C–N Bonds from Nitroarenes

The synthesis can be completed in at most four steps and it tolerates using a-pyridyl carboxylates, malonates, 1,3-dimethylbarbituric acid, 1,3-diones or difurans as the nucleophile and either commercially available 2-nitrobenzyl bromide or through the reduction of 2-

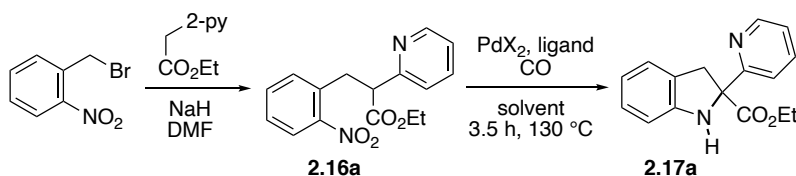
nitrobenzoic acid to its corresponding benzyl alcohol followed by treatment with PBr_3 to form the required benzyl bromide. (Scheme 2.3).



Scheme 2.3 Pd(II)-Catalyzed Synthesis of Polysubstituted Indolines from Nitroarenes

Initially, I wanted to explore the reactivity of **2.16a** when it was exposed to a metal catalyst and reductant (Table 2.1) to explore the hypothesis that $\text{sp}^3\text{-C-H}$ amination could be accomplished using nitroarenes and reductive conditions. $\text{Pd}(\text{OAc})_2$ and phenanthroline and was chosen first catalyst, and $\text{Mo}(\text{CO})_6$ was selected as reductant. These conditions were selected based upon precedent set by a prior Driver group publication.³⁷ Unfortunately, no reaction occurred. Changing the identity of the reductant to carbon monoxide resulted in the production of indoline **2.17a** in a yield of 70% (Table 2.1, entry 1). Initial results were promising, however the issue of maintaining an elevated pressure of harmful carbon monoxide required abandoning the usage of a Schlenk bomb. Instead, a Parr reactor was used. This did limit us to only higher boiling point solvents such as DMF, DMSO or NMP as the conical vial used for the reductive transformation could not be capped tightly to allow CO gas to dissolve into the solvent. Of these high boiling point, polar aprotic solvents NMP was found to be model solvent for the conversion (Table 2.1, entries 1–3). While reducing the catalyst loading from 10 mol % to 5 mol % resulted in an increase in formation of indoline, further reducing the catalyst loading severely attenuated the yield (Table 2.1, entries 3–5). Decreasing the pressure of CO to 1 atm still afforded indoline with a 72% yield, but it was found that 2.0 atm of CO gas resulted in the best yield (Table 2.1, entry 6). Increasing the pressure of CO to 3.0 atm did result in formation of indoline in good yield

(table **2.1**, entry 12). The outer bound of CO pressure was determined to be 2.0 atm as using 4.0 atm attenuated the yield of indoline formation (Table **2.1**, entry 13). Using alternate phenanthroline ligands revealed that more electron-rich ligands decreased the rate of reductive cyclization (Table **2.1**, entries 7–9). Since the usage of other palladium salts failed to improve the synthesis of indoline **2.17a** from **2.16a** (Table **2.1**, entries 10, 11), the conditions stated in entry 4 of Table 1 were selected to further explore the scope of the transformation. In addition to using CO as an alternative reductant to Mo(CO)₆, I tested a CO chemical precursor, however this method of in-situ reductant generation was insufficient in promoting nitroarene reduction (Table **2.1**, entry 14). Inclusion of an additive of 1.0 equiv. of acid did not inhibit reduction of nitrosoarene but did inhibit the electrocyclization to form indoline (Table **2.1**, entry 15). Instead, the nitroarene was reduced to aniline, which subsequently cyclized to form the undesired γ -lactam. We believe that the inclusion of excess proton in the solution produced an unfavorable enol / keto equilibrium resulting in complete attenuation of the nucleophilicity of the 2-pyridyl ester tether.



entry	PdX ₂ (mol %)	Ligand (mol %)	atm CO	additive (equiv.)	solvent	% yield, 2.17a
1	Pd(OAc) ₂ (10)	phen (20)	2.0	—	DMF	70
2	Pd(OAc) ₂ (10)	phen (20)	2.0	—	DMSO	53
3	Pd(OAc) ₂ (10)	phen (20)	2.0	—	NMP	76
4	Pd(OAc) ₂ (5)	phen (10)	2.0	—	NMP	83
5 ^b	Pd(OAc) ₂ (1)	phen (2)	2.0	—	NMP	0
6	Pd(OAc) ₂ (5)	phen (10)	1.0	—	NMP	72
7	Pd(OAc) ₂ (5)	tmphen (20)	2.0	—	NMP	30
8	Pd(OAc) ₂ (5)	4,7-(MeO) ₂ -phen (10)	2.0	—	NMP	71
9	Pd(OAc) ₂ (5)	Bphen (10)	2.0	—	NMP	42
10	PdCl ₂ (5)	phen (10)	2.0	—	NMP	n.r.
11	Pd(TFA) ₂ (5)	phen (10)	2.0	—	NMP	n.r.
12	Pd(OAc) ₂ (5)	phen (10)	3.0	—	NMP	72
13	Pd(OAc) ₂ (5)	phen (10)	4.0	—	NMP	48
14	Pd(OAc) ₂ (5)	phen (10)	—	^c	NMP	n.r.
15	Pd(OAc) ₂ (5)	phen (10)	2.0	PTsOH (1.0)	NMP	0

^a As determined using ¹H NMR spectroscopy using CH₂Br₂ as an internal standard.

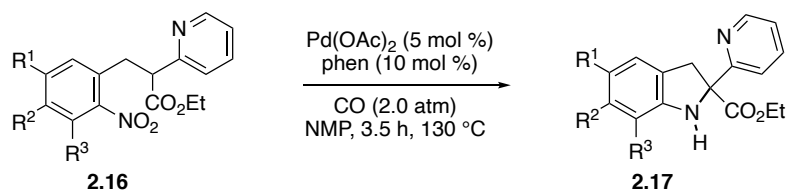
^b 16 h reaction time.

^c 6.0 equiv. CHCl₃ and 3.0 equiv. CsOH added to reaction vessel.

Table 2.1 Development of optimal conditions

Once the optimal conditions had been properly screened and identified, I examined the scope and limitations of the reductive sp³-C–N bond formation by first changing the electronic and steric nature of the nitroarene (Table **2.2**). In general, the yield of Pd-catalyzed reduction of nitroarenes is truncated by the addition of electron-releasing substituents. However, under the conditions we developed, I found that the reductive cyclization was largely unaffected by the

electronic nature of the nitroarene (Table **2.2**, entries 2–9). This reaction can be smoothly carried out with a selection of electron-releasing and minorly electron-withdrawing R¹- or R²-substituents. When a stronger electron-withdrawing CF₃ group was used, the yield was somewhat attenuated (Table **2.2**, entry 5). When methyl was installed in the R₃- position it was observed that reduction of the nitroarene was completely inhibited. This observation, while not unexpected, supports the hypothesis that the metal catalyst coordinates to the nitro-group in order to promote reduction (Table **2.2**, entry 10).⁴⁰



entry	#	R ¹	R ²	R ³	%, yield ^a
1	a	H	H	H	83
2	b	Cl	H	H	65
3	c	F	H	H	72
4	d	Me	H	H	80
5	e	H	CF ₃	H	50
6	f	H	Cl	H	65
7	g	H	F	H	80
8	h	H	Me	H	70
9	i	H	OMe	H	61
10	j	H	H	Me	n.r.

^a Isolated yield of **2.17** after silica gel chromatography.

Table 2.2 Scope and limitations of substituted nitroarenes

Next, I sought to investigate any changes in reactivity of the nitrosoarene when exposed to a catalog of nucleophiles in the hopes of building a library of distinct *N*-heterocyclic frameworks that could be synthesized through the sp³-C–N bond forming reaction (Table **2.3**). Initial modification of the primary test substrate it was discovered that the yield of the reductive cyclization was affected by the steric bulk of ester substituent, but was unaffected by the steric nature about the pyridyl nitrogen (Entries **2.19a**, **2.19b**, **2.19c**). When the pyridyl nitrogen was

changed from the 2-position to the 4-position, the reduction of the nitroarene was completely inhibited and formation of indoline **2.19d** was not observed. This result supported our hypothesis that the positioning of Lewis basic functionalities are key to stabilizing the enol reactive intermediate required to trap the in-situ generated nitrosoarene. Additionally, it was revealed that the inclusion of pyridine as part of the tethered nucleophile was not required to achieve cyclization. Exposure of malonate **2.18e** to our metal catalyzed reductive conditions successfully synthesized indoline **2.19e**. Fortunately, cyclization is not limited to the synthesis of 5-membered *N*-heterocycles. Tetrahydroquinoline **2.19f** was successfully synthesized with a yield of 68%. Tetrahydrobenzoazepine **2.19g** was also synthesized, albeit with a low yield of 12%. I also wanted to probe potential stereoselectivity of the reductive cyclization through exposure of malonate **2.18h**. While the reductive cyclization conditions formed **2.19h** in a moderate yield of 44%, no diastereoselectivity was observed. Synthesis of six-membered rings is not limited to tetrahydroquinoline; oxygen and nitrogen can be included into the nucleophilic tether allowing, efficient access to other complex heterocycles such as benzo-1,3-oxazine **2.19i** and 1,4-dihydroquinazoline **2.19j**. The scope of enolizable nucleophiles able to capture the in-situ generated nitrosoarene is not limited to malonates or 2-pyridylacetic acid ethyl esters. 1,3-dimethylbarbituric acid derivative **2.18k** and 1,3-indandione derivative **2.18l** were also found to be sufficiently nucleophilic to form new sp^3 -C-H bonds, which is a contrast to the decomposition pathway observed when α -cyano- or α -nitro-substituted carboxylates were submitted to reaction conditions. Interestingly, difuran **2.18m** successfully underwent reductive cyclization and ring opening to form indole **2.19m**.⁴¹ With these studies complete, the flexibility of the

reductive cyclization method affording a wide array of *N*-heterocycles using simple *ortho*-substituted nitroarenes has been established.

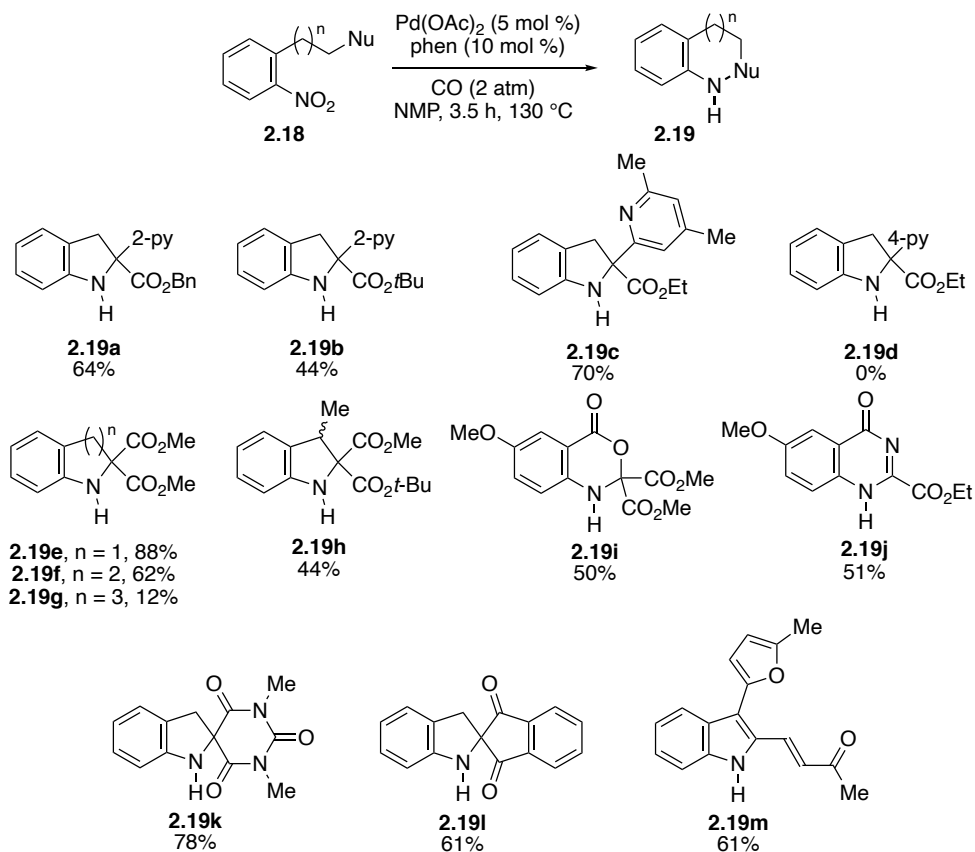
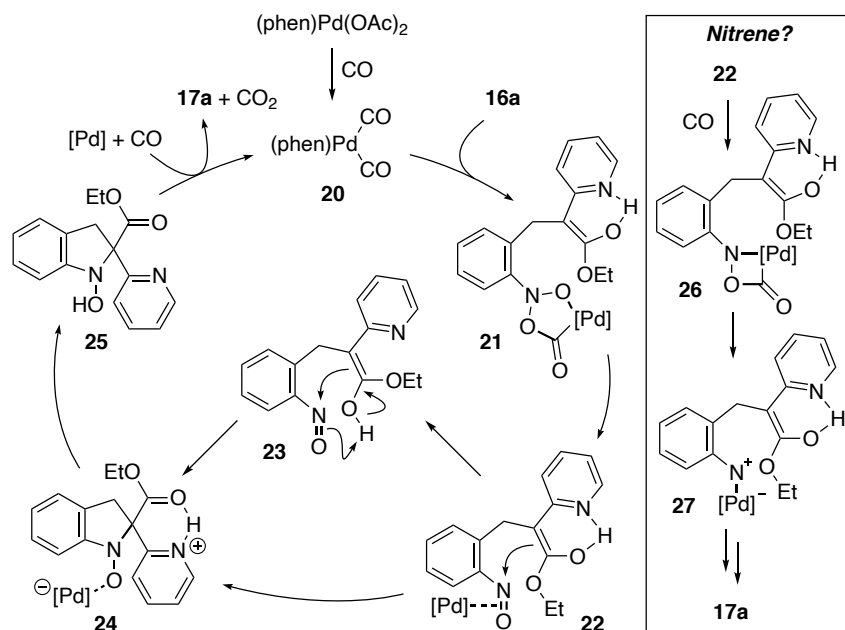


Table 2.3 Investigation of nucleophile scope

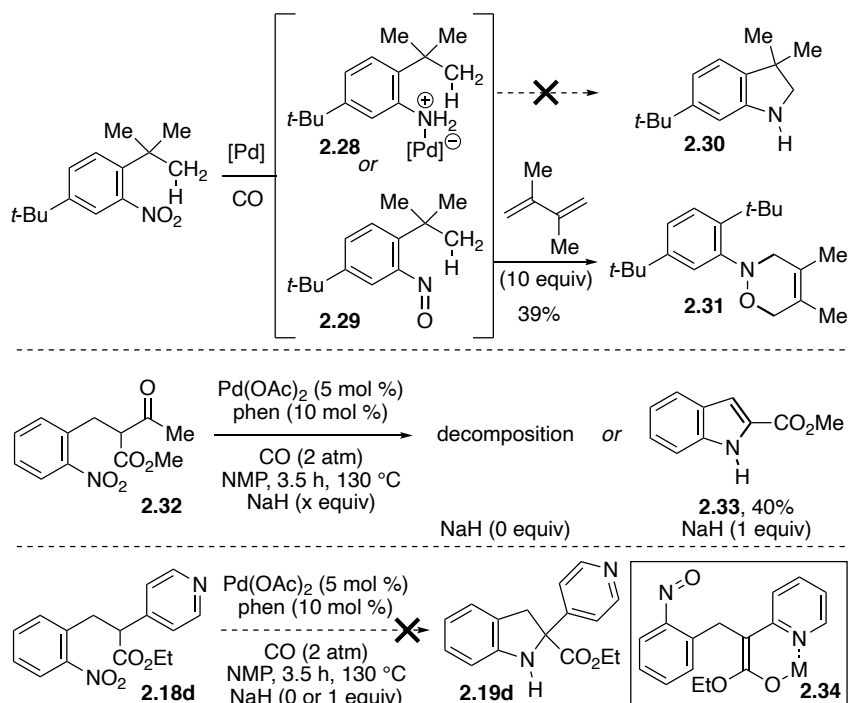
We propose the following mechanism to account for the reductive cyclization formation of $\text{sp}^3\text{-C-N}$ bonds of 2-substituted nitroarenes shown in Scheme **2.4**. Since our data suggests that the successful reaction outcome requires an enolizable tether, we posit that the $\text{sp}^3\text{-C-N}$ bond forming event occurs by way of nucleophilic attack of the enolate onto the nitrosoarene. The active catalyst for nitrosoarene formation and cyclization could be palladium(II) bis-carbonyl species that is generated through CO-mediated reduction of the palladium(II) acetate pre-catalyst. First, nitroarene **2.16a** could oxidatively add to the palladium catalyst, forming palladacycle **2.21**.^{42,43} Decarboxylation could generate nitrosoarene **2.22**, the reactive

intermediate required to accomplish $\text{sp}^3\text{-C-N}$ bond formation.⁴⁴ The nitrosoarene could then be attacked by either the pendant enol or palladium enolate, synthesizing the $\text{sp}^3\text{-C-NAr}$ bond.⁴⁵⁻⁴⁸ The reactive nitrosoarene intermediate could also dissociate from the metal center, proceeded by nucleophilic attack by the enolate.^{49,50} This dissociation prior to the bond forming event could facilitate a nitroso-ene reaction to yield *N*-hydroxyindoline **2.24**.¹⁹⁻²¹ While we are unsure which pathway is followed, we do know that further reduction of *N*-hydroxyindoline **2.25** occurs to form indoline **2.17a**.⁵¹⁻⁵⁴ We also cannot rule out the possibility that nitrosoarene **2.22** could react with an additional carbonyl ligand to produce pallacyclebutane **2.26**. Existence of this palladacycle has been verified by Osborn and co-workers while carrying out mechanistic studies into the palladium-catalyzed carbonylation of nitroarenes, and has been characterized by X-ray crystallography.⁵⁵ Following this, the removal of CO_2 would produce the palladium *N*-aryl nitrene **2.27** that could react with the enol tether, resulting in the indoline product.



Scheme 2.4 Proposed mechanism for Pd-catalyzed $\text{sp}^3\text{-C-N}$ bond formation

To probe the mechanism for the reductive cyclization, I conducted a series of mechanistic experiments (Scheme **2.5**). To begin, I tested for radical intermediates through the addition of 1.0 equivalent TEMPO to the optimized reductive cyclization conditions. Indoline was formed with a yield of 56%, which suggests one of two things. Either radical intermediates are not formed, or, if radical intermediates do form, they do not leave the solvent shell during the reductive cyclization. Next, I wanted to probe the possible existence of an *N*-aryl nitrene and its potential role in the reductive cyclization. To do this, I submitted 2,5-di-*tert*-butylnitrobenzene to reductive $\text{sp}^3\text{-C-N}$ bond formation conditions. Since only full reduction to 2,5-di-*tert*-butylaniline was observed and no C-H activation was achieved, we concluded that the reductive cyclization does not proceed through an *N*-aryl nitrene intermediate. To determine the presence of the nitrosoarene intermediate and to determine if it is bound to palladium, I submitted I submitted 2,5-di-*tert*-butylnitrobenzene to reductive $\text{sp}^3\text{-C-N}$ bond formation conditions and added an excess of 2,3-dimethylbutadiene. The diene intercepted the nitrosoarene, forming oxazine **2.31**. This result further suggests that the reaction proceeds through nitrosoarene and it not bound to palladium.⁵⁶



Scheme 2.5 Mechanistic probes

Next, I explored the effect of acidity and enolization on the reaction outcome by studying the acetoacetate derived **2.32**.^{57–61} When **2.32** was submitted to reaction conditions, no product was formed, and complete decomposition occurred. To verify that the reaction conditions were not decomposing any potential product, I also lowered the reaction temperature to 100 °C but this did not prevent complete decomposition. During optimization, addition of an acid led to complete annunciation of indoline formation and instead led to conversion to lactam (Table **2.1**, entry 15). To remove any excess proton from the reaction solution, NaH was added and 15-crown-5 was added in the same amount to also remove the potentially Lewis acidic sodium ions. These two additives restored the reactivity of **2.32** to afford 1H-indole **2.33**.⁶² Revisiting 4-pyridyl **2.18d** and fully deprotonating it using the conditions that rescued the reactivity of the acetoacetate derived **2.32** did not result in the reductive cyclization using palladium and CO. This was interpreted in one of two ways. First, we were concerned that the exposed nitrogen on the

4-pyridyl tether could be chelating to the metal catalyst, thereby preventing oxidative addition of the nitroarene to the palladium catalyst. To test this hypothesis, a super-stoichiometric amount of pyridine was added to the reaction mixture. Under these conditions indoline **2.17a** was formed, however the yield was somewhat attenuated at 44%. I interpreted this as free pyridine potentially chelating to the active palladium catalyst **2.20**, decreasing its propensity for oxidative addition of the nitroarene. Secondly, since the usage of an alpha-4-pyridyl group should not prevent the reductive cyclization to occur if it proceeded through an ene-reaction posited in intermediate **2.21**, we concluded that $\text{sp}^3\text{-C-N}$ bond formation does not proceed through an ene-type cyclization and the bidentate chelation of the pyridine nitrogen and the oxygen of the ester to the palladium ion is required to facilitate formation of the C-N bond.

In conclusion, I have developed a method affording the palladium-catalyzed reductive cyclization of nitroarenes that allows the conversion of an $\text{sp}^3\text{-C-H}$ bond to an $\text{sp}^3\text{-C-N}$ bond. This method of constructing C-N bonds by way of nucleophilic attack of a variety of malonate derivatives onto the reactive electrophilic nitrosoarene intermediate is mechanistically novel and differentiates itself from other C-H amination reactions, enabling access to *N*-heterocycles of varying ring sizes by changing the identity and tether length of the nucleophile. Building off of this work, additional investigations could be conducted to further the synthetic potential of primary nucleophiles studied in this work in order to more accurately define the electrophilicity of the nitrosoarene intermediate. Following the completion of this work, I continued to study the synthetic potential of the nitrosoarene reactive intermediate to construct other *N*-heterocycles not included in this work.

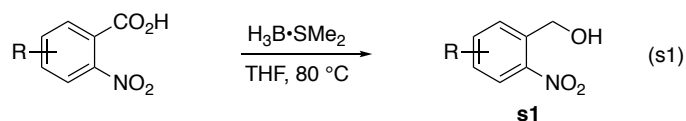
Experimental Section

General. ^1H NMR and ^{13}C NMR spectra were recorded at ambient temperature using 500 MHz or 300 MHz spectrometers. The data are reported as follows: chemical shift in ppm from internal tetramethylsilane on the δ scale, multiplicity (br = broad, s = singlet, d = doublet, t = triplet, q = quartet, m = multiplet), coupling constants (Hz) and integration. High-resolution mass spectra were obtained by peak matching. Melting points are reported uncorrected. Infrared spectroscopy was obtained using a diamond attenuated total reflectance (ATR) accessory. Analytical thin layer chromatography was performed on 0.25 mm extra hard silica gel plates with UV254 fluorescent indicator. Liquid chromatography was performed using forced flow (flash chromatography) of the indicated solvent system on 60Å (40 – 60 μm) mesh silica gel (SiO_2). Medium pressure liquid chromatography (MPLC) was performed to force flow the indicated solvent system down columns that had been packed with 60Å (40 – 60 μm) mesh silica gel (SiO_2). All reactions were carried out under an atmosphere of nitrogen in glassware, which had been oven-dried. Unless otherwise noted, all reagents were commercially obtained and, where appropriate, purified prior to use. Acetonitrile, methanol, toluene, THF, Et_2O , and CH_2Cl_2 were dried by filtration through alumina according to the procedure of Grubbs.⁶³ Metal salts were stored in a nitrogen atmosphere dry box.

I. Preparation of Substituted 2-Nitrobenzyl Alcohols.

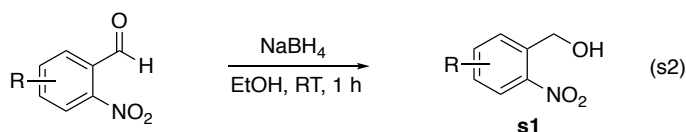
A. General Procedures.

1. Method A.



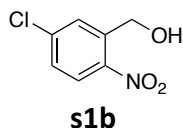
To a 1 M solution of substituted 2-nitrobenzoic acid (1.0 equiv) in THF was added dropwise a 10 M solution of borane dimethylsulfide complex in THF (1.3 equiv). The resulting solution was heated to 80 °C. After 3 hours, the reactives were quenched with the addition of 10 mL of H₂O. The mixture was then extracted with 3 × 30 mL of ethyl acetate. The combined organic phases were washed with 10 mL of a saturated aqueous solution of Na₂CO₃ followed by 10 mL of brine. The resulting organic phase was dried over Na₂SO₄ and filtered. The filtrate was concentrated in *vacuo* to afford the product.

2. Method B.

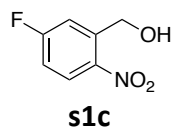


To a 1 M solution of substituted 2-nitrobenzaldehyde (1.0 equiv) in MeOH was added by sodium borohydride (1.1 equiv). After 1 hour, the reactives were quenched with 10 mL of a 1 M aq soln of HCl. The mixture was then extracted with 3 × 30 mL of ethyl acetate. The combined organic phases were washed with 10 mL of a saturated aqueous solution of Na₂CO₃ followed by 10 mL of brine. The resulting organic phase was dried over Na₂SO₄ and filtered. The filtrate was concentrated in *vacuo* to afford the product.

B. Characterization Data.

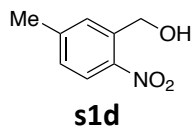


(5-Chloro-2-nitrophenyl)methanol s1b.⁶⁴ Method A was followed using 1.02 g of 5-methoxy-2-nitrobenzoic acid (5.00 mmol) in 25 mL of THF and 0.65 mL of a 10 M soln of $\text{BH}_3 \cdot \text{Me}_2\text{S}$ (6.5 mmol, 1.3 equiv) in THF. Purification by extraction afforded the product as a white solid (0.843 g, 90%). The spectral data matched that reported by Naganawa and co-workers:² ^1H NMR (500 MHz, CDCl_3) δ 8.08 (d, $J = 9.0$ Hz, 1H), 7.81 (d, $J = 2.0$ Hz, 1H), 7.42 (dd, $J = 8.5, 2.5$ Hz, 1H), 5.01 (s, 2H), 2.49 (s, 1H); ^{13}C NMR (125 MHz, CDCl_3) δ 145.4 (C), 140.9 (C), 139.2 (C), 129.4 (CH), 128.3 (CH), 126.6 (CH), 62.0 (CH_2). ATR-FTIR (thin film): 3100–3450, 1604, 1502 cm^{-1} .

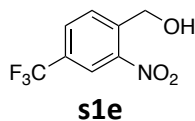


(5-Fluoro-2-nitrophenyl)methanol s1c.⁶⁵ Method B was followed using 0.676 g of 5-fluoro-2-nitrobenzaldehyde (4.00 mmol), 0.166 g of NaBH_4 (4.40 mmol, 1.1 equiv) and 4 mL of MeOH. Purification by extraction afforded the product as a white solid (0.597 g, 87%). The spectral data for **s1c** matched that reported by Engler and co-workers: ^1H NMR (500 MHz, CDCl_3) δ 8.20 (dd, $J = 9.5$ Hz, 5.5 Hz, 1H), 7.53 (dd, $J = 9.5$ Hz, 3 Hz, 1H), 7.12 (m, 1H), 5.04 (d, $J = 5.5$ Hz, 2H), 2.39 (t, $J = 6.0$ Hz, 1H); ^{13}C NMR (125 MHz, CDCl_3) δ 165.8 (d, $J_{\text{CF}} = 254.0$ Hz, C), 149.9 (C), 141.2 (d, $J_{\text{CF}} = 9.12$ Hz, C), 128.1 (d, $J_{\text{CF}} = 9.75$ Hz, CH), 116.1 (d, $J_{\text{C-F}} = 26.6$ Hz, CH), 115.1 (d, $J_{\text{CF}} = 23.4$ Hz, CH),

62.1 (CH₂); ¹⁹F NMR (376 MHz, CDCl₃) δ −102.1. ATR-FTIR (thin film): 3249, 3097, 1523, 1346, 1225, 1039 cm^{−1}.



(5-Methyl-2-nitrophenyl)methanol s1d.⁶⁶ Method A was followed using 0.725 g of 5-methyl-2-nitrobenzoic acid (4.00 mmol) in 20 mL of THF and 0.520 mL of a 10 M soln of BH₃•SMe₂ (5.20 mmol, 1.3 equiv) in THF. Purification by extraction afforded the product as a white solid (0.497 g, 75%). The spectral data for **s1d** matched that reported by Driver and co-workers:⁴ ¹H NMR (500 MHz, CDCl₃) δ 8.02 (d, *J* = 8.3 Hz, 1H), 7.51 (s, 1H), 7.24 (d, *J* = 8.6 Hz, 1H), 4.93 (s, 2H), 2.69 (s, 1H), 2.45 (s, 3H); ¹³C NMR (125 MHz, CDCl₃) δ 145.7 (C), 145.4 (C), 136.8 (C), 130.6 (CH), 129.0 (CH), 125.3 (CH), 62.8 (CH₂), 21.6 (CH₃). ATR-FTIR (thin film): 3291, 2942, 1512, 1334, 1035 cm^{−1}.

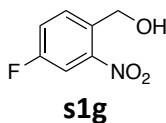


(2-Nitro-4-(trifluoromethyl)phenyl)methanol s1e.⁶⁷ Method A was followed using 0.940 g of 2-nitro-4-trifluoromethylbenzoic acid (4.00 mmol) in 20 mL of THF and 0.520 mL of a 10 M soln of BH₃•SMe₂ (5.2 mmol, 1.3 equiv) in THF. Purification by extraction afforded the product as a white solid (0.619 g, 70%). The spectral data matched that reported by Afzali, Tulveski and co-workers:⁵ mp 68 – 70 °C; ¹H NMR (500 MHz, CDCl₃) δ 8.35 (s, 1H), 8.01 (d, *J* = 8.0 Hz, 1H), 7.92 (d, *J* = 8.0 Hz, 1H), 5.08 (s, 2H) only visible peaks; ¹³C NMR (125 MHz, CDCl₃) δ 147.1 (C), 140.7 (C), 134.6 (q, *J*_{CF}

= 34.9 Hz, C), 129.6 (d, J_{CF} = 3.5 Hz, CH), 122.5 (q, J_{CF} = 202.1 Hz, C), 122.3 (d, J_{CF} = 4.75 Hz, CH), 121.4 (d, J_{CF} = 3.5 Hz, CH) 61.9 (CH₂); ¹⁹F NMR (376 MHz, CDCl₃) δ –63.3. ATR-FTIR (thin film): 2924, 1721, 1330, 1088 cm^{–1}.

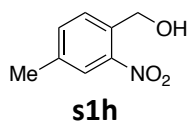


(4-Chloro-2-nitrophenyl)methanol s1f.⁶⁸ Method A was followed using 0.831 g of 4-chloro-2-nitrobenzoic acid (4.00 mmol) in 20 mL of THF and 0.52 mL of a 10 M soln of BH₃•Me₂S (5.20 mmol, 1.3 equiv) in THF. Purification by extraction afforded the product as a yellow solid (0.524 g, 52%). The spectral data for **s1f** matched that reported by Blanc and Bochet:⁶ ¹H NMR (500 MHz, CDCl₃) δ 8.08 (d, J = 1.6 Hz, 1H), 7.72 (d, J = 8.3 Hz, 1H), 7.63 (dd, J = 8.2, 1.7 Hz, 1H), 4.96 (s, 2H), 2.63 (s, 1H); ¹³C NMR (125 MHz, CDCl₃) δ 147.7 (C), 135.4 (C), 134.2 (C), 134.1 (CH), 130.9 (CH), 125.0 (CH), 61.9 (CH₂) ATR-FTIR (thin film): 3279, 1512, 1341, 1031 cm^{–1}.

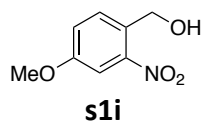


(4-Fluoro-2-nitrophenyl)methanol s1g.⁶⁹ Method A was followed using 0.516 g of 4-fluoro-2-nitrobenzoic acid (2.78 mmol) in 15 mL of THF and a 0.360 mL of a 10 M soln of BH₃•SMe₂ (3.51 mmol, 1.3 equiv) in THF. Purification by extraction afforded the product as a white solid (0.371 g, 78%). (4-Fluoro-2-nitrophenyl)methanol **s1g** was previously reported by Chen and co-workers:⁷ ¹H NMR (500 MHz, CDCl₃) δ 7.82 (d, J = 8.0 Hz, 2.5 Hz, 1H), 7.76 (d, J = 8.5 Hz, 5.5 Hz, 1H), 7.40 (m,

1H), 4.97 (d, $J = 6.0$ Hz, 2H), 2.44 (t, $J = 6.5$ Hz, 1H); ^{13}C NMR (125 MHz, CDCl_3) δ 161.4 (d, $J_{\text{CF}} = 249.8$ Hz, C), 132.8 (C), 131.6 (d, $J_{\text{CF}} = 7.37$ Hz, CH), 121.3 (d, $J_{\text{CF}} = 20.2$ Hz, CH), 112.5 (d, $J_{\text{CF}} = 25.7$ Hz, CH), 62.0 (CH_2), only visible peaks; ^{19}F NMR (376 MHz, CDCl_3) δ -111.7. ATR-FTIR (thin film): 3249, 3096, 1520, 1345, 1038 cm^{-1} .



(4-Methyl-2-nitrophenyl)methanol s1h. Method A was followed using 0.724g of 5-methoxy-2-nitrobenzoic acid (4.00 mmol) in 20 mL of THF and 0.520 mL of a 10 M soln of $\text{BH}_3 \cdot \text{SMe}_2$ (5.20 mmol, 1.3 equiv) in THF. Purification by extraction afforded the product as a white solid (0.501 g, 75%). The spectral data for **s1h** matched that reported by Driver and co-workers:⁴ ^1H NMR (500 MHz, CDCl_3) δ 7.88 (s, 1H), 7.57 (d, $J = 7.0$ Hz, 1H), 7.45 (d, $J = 6.3$ Hz, 1H), 4.88 (s, 2H), 2.75 (s, 1H), 2.43 (s, 3H); ^{13}C NMR (125 MHz, CDCl_3) δ 147.6 (C), 139.1 (C), 134.9 (CH), 133.8 (C), 130.0 (CH), 125.3 (CH), 62.4 (CH_2), 20.8 (CH_3). ATR-FTIR (thin film): 3181–3406, 3080, 1516, 1347 cm^{-1} . HRMS (EI) m/z calculated for $\text{C}_8\text{H}_8\text{O}_3\text{N}$ ($\text{M}-\text{H}$) $^+$: 166.05042, found: 166.05021.

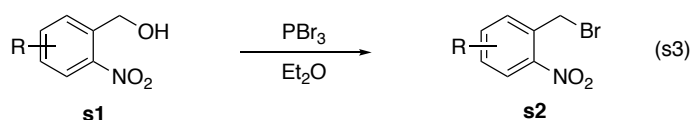


(4-Methoxy-2-nitrophenyl)methanol s1i.⁷⁰ Method A was followed using 1.00 g of 4-methoxy-2-nitrobenzoic acid (5.07 mmol) in 25 mL of THF and 0.659 mL of a 10 M soln of $\text{BH}_3 \cdot \text{SMe}_2$ (6.59 mmol, 1.3 equiv) in THF. Purification by extraction afforded the product as a white solid (0.424 g, 46%). The spectral data for **s1i** matched that reported by Katritzky and co-workers:⁸ ^1H NMR (500

MHz, CDCl₃) δ 7.58 (d, J = 2.9 Hz, 1H), 7.56 (s, 1H), 7.18 (dd, J = 8.6, 2.5 Hz, 1H), 4.85 (s, 2H), 3.87 (s, 3H), 2.73 (s, 1H); ¹³C NMR (125 MHz, CDCl₃) δ 159.4 (C), 148.5 (C), 131.5 (CH), 128.8 (C), 120.4 (CH), 109.7 (CH), 62.3 (CH₂), 55.9 (CH₃). ATR-FTIR (thin film): 3253, 2836, 1512, 1303 cm⁻¹.

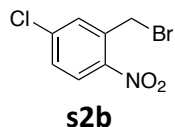
II. Preparation of Substituted 1-(Bromomethyl)-2-nitrobenzenes.

A. General Procedure



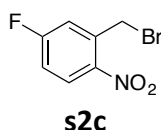
To a solution of substituted (2-nitrophenyl) methanol in Et₂O was added PBr₃ (1.3 equiv.) dropwise. After 3 hours, a saturated solution of NaHCO₃ was added the reaction mixture until a neutral pH was obtained. The resulting solution was extracted with 3 × 10 mL of ethyl acetate and the resulting organic phase was washed with brine. The resulting organic phase was dried over Na₂SO₄, filtered and the filtrate was concentrated *in vacuo* to afford the product.

B. Characterization Data.

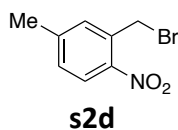


2-(Bromomethyl)-5-chloro-1-nitrobenzene s2b.⁷¹ The general procedure was followed by using 0.815 g of **s1b** (4.42 mmol) in 10 mL of ethyl ether and 0.534 mL of PBr₃ (5.74 mmol). Purification by extraction afforded the product as a yellow oil (0.790 g, 71%). The spectral data of **s2b** matched that reported by McAllister and co-workers:⁷¹ ¹H NMR (500MHz, CDCl₃) 8.01 (d, J = 7.5

Hz, 1H), 7.57 (d, $J = 2.0$ Hz, 1H), 7.45 (dd, $J = 8.5, 2.0$ Hz, 1H), 4.78 (s, 2H); ^{13}C NMR (125 MHz, CDCl_3) δ 146.1 (C), 140.1 (C), 134.8 (C), 132.5 (CH), 129.7 (CH), 127.1 (CH), 28.2 (CH_2). ATR-FTIR (thin film): 3107, 3070, 1519, 1333 cm^{-1} .

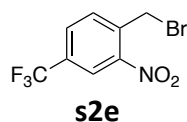


2-(Bromomethyl)-5-fluoro-1-nitrobenzene s2c.⁷² The general procedure was followed by using 0.360 g of **s1c** (2.10 mmol) in 10 mL of ethyl ether and 0.400 mL of PBr_3 (4.20 mmol). Purification by extraction afforded the product as a yellow solid (0.236 g, 48%). The spectral data of **s2c** matched that reported by Rzasa and co-workers: ^1H NMR (500 MHz, CDCl_3) δ 7.78 (dd, $J = 8.5\text{H}, 2.5$ Hz, 1H), 7.58 (dd, $J = 8.0$ Hz, 5.5 Hz, 1H), 7.34 (m, 1H), 4.80 (s, 2H); ^{13}C NMR (125 MHz, CDCl_3) δ 161.9 (d, $J_{\text{CF}} = 251.5$ Hz, C), 148.5 (C), 134.3 (d, $J_{\text{CF}} = 7.62$ Hz, CH), 129.0 (C), 121.0 (d, $J_{\text{CF}} = 20.5$ Hz, CH), 113.3 (d, $J_{\text{CF}} = 25.7$ Hz, CH), 28.0 (CH_2); ^{19}F NMR (376 MHz, CDCl_3) δ -102.7. ATR-FTIR (thin film): 2922, 2853, 1524, 1341, 609 cm^{-1} .



2-(Bromomethyl)-5-methyl-1-nitrobenzene s2d. The general procedure was followed by using 0.502 g of **s1d** (3.00 mmol) in 20 mL of ethyl ether and 0.389 mL of PBr_3 (3.90 mmol). Purification by extraction afforded the product as a yellow solid (0.552 g, 80%). The spectral data of **s2d** matched that reported by McAllister and co-workers: ^1H NMR (500 MHz, CDCl_3) δ 7.91 (d, $J = 8.3$

Hz, 1H), 7.32 (s, 1H), 7.23 (d, $J = 8.3$ Hz, 1H), 4.77 (s, 2H), 2.40 (s, 3H); ^{13}C NMR (125 MHz, CDCl_3) δ 145.5 (C), 145.3 (C), 133.1 (CH), 132.8 (C), 130.2 (CH), 125.7 (CH), 29.5 (CH_2), 21.4 (CH_3). ATR-FTIR (thin film): 3068.2, 1511.9, 1313.3, 826.3 cm^{-1} .



1-(Bromomethyl)-2-nitro-4-(trifluoromethyl)benzene s2e. The general procedure was followed using 0.884 g of **s1e** (4.00 mmol) in 20 mL of ethyl ether and 0.490 mL of PBr_3 (5.20 mmol). Purification by extraction afforded the product as a yellow oil (0.772 g, 68%). The spectral data matched that reported by Driver and co-workers: ^1H NMR (500 MHz, CDCl_3) δ 8.30 (s, 1H), 7.88 (d, $J = 8.0$ Hz, 1H), 7.77 (d, $J = 8.0$ Hz, 1H), 4.85 (s, 2H); ^{13}C NMR (125 MHz, CDCl_3) δ 148.0 (C), 136.6 (C), 133.5 (CH), 130.2 (d, $J_{\text{CF}} = 3.1$ Hz, C), 123.1 (q, $J_{\text{CF}} = 34.1$ Hz, C), 122.8 (d, $J_{\text{CF}} = 3.6$ Hz, CH), 122.5 (q, $J_{\text{CF}} = 271.1$ Hz, C), 27.5 (CH_2); ^{19}F NMR (376 MHz, CDCl_3) δ -63.6. FTIR (thin film): 3120, 1733, 1539, 1130, 1083, 625 cm^{-1} .

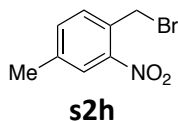


1-(Bromomethyl)-4-chloro-2-nitrobenzene s2f. The general procedure was followed by using 1.00 g of **s1f** (5.30 mmol) in 15 mL of diethyl ether and 0.989 mL of PBr_3 (10.6 mmol). Purification by extraction afforded the product as yellow oil (1.28 g, 97%). The spectral data matched of **s2f** that reported by Driver and co-workers: ^1H NMR (500 MHz, CDCl_3) δ 7.98 (d, $J = 1.8$ Hz, 1H), 7.56

(dd, $J = 8.3, 2.0$ Hz, 1H), 7.52 (d, $J = 8.3$ Hz, 1H), 4.76 (s, 2H); ^{13}C NMR (125 MHz, CDCl_3) δ 148.2 (C), 135.4 (C), 133.8 (CH), 133.7 (CH), 131.4 (C), 125.6 (CH), 28.1 (CH_2). ATR-FTIR (thin film): 3086, 2866, 1526, 1343 cm^{-1} .



2-(Bromomethyl)-4-fluoro-1-nitrobenzene s2f. The general procedure was followed by using 0.360 g of **s1g** (2.10 mmol) in 10 mL of ethyl ether and 0.400 mL of PBr_3 (4.20 mmol). Purification by extraction afforded the product as a yellow solid (0.220 g, 45%). The spectral data of **s2g** matched that reported by Rzas and co-workers: ^1H NMR (500 MHz, CDCl_3) δ 8.14 (m, 1H), 7.30 (dt, $J = 8.5$ Hz, 2.5 Hz, 1H), 7.16 (m, 1H), 4.82 (d, $J = 3.5$ Hz, 2H); ^{13}C NMR (125 MHz, CDCl_3) δ 164.7 (d, $J_{\text{CF}} = 255.8$ Hz, C), 143.9 (C), 136.3 (d, $J_{\text{CF}} = 9.12$ Hz, C), 128.5 (d, $J_{\text{CF}} = 10.7$ Hz, CH), 119.5 (d, $J_{\text{CF}} = 52.8$ Hz, CH), 116.5 (d, $J_{\text{CF}} = 22.5$ Hz, CH), 28.4 (CH_2), ^{19}F NMR (376 MHz, CDCl_3) δ -108.8. ATR-FTIR (thin film): 3065, 1531, 1346, 1240, 608 cm^{-1} .

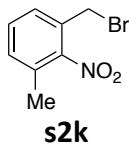


1-(Bromomethyl)-4-methyl-2-nitrobenzene s2h. The general procedure was followed by using 0.700 g of **s1h** (4.19 mmol) in 10 mL of diethyl ether and 0.510 mL of PBr_3 (5.43 mmol). Purification by extraction afforded the product as yellow oil (0.791 g, 82%). The spectral data of **s2h** matched that reported by McAllister and co-workers: ^1H NMR (500MHz, CDCl_3) δ 7.84 (s, 1H),

7.44 – 7.39 (m, 2H), 4.79 (s, 2H), 3.29 (s, 3H); ^{13}C NMR (125 MHz, CDCl_3) δ 147.8 (C), 140.5 (C), 134.5 (CH), 132.4 (CH), 129.9 (C), 125.9 (CH), 29.1 (CH_2), 21.0 (CH_3). ATR-FTIR (thin film): 3056, 2924, 2870, 1523, 1343 cm^{-1} . HRMS (EI) m/z calculated for $\text{C}_8\text{H}_8\text{O}_2\text{NBr}$ (M) $^+$: 228.97383, found: 228.97442.

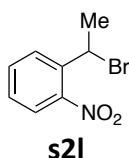


1-(Bromomethyl)-4-methoxy-2-nitrobenzene s2i. The general procedure was followed by using 0.900 g of **s1i** (4.91 mmol) in 15 mL of diethyl ether and 0.600 mL of PBr_3 (6.38 mmol). Purification by extraction afforded the product as a yellow oil (0.725 g, 60%). The spectral data of **s2i** matched that reported by McAllister and co-workers: ^1H NMR (500 MHz, CDCl_3) δ 7.51 (d, J = 2.4 Hz, 1H), 7.43 (d, J = 8.6 Hz, 1H), 7.10 (dd, J = 8.5, 2.4 Hz, 1H), 4.77 (s, 2H), 3.86 (s, 3H); ^{13}C NMR (125 MHz, CDCl_3) δ 160.1 (C), 148.6 (C), 133.6 (CH), 124.7 (C), 119.9 (CH), 110.5 (CH), 56.0 (CH_3), 29.3 (CH_2). ATR-FTIR (thin film): 2952, 1515, 1363, 1282 cm^{-1} .



1-(Bromomethyl)-3-methyl-2-nitrobenzene s2k. The general procedure was followed using 0.884 g of (3-methyl-2-nitrophenyl)methanol (4.00 mmol) in 20 mL of ethyl ether and 0.490 mL of PBr_3 (5.20 mmol). Purification by extraction afforded the product as a yellow oil (0.690 g, 75%). The spectral data of **s2k** matched that reported by McAllister and co-workers: ^1H NMR (500 MHz,

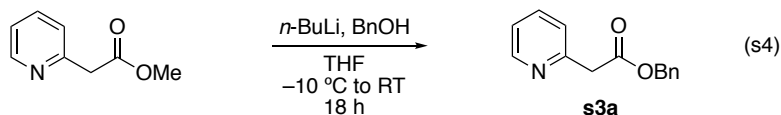
CDCl₃) δ 7.39 – 7.34 (m, 2H), 7.27 (dd, J = 7.2, 1.8 Hz, 1H), 4.47 (s, 2H), 2.34 (s, 3H); ¹³C NMR (125 MHz, CDCl₃) δ 150.6 (C), 131.9 (CH), 130.9 (C), 130.7 (CH), 129.7 (C), 129.0 (CH), 26.9 (CH₂), 17.7 (CH₃). FTIR (thin film): 3002, 1710, 1528, 1362, 1219 cm⁻¹.



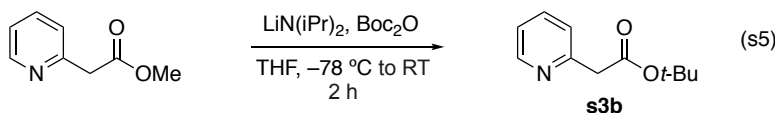
1-(1-Bromoethyl)-2-nitrobenzene s2I.⁷³ The general procedure was followed using 0.501 g of 1-(2-nitrophenyl)ethan-1-ol (4.00 mmol) in 20 mL of ethyl ether and 0.560 mL of PBr₃ (6.00 mmol). Purification by extraction afforded the product as a yellow oil (0.506 g, 55%). The spectral data of **s2I** matched that reported by Deveraj and co-workers:¹¹ ¹H NMR (500 MHz, CDCl₃) δ 7.88 (d, J = 8.0 Hz, 1H), 7.82 (d, J = 8.0 Hz, 1H), 7.63 (t, J = 7.5 Hz, 1H), 7.42 (t, J = 8.0 Hz, 1H), 5.80 (q, J = 6.5 Hz, 1H), 2.07 (d, J = 7.0 Hz, 3H); ¹³C NMR (125 MHz, CDCl₃) δ 147.4 (C), 137.8 (C), 133.6 (CH), 130.0 (CH), 129.1 (CH), 124.5 (CH), 42.0 (CH), 27.3 (CH₃). ATR-FTIR (thin film): 2980, 1725, 1515, 1349, 680 cm⁻¹.

III. Synthesis of Substituted Ethyl 3-(2-Nitrophenyl)-2-(pyridin-2-yl)propanoates.

A. Syntheses of 2-Pyridyl Acetates.

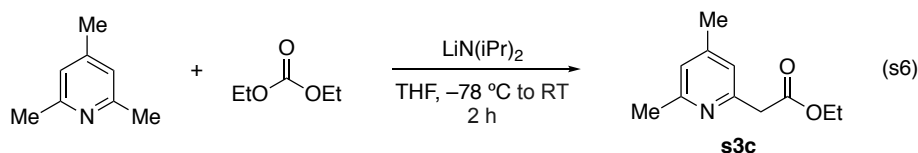


Benzyl 2-(pyridin-2-yl)acetate s3a. To a cooled (−10 °C) stirred solution of benzyl alcohol (625 μ L, 6.0 mmol, 2.0 equiv) in 3.0 mL of dry THF was added 2.4 mL of a 2.5 M solution of *n*-BuLi in hexanes (6.0 mmol, 2.0 equiv). After 10 min, 410 mg of methyl 2-pyridylacetate (3.0 mmol, 1.0 equiv.) in 3.0 mL of dry THF was added dropwise, and reaction mixture was allowed to warm to room temperature. After 18 hours, the reactives were quenched with 10 mL of a saturated NH₄Cl solution and 10 mL of water. The resulting solution was extracted with 3 \times 10 mL of ethyl acetate and the combined extracts were washed with brine. The resulting organic phase was dried over Na₂SO₄, filtered and the filtrate was concentrated *in vacuo*. Purification by MPLC (20:80 EtOAc: hexanes) afforded the product as light yellow oil (0.212 g, 31%). The spectral data of the product matched that reported by Glorius and co-workers:⁷³ ¹H NMR (500 MHz, CDCl₃) δ 8.57 (d, *J* = 4.8 Hz, 1H), 7.67 (t, *J* = 7.7 Hz, 1H), 7.32 (m, 6H), 7.21 (m, 1H), 5.17 (s, 2H), 3.93 (s, 2H); ¹³C NMR (125 MHz, CDCl₃) δ 170.3 (C), 154.1 (C), 149.2 (CH), 137.0 (CH), 135.7 (C), 128.5 (CH), 128.3 (CH), 128.2 (CH), 124.1 (CH), 122.3 (CH), 66.8 (CH₂), 43.6 (CH₂). ATR-FTIR (thin film): 3033, 1732, 1591, 1150 cm^{−1}.



***tert*-Butyl 2-(pyridin-2-yl)acetate s3b.** To a cold stirred solution of diisopropylamine (420 μ L, 3.0 mmol, 1.0 equiv) in 0.6 mL of dry THF was added 1.2 mL of a 2.5 M solution of *n*-BuLi in hexanes (3.0 mmol, 1.0 equiv.) at −78 °C. After 30 minutes, 299 mg of methyl 2-pyridylacetate (3.21 mmol, 1.07 equiv) in 0.6 mL of dry THF was added dropwise. After 1 hour, 720 mg of di-*tert*-butyl dicarbonate (3.3 mmol, 1.1 equiv) was added and the reaction mixture was allowed to warm to

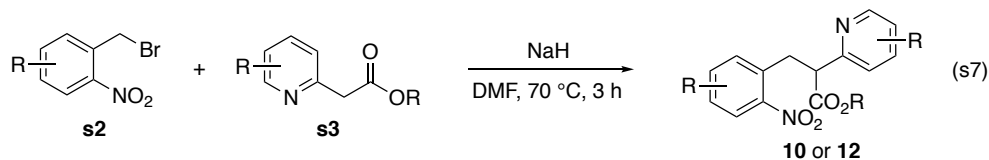
room temperature. After 2 hours, the reactives were quenched with 10 mL of a saturated NH_4Cl solution and 10 mL of water. The resulting solution was extracted with 3×10 mL of ethyl acetate and the combined extracts were washed with brine. The resulting organic phase was dried over Na_2SO_4 , filtered and the filtrate was concentrated *in vacuo*. Purification by MPLC (10:90 EtOAc:hexanes) afforded the product as light yellow oil (0.120 g, 21%). The spectral data of the product matched that reported by Glorius and co-workers: ^1H NMR (500 MHz, CDCl_3) δ 8.54 (d, J = 4.8 Hz, 1H), 7.66 (t, J = 8.2 Hz, 1H), 7.30 (d, J = 7.8 Hz, 1H), 7.19 (m, 1H), 3.78 (s, 2H), 1.44 (s, 9H); ^{13}C NMR (125 MHz, CDCl_3) δ 169.8 (C), 154.8 (C), 149.0 (CH), 136.9 (CH), 124.0 (CH), 122.0 (CH), 81.3 (C), 44.8 (CH_2), 28.0 (CH_3). ATR-FTIR (thin film): 2978, 1727, 1591, 1393 cm^{-1} .



Ethyl 2-(4,6-dimethylpyridin-2-yl)acetate s3c.⁷⁵ To a cold solution of 2,4,6-trimethyl pyridine (0.363 g, 3.00 mmol, 1.0 equiv) in 6 mL of THF was added a 1.95 mL of a 2.0 M solution of lithium diisopropyl amide (3.90 mmol, 1.3 equiv) in THF at -78°C . After 20 minutes, 0.330 mL of diethyl carbonate (3.30 mmol, 1.3 equiv) was added and the solution was allowed to warm to room temperature. After 2 hours, the reactives were quenched with 10 mL of a saturated aq soln of NH_4Cl . The resulting solution was extracted with 3×10 mL of ethyl acetate and the combined extracts were washed with brine. The resulting organic phase was dried over Na_2SO_4 , filtered and the filtrate was concentrated *in vacuo*. The crude product was purified by azeotropic distillation using heptane as the entrainer to afford the product as a yellow oil (0.193 g, 33%), which was

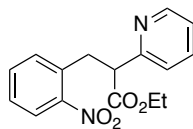
used in the subsequent step without further purification. The spectral data of **s3c** matched that reported by Compagnon and co-workers:⁷⁵ ¹H NMR (500 MHz, CDCl₃) δ 6.88 (s, 1H), 6.83 (s, 1H), 4.13 (q, *J* = 7.5 Hz, 2H), 3.72 (s, 2H), 2.45 (s, 3H), 2.25 (s, 3H), 1.22 (t, *J* = 7.0 Hz, 3H); ¹³C NMR (125 MHz, CDCl₃) δ 171.0 (C), 157.8 (C), 153.3 (C), 147.9 (C), 122.7 (CH), 121.7 (CH), 60.9 (CH₂), 43.8 (CH₂), 24.1 (CH₃), 20.8 (CH₃), 14.2 (CH₃); ATR-FTIR (thin film): 2980, 2923, 1732, 1151 cm⁻¹.

B. General Procedure for Synthesis of Substituted Ethyl-3-(2-nitrophenyl)-2-(pyridine-2-yl)propanoates.



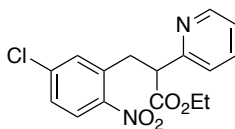
To a solution of 0.048 g of sodium hydride (1.20 mmol, 1.2 equiv) in 6 mL of DMF was slowly added 0.165 g of ethyl-2-pyridyl acetate (1.00 mmol, 1.0 equiv). The reaction mixture was heated to 70 °C. After 15 minutes, the solution was cooled to 0 °C, and 0.216 g of 2-nitrobenzyl bromide (1.00 mmol, 1.0 equiv.) was added. The reaction mixture was heated to 70 °C. After 3 h, the reaction mixture was cooled to room temperature and the reactives were quenched with 10 mL of H₂O. The solution was extracted with 3 × 15 mL of ethyl acetate, and the combined extracts were washed with 2 × 10 mL of brine. The resulting organic phase was dried over Na₂SO₄, filtered and the filtrate was concentrated *in vacuo*. Purification by MPLC (10:90 to 20:80 EtOAc:hexanes) afforded the product.

C. Characterization Data.



10a

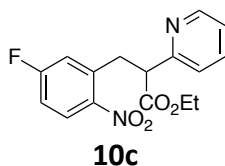
Ethyl 3-(2-nitrophenyl)-2-(pyridin-2-yl)propanoate 10a. The general procedure was followed by using 0.330 g of ethyl 2-pyridylacetate (2.0 mmol), 0.096 g of sodium hydride (2.40 mmol, 60 wt % in oil), 0.432 g of 2-nitrobenzyl bromide (2.00 mmol) in 12 mL of dry DMF. Purification by MPLC (25:75 EtOAc:hexanes) afforded the product as a light yellow oil (0.542 g, 90%): ^1H NMR (500 MHz, CDCl_3) δ 8.59 (d, J = 4.0 Hz, 1H), 7.93 (d, J = 7.7 Hz, 1H), 7.59 (td, J = 11.5, 1.8 Hz, 1H), 7.39 (t, J = 7.5 Hz, 1H), 7.34 – 7.31 (m, 1H), 7.24 (d, J = 1.0 Hz, 1H), 7.21 (d, J = 7.3 Hz, 1H), 7.18 – 7.15 (m, 1H), 4.25 (t, J = 7.5 Hz, 1H), 4.11 (q, J = 7.2 Hz, 2H), 3.75 (dd, J = 13.7, 8.0 Hz, 1H), 3.52 (dd, J = 13.6, 6.9 Hz, 1H), 1.12 (t, J = 7.2 Hz, 3H); ^{13}C NMR (125 MHz, CDCl_3) δ 171.8 (C), 157.8 (C), 149.6 (CH), 149.5 (C), 136.8 (CH), 134.3 (C), 133.3 (CH), 132.8 (CH), 127.7 (CH), 124.9 (CH), 123.5 (CH), 122.4 (CH), 61.1 (CH_2), 54.0 (CH), 35.3 (CH_2), 14.0 (CH_3). ATR-FTIR (thin film): 2981, 1730, 1522, 1344, 1289, 1214, 1160 cm^{-1} . HRMS (ESI) m/z calculated for $\text{C}_{16}\text{H}_{16}\text{N}_2\text{O}_4$ ($\text{M}+\text{H}$) $^+$: 301.1188; found 301.1183.



10b

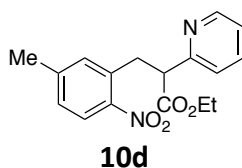
Ethyl 3-(5-chloro-2-nitrophenyl)-2-(pyridin-2-yl)propanoate 10b. The general procedure was followed by using 0.330 g of ethyl 2-pyridylacetate (2.0 mmol), 0.0960 g of sodium hydride (2.40 mmol, 60 wt % in oil), 0.500 g of 1-(bromomethyl)-5-chloro-2-nitrobenzene (2.00 mmol) in 12 mL

of dry DMF. Purification by MPLC (25:75 EtOAc:hexanes) afforded the product as a light yellow oil (0.260 g, 39%): ^1H NMR (500 MHz, CDCl_3) δ 8.5 (d, J = 3.5 Hz, 1H), 7.90 (d, J = 4.0 Hz, 1H), 7.62 (td, J = 7.5, 1.5 Hz, 1H), 7.37 (dd, J = 9.0, 2.0 Hz, 1H), 7.25 – 7.17 (m, 3H), 4.21 (t, J = 7.0 Hz, 1H), 4.12 (dq, J = 4.5, 2.5 Hz, 2H), 3.72 (dd, J = 13.5, 8.0 Hz, 1H), 3.50 (dd, J = 13.5, 7.0 Hz, 1H), 1.14 (t, J = 7.0 Hz, 3H); ^{13}C NMR (125 MHz, CDCl_3) δ 171.6, 157.4, 149.6, 147.6, 139.2, 136.9, 136.4, 133.2, 127.9, 126.4, 123.5, 122.6, 61.3, 53.7, 35.1, 14.1. ATR-FTIR (thin film): 2970, 1733, 1695, 1524, 1471, 1436, 1173 cm^{-1} . HRMS (ESI) m/z calculated for $\text{C}_{16}\text{H}_{15}\text{ClN}_2\text{O}_4$ ($\text{M}+\text{H}$) $^+$: 335.0799; found 335.0791.

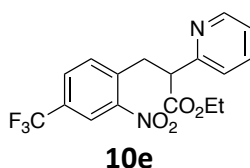


Ethyl 3-(5-fluoro-2-nitrophenyl)-2-(pyridin-2-yl)propanoate 10c. The general procedure was followed by using 0.330 g of ethyl 2-pyridylacetate (2.00 mmol), 0.096 g of sodium hydride (2.40 mmol, 60 wt % in oil), 0.500 g of 1-(bromomethyl)-4-fluoro-2-nitrobenzene (2.00 mmol) in 12 mL of dry DMF. Purification by MPLC (25:75 EtOAc:hexanes) afforded the product as a light yellow oil (0.243 g, 36%): ^1H NMR (500 MHz, CDCl_3) δ 8.57 – 8.56 (m, 1H), 8.01 (dd, J = 5.5, 3.5 Hz, 1H), 7.61 (dt, J = 7.5, 1.0 Hz, 1H), 7.22 (d, J = 7.5 Hz, 1H), 7.23 – 7.16 (m, 1H), 7.01 – 6.95 (m, 2H), 4.23 (t, J = 7.5 Hz, 1H), 4.11 (q, J = 7.0 Hz, 2H), 3.74 (dd, J = 13.5, 8.0 Hz, 1H), 3.52 (dd, J = 13.5, 7.0 Hz, 1H), 1.13 (t, J = 7.5 Hz, 3H); ^{13}C NMR (125 MHz, CDCl_3) δ 171.6 (C), 164.3 (d, J_{CF} = 254.6 Hz, C), 157.4 (C), 149.6 (CH), 145.4 (C), 138 (d, J_{CF} = 9.25, C), 136.9 (CH), 127.8 (d, J_{CF} = 10.6 Hz, CH), 123.5 (CH), 122.3 (CH), 120.0 (d, J_{CF} = 23.8 Hz, CH), 114.8 (d, J_{CF} = 22.3 Hz, CH), 61.2 (CH_2), 53.7 (CH),

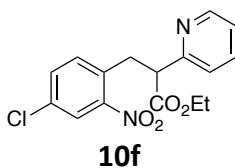
35.4 (CH₂) 14.0 (CH₃); ¹⁹F NMR (376 MHz, CDCl₃) δ –104.5. ATR-FTIR (thin film): 3078, 1744, 1711, 1533, 1359, 1219 cm⁻¹. HRMS (ESI) m/z calculated for C₁₆H₁₅FN₂O₄ (M+H)⁺: 319.1094; found 319.1088.



Ethyl 3-(5-methyl-2-nitrophenyl)-2-(pyridin-2-yl)propanoate 10d. The general procedure was followed by using 0.160 g of ethyl 2-pyridylacetate (0.970 mmol), 0.046 g of sodium hydride (1.16 mmol, 60 wt % in oil), 0.223 g of 2-(bromomethyl)-4-methyl-1-nitrobenzene (0.970 mmol) in 6.0 mL of dry DMF. Purification by MPLC (25:75 EtOAc:hexanes) afforded the product as colorless oil (0.198 g, 65%): ¹H NMR (500 MHz, CDCl₃) δ 8.58 (d, *J* = 3.3 Hz, 1H), 7.88 (d, *J* = 8.5 Hz, 1H), 7.60 (t, *J* = 7.6 Hz, 1H), 7.21 (d, *J* = 7.7 Hz, 1H), 7.16 (t, *J* = 6.1 Hz, 1H), 7.11 (d, *J* = 8.1 Hz, 1H), 7.03 (s, 1H), 4.23 (t, *J* = 7.3 Hz, 1H), 4.11 (q, *J* = 7.0 Hz, 2H), 3.73 (dd, *J* = 13.4, 8.3 Hz, 1H), 3.50 (dd, *J* = 13.4, 6.6 Hz, 1H), 2.29 (s, 3H), 1.13 (t, *J* = 7.2 Hz, 3H); ¹³C NMR (125 MHz, CDCl₃) δ 171.9 (C), 158.0 (C), 149.6 (CH), 147.0 (C), 144.1 (C), 136.7 (CH), 134.4 (C), 133.9 (CH), 128.2 (CH), 125.2 (CH), 123.4 (CH), 122.3 (CH), 61.1 (CH₂), 54.0 (CH), 35.5 (CH₂), 21.3 (CH₃), 14.1 (CH₃). ATR-FTIR (thin film): 2981, 1731, 1588, 1517, 1216, 1173, 1159 cm⁻¹. HRMS (ESI) m/z calculated for C₁₇H₁₈N₂O₄ (M+H)⁺: 315.1345; found 315.1341.

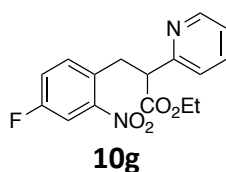


Ethyl 3-(2-nitro-4-(trifluoromethyl)phenyl)-2-(pyridin-2-yl)propanoate 10e. The general procedure was followed using 0.117 g of ethyl 2-pyridylacetate (0.710 mmol), 0.025 g of sodium hydride (0.710 mmol, 60 wt % in oil), 0.200 g of 1-(bromomethyl)-2-nitro-4-(trifluoromethyl)benzene (0.710 mmol) in 5 mL of dry DMF. Purification by MPLC (25:75 EtOAc:hexanes) afforded the product as a yellow oil (0.040 g, 15%): ^1H NMR (500 MHz, CDCl_3) δ 8.58 (d, J = 3.5 Hz, 1H), 8.19 (s, 1H), 7.64 (t, J = 8.0 Hz, 2H), 7.45 (d, J = 8.0 Hz, 1H), 7.23 – 7.18 (m, 2H), 4.11 (q, J = 7.0 Hz, 2H), 3.80 (dd, J = 13.5, 8.0 Hz, 1H), 3.58 (dd, J = 13.5, 7.0 Hz, 1H), 1.13 (t, J = 7.0 Hz, 3H); ^{13}C NMR (125 MHz, CDCl_3) δ 171.5 (C), 157.2 (C), 149.7 (CH), 149.4 (CH), 138.4 (CH), 136.9 (C), 134.4 (C), 130.4 (q, J_{CF} = 25.0 Hz, C), 129.1 (CH), 123.5 (CH), 122.8 (q, J_{CF} = 270.1 Hz, C), 122.6 (CH), 122.2 (d, J_{CF} = 3.6 Hz, CH), 61.3 (CH_2), 53.7 (CH), 35.0 (CH_2), 14.0 (CH_3); ^{19}F NMR (376 MHz, CDCl_3) δ –63.2. ATR-FTIR (thin film): 2984, 1732, 1538, 1323, 1129, 1088 cm^{-1} . HRMS (ESI) m/z calculated for $\text{C}_{17}\text{H}_{15}\text{F}_3\text{N}_2\text{O}_4$ ($\text{M}+\text{H}$) $^+$: 369.1062; found 369.1058.

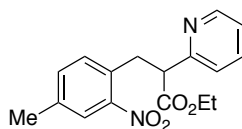


Ethyl 3-(4-chloro-2-nitrophenyl)-2-(pyridin-2-yl)propanoate 10f. The general procedure was followed by using 0.330 g of ethyl 2-pyridylacetate (2.00 mmol), 0.096 g of sodium hydride (2.40 mmol, 60 wt % in oil), 0.500 g of 1-(bromomethyl)-4-chloro-2-nitrobenzene (2.00 mmol) in 12 mL of dry DMF. Purification by MPLC (25:75 EtOAc:hexanes) afforded the product as a light yellow oil (0.243 g, 36%): ^1H NMR (500 MHz, CDCl_3) δ 8.5 (d, J = 4.0 Hz, 1H), 7.90 (d, J = 2.0 Hz, 1H), 7.59 (td, J = 7.5, 1.0 Hz, 1H), 7.37 (dd, J = 8.5, 2.0 Hz, 1H), 7.20 – 7.15 (m, 3H), 7.21 (d, J = 7.3 Hz, 1H),

4.19 (t, $J = 7.5$ Hz, 1H), 4.08 (q, $J = 7.0$ Hz, 2H), 3.69 (dd, $J = 13.5, 8.0$ Hz, 1H), 3.46 (dd, $J = 13.5, 7.0$ Hz, 1H), 1.10 (t, $J = 7.0$ Hz, 3H); ^{13}C NMR (125 MHz, CDCl_3) δ 171.6 (C), 157.4 (C), 149.6 (CH), 136.9 (CH), 134.5 (C), 133.2 (CH), 132.8 (C), 127.8 (CH), 124.9 (CH), 123.5 (CH), 122.5 (CH), 61.1 (CH_2), 53.8 (CH), 34.7 (CH_2), 14.0 (CH_3). ATR-FTIR (thin film): 2981, 1730, 1589, 1346, 1145, 1047, cm^{-1} . HRMS (ESI) m/z calculated for $\text{C}_{16}\text{H}_{15}\text{ClN}_2\text{O}_4$ ($\text{M}+\text{H}$) $^+$: 335.0799; found 335.0799.

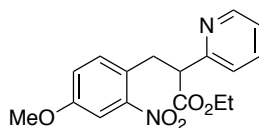


Ethyl 3-(4-fluoro-2-nitrophenyl)-2-(pyridin-2-yl)propanoate 10g. The general procedure was followed by using 0.330 g of ethyl 2-pyridylacetate (2.00 mmol), 0.0960 g of sodium hydride (2.40 mmol, 60 wt % in oil), 0.500 g of 1-(bromomethyl)-4-fluoro-2-nitrobenzene (2.00 mmol) in 12 mL of dry DMF. Purification by MPLC (25:75 EtOAc:hexanes) afforded the product as a light yellow oil (0.243 g, 36%): ^1H NMR (500 MHz, CDCl_3) δ 8.58 (d, $J = 4.0$ Hz, 1H), 7.67 (dd, $J = 8.5, 2.5$ Hz, 1H), 7.62 (t, $J = 8.0$ Hz, 1H), 7.28 – 7.27 (m, 1H), 7.22 – 7.17 (m, 2H), 7.15 – 7.11 (m, 1H), 4.21 (t, $J = 7.0$ Hz, 1H), 4.15 (q, $J = 7.0$ Hz, 2H), 3.72 (dd, $J = 14.0, 8.5$ Hz, 1H), 3.49 (dd, $J = 14.0, 7.0$ Hz, 1H), 1.13 (t, $J = 7.0$ Hz, 3H); ^{13}C NMR (125 MHz, CDCl_3) δ 171.7 (C), 161.8 (C), 159.8 (C), 157.5 (C), 149.6 (CH), 137.0 (CH), 135.0 (d, $J_{\text{CF}} = 7.4$ Hz, CH), 130.2 (d, $J_{\text{CF}} = 3.8$ Hz, C), 123.5 (CH), 122.5 (CH), 120.2 (d, $J_{\text{CF}} = 20.8$ Hz, CH), 112.3 (d, $J_{\text{CF}} = 26.3$ Hz, CH), 61.2 (CH_2), 53.9 (CH), 34.7 (CH_2), 14.0 (CH_3); ^{19}F NMR (376 MHz, CDCl_3) δ -110.6. ATR-FTIR (thin film): 2983, 1731, 1586, 1525, 1343 cm^{-1} . HRMS (ESI) m/z calculated for $\text{C}_{16}\text{H}_{15}\text{FN}_2\text{O}_4$ ($\text{M}+\text{H}$) $^+$: 319.1094; found 319.1088.



10h

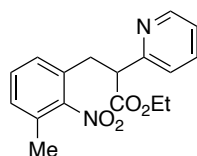
Ethyl 3-(4-methyl-2-nitrophenyl)-2-(pyridin-2-yl)propanoate 10h. The general procedure was followed by using 0.358 g of ethyl 2-pyridylacetate (0.217 mmol), 0.113 g of sodium hydride (2.82 mmol, 60 wt % in oil), 0.500 g of 2-(bromomethyl)-5-methyl-1-nitrobenzene (0.217 mmol) in 6.0 mL of dry DMF. Purification by MPLC (20:80 EtOAc:hexanes) afforded the product as a yellow oil (0.260 g, 41%): ^1H NMR (500 MHz, CDCl_3) δ 8.56 (dd, J = 3.0, 1.0 Hz, 1H), 7.73 (s, 1H), 7.60 (dt, J = 6.0, 1.0 Hz, 1H), 7.19 (t, J = 7.5 Hz, 2H), 7.17 – 7.14 (m, 1H), 7.11 (d, J = 8.0 Hz, 1H), 4.22 (t, J = 7.0 Hz, 1H), 4.10 (q, J = 7.0 Hz, 2H), 3.69 (dd, J = 13.5, 8.0 Hz, 1H), 3.45 (dd, J = 14.0, 7.0 Hz, 1H), 2.34 (s, 3H), 1.17 (t, J = 7.0 Hz, 3H); ^{13}C NMR (125 MHz, CDCl_3) δ 171.9 (C), 157.9 (C), 149.6 (CH), 149.2 (C), 138.0 (C), 136.8 (CH), 133.7 (C), 133.1 (CH), 131.1 (CH), 125.1 (CH), 123.4 (CH), 122.3 (CH), 61.1 (CH_2), 54.1 (CH), 35.0 (CH_2), 20.7 (CH_3), 14.1 (CH_3). ATR-FTIR (thin film): 2981, 1734, 1589, 1570, 1215 cm^{-1} . HRMS (ESI) m/z calculated for $\text{C}_{17}\text{H}_{18}\text{N}_2\text{O}_4$ ($\text{M}+\text{H}$) $^+$: 315.1345; found 315.1341.



10i

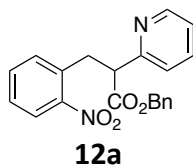
Ethyl 3-(4-methoxy-2-nitrophenyl)-2-(pyridin-2-yl)propanoate 10i. The general procedure was followed by using 0.380 g of ethyl 2-pyridylacetate (2.3 mmol), 0.112 g of sodium hydride (2.8 mmol, 60 wt % in oil), 0.598 g of 1-(bromomethyl)-4-methoxy-2-nitrobenzene (2.3 mmol) in 14.0 mL of dry THF. Purification by MPLC (25:75 EtOAc:hexane) afforded the product as a brown oil

(0.235 g, 31%): ^1H NMR (500 MHz, CDCl_3) δ 8.57 (d, J = 4.6 Hz, 1H), 7.61 (t, J = 7.7 Hz, 1H), 7.45 (d, J = 2.8 Hz, 1H), 7.23 (m, 1H), 7.17 (m, 2H), 6.94 (m, 1H), 4.24 (t, J = 7.6 Hz, 1H), 4.11 (q, J = 7.1 Hz, 2H), 3.81 (s, 3H), 3.67 (dd, J = 13.8, 8.1 Hz, 1H), 3.44 (dd, J = 13.6, 7.0 Hz, 1H), 1.13 (t, J = 7.1 Hz, 3H); ^{13}C NMR (125 MHz, CDCl_3) δ 171.9 (C), 158.6 (C), 157.8 (C), 149.7 (C), 149.3 (CH), 137.0 (CH), 134.2 (CH), 126.1 (C), 123.6 (CH), 122.4 (CH), 119.6 (CH), 109.4 (CH), 61.1 (CH_2), 55.7 (CH_3), 54.0 (CH), 34.8 (CH_2), 14.1 (CH_3). ATR-FTIR (thin film): 2979, 1730, 1589, 1249, 1033 cm^{-1} . HRMS (ESI) m/z calculated for $\text{C}_{17}\text{H}_{18}\text{N}_2\text{O}_5$ ($\text{M}+\text{H}$) $^+$: 331.1294; found 331.1293.

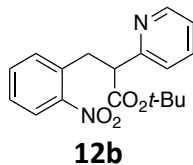


10j

Ethyl 3-(3-methyl-2-nitrophenyl)-2-(pyridin-2-yl)propanoate 10j. The general procedure was followed by using 0.358 g of ethyl 2-pyridylacetate (2.17 mmol), 0.104 g of sodium hydride (2.60 mmol, 60 wt % in oil), 0.500 g of 1-(bromomethyl)-3-methyl-2-nitrobenzene (2.17 mmol) in 10 mL of dry DMF. Purification by MPLC (25:75 EtOAc:hexanes) afforded the product as a light yellow oil (0.134 g, 35%): ^1H NMR (500 MHz, CDCl_3) δ 8.56 (d, J = 4.0 Hz, 1H), 7.58 (t, J = 7.5 Hz, 1H), 7.15 – 7.13 (m, 3H), 7.10 (d, J = 5.0 Hz, 1H), 6.98 (d, J = 5.0 Hz, 1H), 4.11 (q, J = 6.5 Hz, 2H), 3.45 (dd, J = 14.0, 8.0 Hz, 2H), 3.18 (dd, J = 14.5, 7.5 Hz, 1H), 2.28 (s, 3H), 1.13 (t, J = 7.0 Hz, 3H); ^{13}C NMR (125 MHz, CDCl_3) δ 171.7 (C), 157.5 (C), 152.0 (C), 149.6 (CH), 136.8 (CH), 130.5 (C), 129.8 (CH), 129.7 (C), 129.6 (CH), 129.0 (CH), 123.5 (CH), 122.4 (CH), 61.2 (CH_2), 54.1 (CH_3), 33.5 (CH_2), 17.5 (CH), 14.0 (CH_3). ATR-FTIR (thin film): 2982, 1731, 1589, 1523, 1158 cm^{-1} . HRMS (ESI) m/z calculated for $\text{C}_{17}\text{H}_{18}\text{N}_2\text{O}_4$ ($\text{M}+\text{H}$) $^+$: 315.1345; found 315.1341.

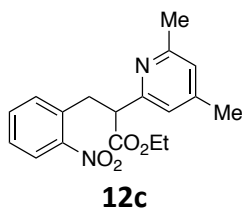


Benzyl 3-(2-nitrophenyl)-2-(pyridin-2-yl)propanoate 12a. The general procedure was followed by using 0.200 g of benzyl 2-pyridylacetate (0.880 mmol), 0.0430 g of sodium hydride (1.06 mmol, 60 wt % in oil), 0.190 g of 2-nitrobenzyl bromide (0.880 mmol) in 6.0 mL of dry DMF. Purification by MPLC (25:75 EtOAc:hexanes) afforded the product as a light yellow oil (0.123 g, 39%): ^1H NMR (500 MHz, CDCl_3) δ 8.58 (d, J = 4.8 Hz, 1H), 7.93 (d, J = 7.7 Hz, 1H), 7.59 (t, J = 7.6 Hz, 1H), 7.35 – 7.14 (m, 10H), 5.11 (s, 2H), 4.34 (t, J = 7.3 Hz, 1H), 3.78 (dd, J = 13.6, 7.9 Hz, 1H), 3.55 (dd, J = 13.7, 6.7 Hz, 1H); ^{13}C NMR (125 MHz, CDCl_3) δ 171.7 (C), 157.6 (C), 149.6 (CH), 149.4 (C), 136.9 (CH), 135.7 (C), 134.1 (C), 133.3 (CH), 132.9 (CH), 128.4 (CH), 128.1 (CH), 127.9 (CH), 127.7 (CH), 124.9 (CH), 123.6 (CH), 122.5 (CH), 66.7 (CH_2), 54.0 (CH), 35.3 (CH_2). ATR-FTIR (thin film): 3065, 1733, 1522, 1434, 1344, 1213 cm^{-1} . HRMS (ESI) m/z calculated for $\text{C}_{21}\text{H}_{18}\text{N}_2\text{O}_4$ ($\text{M}+\text{H}$) $^+$: 363.1345; found 363.1340.



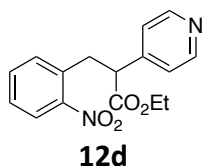
tert-Butyl 3-(2-nitrophenyl)-2-(pyridin-2-yl)propanoate 12b. The general procedure was followed by using 0.0780 g of *tert*-butyl 2-pyridylacetate (0.400 mmol), 0.0190 g of sodium hydride (0.480 mmol, 60 wt % in oil), 0.0860 g of 2-nitrobenzyl bromide (0.400 mmol) in 2.4 mL

of dry DMF. Purification by MPLC (25:75 EtOAc:hexanes) afforded the product as a light yellow oil (0.0880 g, 67%): ^1H NMR (500 MHz, CDCl_3) δ 8.56 (d, J = 4.4 Hz, 1H), 7.90 (d, J = 8.1 Hz, 1H), 7.59 (t, J = 7.6 Hz, 1H), 7.38 (t, J = 7.4 Hz, 1H), 7.31 (t, J = 8.1 Hz, 1H), 7.26 (d, J = 7.0 Hz, 1H), 7.19 (d, J = 9.0 Hz, 1H), 7.16 – 7.14 (m, 1H), 4.16 (t, J = 7.5 Hz, 1H), 3.70 (dd, J = 13.8, 8.1 Hz, 1H), 3.50 (dd, J = 13.6, 7.0 Hz, 1H), 1.31 (s, 9H); ^{13}C NMR (125 MHz, CDCl_3) δ 170.9 (C), 158.1 (C), 149.5 (C), 149.3 (CH), 136.8 (CH), 134.4 (C), 133.2 (CH), 132.7 (CH), 127.5 (CH), 124.8 (CH), 123.3 (CH), 122.2 (CH), 81.3 (C), 54.5 (CH), 35.1 (CH_2), 27.8 (CH_3). ATR-FTIR (thin film): 2978, 1724, 1522, 1471, 1434, 1366, cm^{-1} . HRMS (ESI) m/z calculated for $\text{C}_{18}\text{H}_{20}\text{N}_2\text{O}_4$ ($\text{M}+\text{H}$) $^+$: 329.1501; found 329.1494.

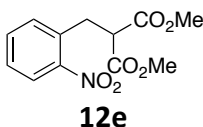


Ethyl 2-(4,6-dimethylpyridin-2-yl)-3-(2-nitrophenyl)propanoate 12c. The general procedure was followed by using 0.100 g of **s3a** (0.052 mmol), 0.031 g of sodium hydride (0.78 mmol, 60 wt % in oil), 0.112 g of 2-nitrobenzyl bromide (0.052 mmol) in 5 mL of dry DMF. Purification by HPLC (20:80 EtOAc:hexanes) afforded the product as a yellow oil (0.070 g, 41%): ^1H NMR (500 MHz, CDCl_3) δ 7.91 (d, J = 7.8 Hz, 1H), 7.41 (t, J = 7.0 Hz, 1H), 7.31 (q, J = 5.5 Hz, 2H), 6.84 (d, J = 7.5 Hz, 2H), 4.16 (t, J = 7.0 Hz, 1H), 4.09 (q, J = 7.0 Hz, 2H), 3.72 (dd, J = 13.5, 8.5 Hz, 1H), 3.52 (dd, J = 13.5, 7.0 Hz, 1H), 2.46 (s, 3H), 2.25 (s, 3H), 1.13 (t, J = 7.0 Hz, 3H); ^{13}C NMR (125 MHz, CDCl_3) δ 172.2 (C), 158.0 (C), 156.8 (C), 149.6 (C), 147.9 (C), 134.5 (C), 133.1 (CH), 132.7 (CH), 127.5 (CH), 124.8 (CH), 122.9 (CH), 120.9 (CH), 60.9 (CH_2), 53.9 (CH_3), 35.0 (CH_2), 24.3 (CH), 20.9 (CH_3), 14.0

(CH₃). ATR-FTIR (thin film): 2981, 1731, 1608, 1523, 1175 cm⁻¹. HRMS (ESI) m/z calculated for C₁₈H₂₀N₂O₄ (M+H)⁺: 329.1501; found 329.1494.

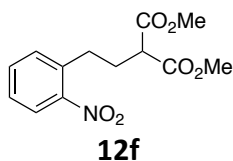


ethyl 3-(2-nitrophenyl)-2-(pyridin-4-yl)propanoate 12d. The general procedure was followed using 0.330 g of ethyl-4-pyridyl acetate (2.00 mmol), 0.096 g of sodium hydride (2.60 mmol, 60 wt % in oil), 0.432 g of 2-nitrobenzyl bromide (2.00 mmol) in 4 mL of DMF. Purification by MPLC (1:99 to 30:70 EtOAc:hexanes) afforded the product as a yellow oil (0.240 g, 41%): ¹H NMR (500 MHz, CDCl₃) δ 8.55 (d, *J* = 5.5 Hz, 2H), 7.99 (dd, *J* = 8.5, 1.0 Hz, 1H), 7.45 (td, *J* = 7.5, 1.5 Hz, 1H), 7.38 (td, *J* = 8.0, 1.0 Hz, 1H), 7.25 (d, *J* = 5.5 Hz, 2H), 7.22 – 7.21 (m, 1H), 4.11 – 4.05 (m, 2H), 4.03 (q, *J* = 3.0 Hz, 1H), 3.61 (dd, *J* = 13.5, 9.0 Hz, 1H), 3.32 (dd, *J* = 13.5, 6.0 Hz, 1H), 1.12 (t, *J* = 7.5 Hz, 3H); ¹³C NMR (125 MHz, CDCl₃) δ 171.8 (C), 150.2 (C), 149.9 (C), 149.2 (CH), 147.1 (CH), 133.3 (C), 133.2 (CH), 133.1 (CH), 128.2 (CH), 125.2 (CH), 123.1 (CH), 120.6 (CH), 61.4 (C), 51.4 (CH), 37.0 (CH₂), 14.0 (CH₃). ATR-FTIR (thin film): 2983, 1730, 1597, 1524, 1344, 908 cm⁻¹. HRMS (ESI) m/z calculated for C₁₆H₁₆N₂O₄ (M+H)⁺: 301.1888; found 301.1881.

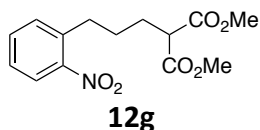


Dimethyl 2-(2-nitrobenzyl)malonate 12e.⁷⁶ The general procedure was followed by using 0.170 mL of dimethyl malonate (1.10 mmol), 0.0440 g of sodium hydride (1.10 mmol, 60 wt % in oil),

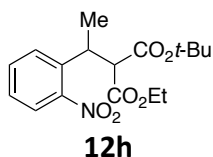
0.216 g of 2-nitrobenzyl bromide (1.00 mmol) in 4 mL of DMF. Purification by MPLC (3:97 to 10:90 EtOAc:hexanes) afforded the product as a light yellow solid (0.182 g, 68%). Malonate **12e** was previously reported by Pratt and co-workers:⁷⁶ mp 40 – 42 °C ¹H NMR (500 MHz, CDCl₃) δ 8.00 (d, *J* = 8.0 Hz, 1H), 7.53 (t, *J* = 7.5 Hz, 1H), 7.43 – 7.38 (m, 2H), 3.92 (t, *J* = 7.5 Hz, 1H), 3.70 (s, 6H), 3.51 (d, *J* = 7.5 Hz, 2H); ¹³C NMR (125 MHz, CDCl₃) δ 168.9 (C), 142.2 (C), 140.9 (C), 133.3 (CH), 133.0 (CH), 128.3 (CH), 125.3 (CH), 52.7 (CH₃), 52.2 (CH), 32.2 (CH₂). ATR-FTIR (thin film): 3001, 2956, 1740, 1715, 1522, 1435, 1344, 1216, 1142, 858, 787 cm⁻¹. HRMS (ESI) *m/z* calculated for C₁₃H₁₃NO₆Na (M+H)⁺: 291.0641, found: 298.0647.



Dimethyl 2-(2-nitrophenethyl)malonate 12f.⁷⁷ The general procedure was followed by using 0.170 mL of dimethyl malonate (1.10 mmol), 0.0440 g of sodium hydride (1.10 mmol, 60 wt % in oil), 0.230 g of 2-nitrophenethyl bromide (1.00 mmol) in 4 mL of DMF. Purification by MPLC (3:97 to 10:90 EtOAc:hexanes) afforded the product as a yellow liquid (0.211 g, 75%). Malonate **12f** was previously reported by Dale and Strobel:⁷⁷ ¹H NMR (500 MHz, CDCl₃) δ 7.92 (d, *J* = 8.5 Hz, 1H), 7.53 (t, *J* = 7.5 Hz, 1H), 7.36 (m, 2H), 3.75 (s, 6H), 3.45 (t, *J* = 7.5 Hz, 1H), 2.93 (t, *J* = 8.0 Hz, 2H), 2.26 (q, *J* = 7.5 Hz, 2H); ¹³C NMR (125 MHz, CDCl₃) δ 169.4 (C), 149.2 (C), 135.8 (C), 133.2 (CH), 132.1 (CH), 127.5 (CH), 124.9 (CH), 52.6 (CH₃), 51.2 (CH), 30.5 (CH₂), 29.6 (CH₂). ATR-FTIR (thin film): 2952, 2921, 2854, 1729, 1609, 1523, 1434, 1345, 1224, 1197, 1153, 859 cm⁻¹. HRMS (ESI) *m/z* calculated for C₁₃H₁₆NO₆ (M+H)⁺: 282.0978, found: 282.0974.



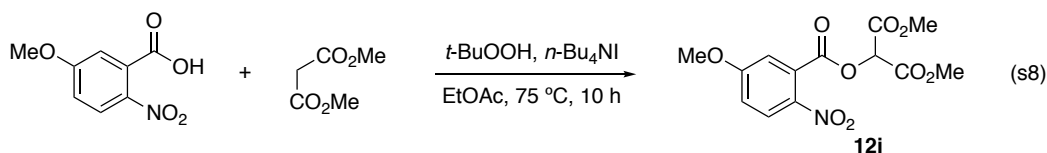
Dimethyl 2-(3-(2-nitrophenyl)propyl)malonate 12g. The general procedure was followed by using 0.1602 g of dimethyl malonate (1.00 mmol), 0.0400 g of sodium hydride (1.00 mmol, 60 wt % in oil), 0.2430 g of 1-(3-bromopropyl)-2-nitrobenzene (1.00 mmol) in 4.0 mL of DMF. Purification by MPLC (3:97 to 10:90 EtOAc:hexanes) afforded the product as a brown liquid (0.207 g, 70%): ^1H NMR (500 MHz, CDCl_3) δ 7.88 (d, J = 7.5 Hz, 1H), 7.50 (t, J = 7.5 Hz, 1H), 7.34 (t, J = 8.0 Hz, 2H), 3.73 (s, 6H), 3.40 (t, J = 7.5 Hz, 1H), 2.90 (t, J = 8.0 Hz, 2H), 2.00 (q, J = 7.5 Hz, 2H), 1.70 – 1.67 (m, 2H); ^{13}C NMR (125 MHz, CDCl_3) δ 169.6 (C), 149.3 (C), 136.6 (C), 132.9 (CH), 131.9 (CH), 121.2 (CH), 124.8 (CH), 52.6 (CH_3), 51.4 (CH), 32.6 (CH_2), 28.6 (CH_2), 28.3 (CH_2). ATR-FTIR (thin film): 2954, 2869, 1731, 1609, 1576, 1434, 1345, 1151 cm^{-1} . HRMS (ESI) m/z calculated for $\text{C}_{14}\text{H}_{18}\text{NO}_6$ ($\text{M}+\text{H}$) $^+$: 296.1134, found: 296.1130.



1-(*tert*-Butyl) 3-ethyl 2-(1-(2-nitrophenyl)ethyl)malonate 12h. The general procedure was followed using 0.188 g of *tert*-butyl ethyl malonate (1.00 mmol), 0.0400 g of sodium hydride (1.00 mmol, 60 wt % in oil), 0.230 g of 1-(1-bromoethyl)-2-nitrobenzene (1.00 mmol) in 4 mL of DMF. Purification by MPLC (1:99 to 5:95 EtOAc:hexanes) afforded the product, a 40:60 mixture of diastereomers, as a yellow liquid (0.160 g, 47%). Diagnostic peaks for the major diastereomer: ^1H

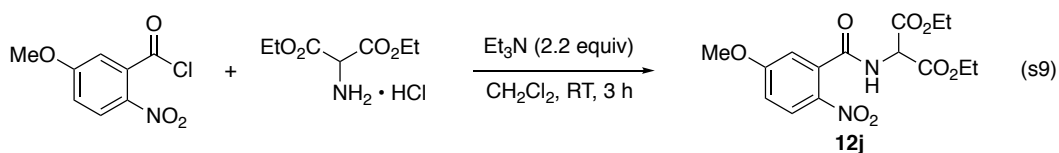
NMR (500 MHz, CDCl₃) δ 7.75 – 7.71 (m, 1H), 7.53 (q, J = 5.0 Hz, 1H), 7.40 (dd, J = 4.5, 3.0 Hz, 1H), 7.33 (q, J = 7.5 Hz, 1H), 4.26 – 4.19 (m, 2H), 4.02 – 3.90 (m, 1H), 3.61 (dd, J = 17.0, 6.5 Hz, 1H), 1.40 (d, J = 6.9 Hz, 1.2H), 1.39 (d, J = 6.8 Hz, 1.8H), 1.27 (t, J = 9.0 Hz, 2.1H), 1.15 (s, 5.7H), 1.02 (t, J = 7.0 Hz, 1.22H); ¹³C NMR (125 MHz, CDCl₃) δ 168.0 (C), 166.4 (C), 150.3 (C), 138.3 (C), 132.5 (CH), 128.4 (CH), 127.3 (CH), 124.2 (CH), 82.4 (C), 61.5 (CH₂), 59.5 (CH₃), 34.2 (CH), 27.4 (CH₃), 20.3 (CH), 14.1 (CH). ATR-FTIR (thin film): 2980, 1704, 1527, 1368, 1241 cm⁻¹. HRMS (ESI) m/z calculated for C₁₇H₂₃NO₆ (M+H)⁺: 360.1423; found 360.1417.

IV. Synthesis of Substrates 12i – 12m.



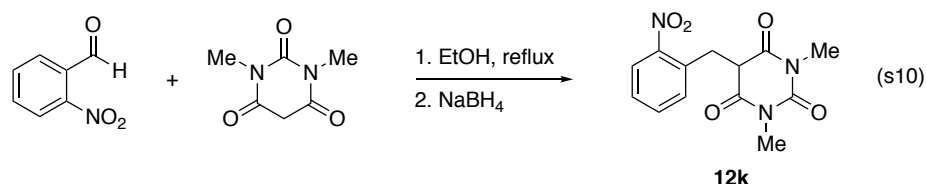
Dimethyl 2-((5-methoxy-2-nitrobenzoyl)oxy)malonate 12i. To a stirring mixture of 0.197 g of 5-methoxy-2-nitrobenzoic acid (1.00 mmol), 0.132 g of dimethyl malonate (1.00 mmol) and 0.037 g of Bu₄NI (0.10 mmol) in 5 mL of EtOAc was added 0.36 mL of *t*-butyl hydroperoxide (5.5 M in decane, 2.0 mmol). The resulting mixture was heated to 75 °C. After 10 h, the reaction mixture was cooled to room temperature and poured into 10 mL of a 1:1 mixture (v/v) of Na₂S₂O₃ and NaHCO₃. The mixture was extracted with 2 × 10 mL of ethyl acetate, and the combined organic phases were washed with 10 mL of brine. The resulting organic phase was dried over Na₂SO₄, filtered and the filtrate was concentrated *in vacuo*. Purification by MPLC (3:97 to 10:90 EtOAc:hexanes) afforded the product as a colorless oil (0.216 g, 54%): ¹H NMR (500 MHz, CDCl₃)

δ 8.08 (d, J = 9.0 Hz, 1H), 7.16 (d, J = 3.0 Hz, 1H), 7.04 (dd, J = 9.0 Hz, 3.0 Hz, 1H), 5.81 (s, 1H), 3.92 (s, 3H), 3.86 (s, 6H); ^{13}C NMR (125 MHz, CDCl_3) δ 164.5 (C), 164.2 (C), 163.6 (C), 139.6 (C), 129.6 (C), 126.8 (CH), 116.3 (CH), 114.6 (CH), 72.5 (CH), 56.3 (CH_3), 53.5 (CH_3). ATR-FTIR (thin film): 3285, 2918, 1744, 1639, 1605, 1582, 1520, 1485, cm^{-1} . HRMS (ESI) m/z calculated for $\text{C}_{13}\text{H}_{13}\text{NO}_9\text{Na}$ ($\text{M}+\text{Na}$) $^+$: 350.0488, found: 350.0493.

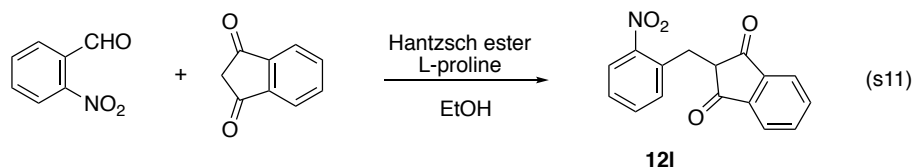


Diethyl 2-(5-methoxy-2-nitrobenzamido)malonate 12j. To a solution of 0.394 g of 5-methoxy-2-nitrobenzoic acid (2.00 mmol) in 5 mL of dichloromethane was added 0.254 g of oxalyl chloride (2.00 mmol, 1.0 equiv). After 15 h, the reaction mixture was concentrated *in vacuo*. To the resulting residue was added 5 mL of dichloromethane, followed by 0.423 g of diethyl aminomalonate hydrochloride (2.00 mmol, 1.0 equiv) and 0.61 mL of triethylamine (4.40 mmol, 2.2 equiv). After 3 h, the reactives were quenched with 10 mL of H_2O . The solution was extracted with 3×15 mL of ethyl acetate, and the combined extracts were washed with 2×10 mL of brine. The resulting organic phase was dried over Na_2SO_4 , filtered and the filtrate was concentrated *in vacuo*. Purification by MPLC (10:90 to 20:80 EtOAc:hexanes) afforded the product as a white solid (0.160 g, 23%): mp 118 – 120 $^\circ\text{C}$; ^1H NMR (500 MHz, CDCl_3) δ 8.16 – 8.14 (m, 1H), 7.02 – 7.00 (m, 2H), 6.78 (d, J = 6.5 Hz, 1H), 5.36 (d, J = 7.0 Hz, 1H), 4.36 – 4.30 (m, 4H), 3.92 (s, 3H), 1.34 (t, J = 7.0 Hz, 6H); ^{13}C NMR (125 MHz, CDCl_3) δ 166.0 (C), 165.9 (C), 163.8 (C), 134.4 (C), 127.3 (CH), 115.4 (CH), 114.0 (CH), 62.9 (CH_3), 56.9 (C), 56.3 (CH), 14.0 (CH_3) only peaks visible. ATR-FTIR (thin

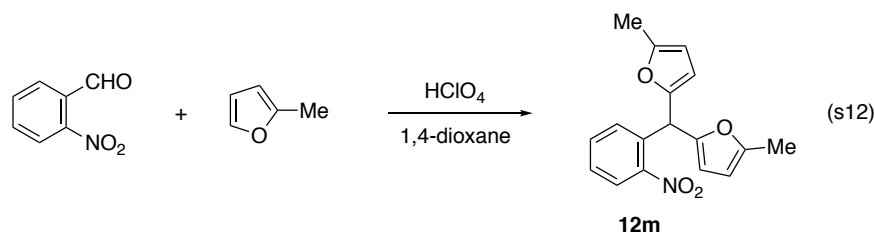
film): 3284, 2989, 1751, 1737, 1648, 1519 cm^{-1} . HRMS (ESI) m/z calculated for $\text{C}_{15}\text{H}_{18}\text{N}_2\text{O}_8$ ($\text{M}+\text{H}$) $^{+}$: 355.1141; found 355.1133.



1,3-Dimethyl-5-(2-nitrobenzyl)pyrimidine-2,4,6(1H,3H,5H)-trione 12k.⁷⁸ To a stirring mixture of 0.604 g of 2-nitrobenzaldehyde (4.00 mmol) in 10 mL of ethanol was added 0.624 g of 1,3-dimethylbarbituric acid (4.00 mmol). The mixture was heated to reflux. After 10 minutes, the reaction mixture was cooled to room temperature, and 0.304 g of sodium borohydride (8.00 mmol) was added. After 1 h, the reaction mixture was concentrated *in vacuo*, and the resulting residue was purified using MPLC (3:97 to 10:90 EtOAc:hexanes) to afford the product as a yellow solid (0.885 g, 76%). **12k** was previously reported by Terent'ev and co-workers:⁷⁸ mp 143 – 144 °C; ¹H NMR (500 MHz, CDCl₃) δ 7.97 (d, J = 8.0 Hz, 1.0 Hz, 1H), 7.58 (dt, J = 8.0 Hz, 1.5 Hz, 1H), 7.46 – 7.42 (m, 2H), 3.84 (t, J = 7.0 Hz, 1H), 3.72 (d, J = 7.0 Hz, 2H), 3.26 (s, 6H); ¹³C NMR (125 MHz, CDCl₃) δ 167.4 (C), 151.4 (C), 149.4 (C), 133.2 (CH), 132.9 (CH), 132.1 (C), 128.6 (CH), 125.2 (CH), 50.3 (CH), 33.0 (CH₂), 28.8 (CH₃). ATR-FTIR (thin film): 2864, 1745, 1694, 1660, 1518, 1447, 1415, 1378, 1332, 1273, 1089, 1042 cm^{-1} . HRMS (ESI) m/z calculated for $\text{C}_{13}\text{H}_{14}\text{N}_3\text{O}_5$ ($\text{M}+\text{H}$) $^{+}$: 292.0933, found: 292.0925.

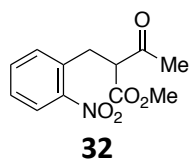


2-(2-Nitrobenzyl)-1H-indene-1,3(2H)-dione 12I.⁷⁹ To a mixture of 0.100 g of 2-nitrobenzaldehyde (0.66 mmol), 0.096 g of 1,3-indanedione (0.66 mmol), 0.167 g of Hantzsch ester (0.660 mmol) in 0.20 mL of ethanol was added 0.015 g of L-proline (0.13 mmol). After 3 h, the reaction mixture was concentrated *in vacuo*, and the resulting residue was purified by MPLC (3:97 to 10:90 EtOAc:hexanes) to afford the product as a yellow solid (0.133 g, 72%). **12I** was previously reported by Arens and co-workers:⁷⁹ mp (dec) 156 – 158 °C; ¹H NMR (500 MHz, CDCl₃) δ 8.02 (dd, *J* = 8.0 Hz, 1.0 Hz, 1H), 7.97 – 7.95 (m, 2H), 7.85 – 7.83 (m, 2H), 7.56 (dt, *J* = 7.5 Hz, 1.0 Hz, 1H), 7.50 (dd, *J* = 8.0 Hz, 1.5 Hz, 1H), 7.42 (dt, *J* = 8.5 Hz, 1.0 Hz, 1H), 3.52 (d, *J* = 7.5 Hz, 2H), 3.46 (dd, *J* = 8.5 Hz, 7.5 Hz, 1H); ¹³C NMR (125 MHz, CDCl₃) δ 198.9 (C), 149.4 (C), 141.9 (CH), 135.8 (CH), 133.2 (C), 133.1 (CH), 128.1 (CH), 125.1 (CH), 123.4 (CH), 53.4 (CH), 30.0 (CH₂), only visible peaks. ATR-FTIR (thin film): 3072, 2848, 1743, 1698, 1590, 1577, 1522, 1403, 1353, 1332, 1298, 1271, 1208, 1183, 1054 cm⁻¹. HRMS (ESI) *m/z* calculated for C₁₆H₁₂NO₄ (M+H)⁺: 282.0766, found: 282.0758.



5,5'-((2-Nitrophenyl)methylene)bis(2-methylfuran) 12m.⁸⁰ To a solution of 0.151 g of 2-nitrobenzaldehyde (1.0 mmol) and 0.164 g of 2-methylfuran (2.0 mmol) in 4 mL of 1,4-dioxane was added 0.060 mL of a 70% aq soln of HClO₄. The reaction mixture was heated to 70 °C. After

1 h, the reaction mixture was cooled to room temperature and then poured into 20 mL of cold water. The resulting mixture was extracted with 2 × 10 mL of ethyl acetate, and the combined organic phases were washed with 10 mL of brine. The resulting organic phase was dried over Na₂SO₄, filtered and the filtrate was concentrated *in vacuo*. The resulting residue was purified by MPLC (3:97 to 10:90 EtOAc:hexanes) to afford the product as a brown solid (0.214 g, 72%). Difuran **12m** was previously reported by Jones and McKinley:⁸⁰ mp 78 – 80 °C; ¹H NMR (500 MHz, CDCl₃) δ 7.93 (dd, *J* = 8.0 Hz, 1.0 Hz, 1H), 7.53 (dt, *J* = 8.0 Hz, 1.0 Hz, 1H), 7.39 (dt, *J* = 8.0 Hz, 1.5 Hz, 1H), 7.35 (dd, *J* = 8.0 Hz, 1.0 Hz, 1H), 6.21 (s, 1H), 5.91 (d, *J* = 3.0 Hz, 2H), 5.88 (d, *J* = 3.0 Hz, 2H), 2.23 (s, 6H); ¹³C NMR (125 MHz, CDCl₃) δ 151.9 (C), 150.8 (C), 148.8 (C), 134.5 (C), 132.9 (CH), 131.0 (CH), 127.9 (CH), 124.8 (CH), 109.1 (CH), 106.2 (CH), 39.9 (CH), 13.6 (CH₃). ATR-FTIR (thin film): 2919, 1604, 1562, 1520, 1476, 1446, 1348, 1216, 1021, 1004, 968 cm⁻¹. HRMS (ESI) *m/z* calculated for C₁₇H₁₅NO₄ (M+H)⁺: 297.1079, found: 297.1090.

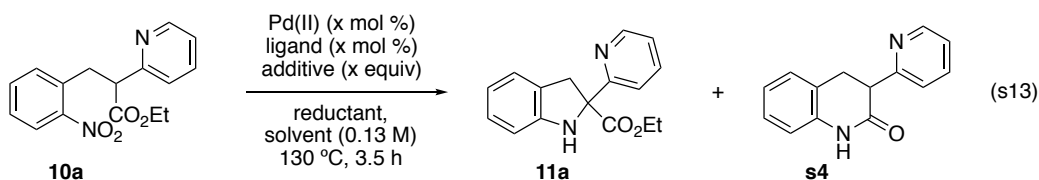


Methyl 2-(2-nitrobenzyl)-3-oxobutanoate 32.¹⁵ The general procedure was followed using 0.432 g of 2-nitrobenzyl bromide (2.00 mmol), 0.232 g of methyl acetoacetate (2.00 mmol), 0.080 g of NaH (2.00 mmol, 60 % wt. in oil) in 5 mL DMF. Purification by MPLC (1:99 to 5:95 EtOAc:hexanes) afforded the product as a yellow liquid (0.251 g, 59%). Nitroarene **26** was previous reported by Dale and Strobel.¹⁵ ¹H NMR (500 MHz, CDCl₃) δ 7.96 (d, *J* = 8.0 Hz, 1H), 7.50 (t, *J* = 7.5 Hz, 1H), 7.39 (d, *J* = 7.0 Hz, 2H), 4.01 – 3.99 (m, 1H), 3.66 (s, 3H), 3.45 (dd, *J* = 13.5, 5.5 Hz, 1H), 3.33 (dd, *J*

= 14, 8.5 Hz, 1H), 2.24 (s, 3H); ^{13}C NMR (125 MHz, CDCl_3) δ 201.8 (C), 169.1 (C), 149.0 (C), 133.6 (C), 133.4 (CH), 133.4 (CH), 128.2 (CH), 125.2 (CH), 59.5 (CH_3), 52.6 (CH_3), 31.3 (CH_2), 29.7 (CH).
 ATR-FTIR (thin film): cm^{-1} 2952, 1741, 1715, 1609, 1522, 1344, 1219 cm^{-1} .

V. Development of Pd-Catalyzed Indoline Synthesis.

A. Optimization of Reaction Conditions.



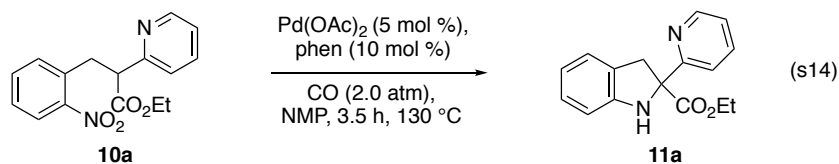
A conical vial was charged with 0.060 g of the substrate (0.020 mmol, 1.0 equiv), Pd^{II} salt, ligand, and 1.5 mL of solvent. The vial was loosely capped and placed into a Parr reactor. The reactor was sealed, evacuated and charged with CO gas. The Parr reactor was then heated to 130 °C. After 3.5 h, the solution was cooled to room temperature and diluted with 10 mL of saturated NaHCO_3 . The mixture was extracted with 3×10 mL of ethyl acetate. The organic phase was dried over Na_2SO_4 , filtered and the filtrate was concentrated in *vacuo*. The resulting residue was analyzed by ^1H NMR spectroscopy using CH_2Br_2 as an internal standard to determine the reaction progress.

Table s1. Optimization of Pd-catalyzed reductive amination reaction.

entry	Pd(II)	mol %	ligand	mol %	reductant	atm	additive	(equiv)	solv	yield % ^a	17a:s4
1	Pd(OAc) ₂	1.0	phen	2.0	CO	2.0	—	—	NMP	0	0:0
2	Pd(OAc) ₂	5.0	phen	10.0	Mo(CO) ₆	2.0 equiv	—	—	NMP	0	0:0
3	Pd(OAc) ₂	5.0	phen	20.0	CO	2.0	—	—	NMP	60	100:0
4	Pd(OAc) ₂	20.0	phen	40.0	CO	2.0	—	—	NMP	56	100:0
5	Pd(OAc) ₂	10.0	phen	20.0	CO	2.0	—	—	NMP	76	100:0
6	Pd(OAc) ₂	10.0	phen	20.0	CO	2.0	—	—	DMF	70	100:0
7	Pd(OAc) ₂	10.0	phen	20.0	CO	2.0	—	—	DMSO	53	100:0
8	Pd(OAc) ₂	5.0	phen	10.0	CO	2.0	—	—	NMP	83	100:0
9	Pd(OAc) ₂	5.0	phen	10.0	CO	1.0	—	—	NMP	72	100:0
10	Pd(OAc) ₂	5.0	phen	10.0	CO	3.0	—	—	NMP	72	100:0
11	Pd(OAc) ₂	5.0	phen	10.0	CO	4.0	—	—	NMP	48	100:0
12	Pd(OAc) ₂	5.0	phen	10.0	CHCl ₃	6.0 equiv	CsOH	3.0	NMP	0	0:0
13	Pd(OAc) ₂	5.0	phen	10.0	CHCl ₃	6.0 equiv	KOH	3.0	NMP	0	0:0
14	Pd(TFA) ₂	5.0	phen	10.0	CO	2.0	—	—	NMP	0	0:0
15	Pd(dppf) Cl	5.0	phen	10.0	CO	2.0	—	—	NMP	0	0:0
16	Pd(OAc) ₂	10.0	phen	20.0	CO	2.0	pTsoH	1.0	NMP	74	0:100
17	Pd(OAc) ₂	10.0	phen	20.0	CO	2.0	Cs ₂ CO ₃	1.0	NMP	55	100:0
18	Pd(OAc) ₂	10.0	phen	20.0	CO	2.0	NaHCO ₃	2.0	NMP	24	100:0
19	Pd(OAc) ₂	5.0	phen	10.0	CO	2.0	MeOH	1.0	NMP	64	63:37
20	Pd(OAc) ₂	10.0	4,7-(MeO) ₂ phen	20.0	CO	2.0	—	—	NMP	71	100:0
21	Pd(OAc) ₂	10.0	BPhen	20.0	CO	2.0	—	—	NMP	42	100:0
22	Pd(OAc) ₂	10.0	phen	20.0	CO	2.0	H ₂ O	1.0	NMP	15	0:100

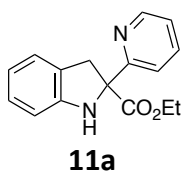
^a As determined using ¹H NMR spectroscopy using CH₂Br₂ as the internal standard.

B. Optimal Conditions.



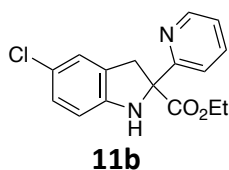
A conical vial was charged with 0.0600 g of the substrate (0.02 mmol, 1.0 equiv), 0.0022 g of Pd(OAc)₂ (0.005 mmol, 5 mol %), 0.004 g of 1,10-phenanthroline (0.010 mmol, 10 mol %), and 1.5 mL of NMP. The vial was loosely capped and placed into a Parr reactor. The reactor was sealed, evacuated and charged with CO gas. The Parr reactor was then heated to 130 °C. After 3.5 h, the solution was cooled to room temperature and diluted with 10 mL of saturated NaHCO₃. The mixture was extracted with 3 × 10 mL of ethyl acetate. The organic phase was dried over Na₂SO₄, filtered and the filtrate was concentrated in *vacuo*. The resulting residue was dry loaded onto celite and purified by MPLC (2:98 to 15:85 EtOAc:hexanes) to afford the product.

C. Characterization Data.

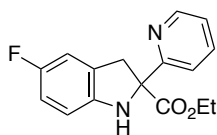


Ethyl 2-(pyridin-2-yl)indoline-2-carboxylate 11a. The general procedure was followed by using 0.060 g of **10a** (0.200 mmol), 0.0022 g of Pd(OAc)₂ (0.010 mmol), 0.0036 g of phenanthroline (0.020 mmol) in 1.5 mL of NMP. Purification by MPLC (25:75 EtOAc:hexanes) afforded the product as a yellow oil (0.050 g, 83%): ¹H NMR (500 MHz, CDCl₃) δ 8.56 (d, *J* = 4.4 Hz, 1H), 7.71 (t, *J* = 7.7 Hz, 1H), 7.62 (d, *J* = 7.9 Hz, 1H), 7.23 – 7.20 (m, 1H), 7.09 – 7.05 (m, 2H), 6.79 – 6.74 (m,

2H), 4.21 – 4.18 (m, 2H), 4.07 (d, $J = 16.1$ Hz, 1H), 3.51 (d, $J = 16.3$ Hz, 1H), 1.20 (t, $J = 7.1$ Hz, 3H) only visible peaks; ^{13}C NMR (125 MHz, CDCl_3) δ 173.6 (C), 161.0 (C), 149.2 (C), 148.9 (CH), 137.1 (CH), 127.7 (CH), 126.5 (C), 124.5 (CH), 122.7 (CH), 120.7 (CH), 119.6 (CH), 110.0 (CH), 74.7 (C), 62.0 (CH_2), 40.3 (CH_2), 14.0 (CH_3); ATR-FTIR (thin film): cm^{-1} 3362, 2981, 1732, 1610, 1588, 1485, cm^{-1} . HRMS (ESI) m/z calculated for $\text{C}_{16}\text{H}_{16}\text{N}_2\text{O}_2$ ($\text{M}+\text{H}$) $^+$: 269.1290; found 269.1288.

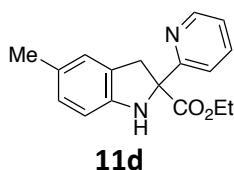


Ethyl 5-chloro-2-(pyridin-2-yl)indoline-2-carboxylate 11b. The general procedure was followed by using 0.0668 g of **10b** (0.200 mmol), 0.0023 g of $\text{Pd}(\text{OAc})_2$ (0.010 mmol), 0.0036 g of phenanthroline (0.020 mmol) in 1.5 mL of NMP. Purification by MPLC (15:85 EtOAc:hexane) afforded the product as a yellow oil (0.0393 g, 65%): ^1H NMR (500 MHz, CDCl_3) δ 8.55 (d, $J = 4.5$ Hz, 1H), 7.71 (t, $J = 7.5$ Hz, 1H), 7.57 (d, $J = 8.0$ Hz, 1H), 7.22 (t, $J = 5.5$ Hz, 1H), 6.97 (d, $J = 7.5$ Hz, 1H), 6.73 (s, 1H), 6.70 (d, $J = 7.5$ Hz, 1H), 4.22 – 4.16 (m, 2H), 4.00 (d, $J = 16.5$ Hz, 1H), 3.44 (d, $J = 16.5$ Hz, 1H), 1.19 (t, $J = 7.5$ Hz, 3H); ^{13}C NMR (125 MHz, CDCl_3) δ 173.2 (C), 160.5 (C), 150.4 (C), 148.9 (CH), 137.1 (C), 133.3 (CH), 125.2 (C), 125.1 (CH), 122.9 (CH), 120.5 (CH), 119.4 (CH), 110.1 (CH), 75.1 (C), 62.2 (CH_2), 39.6 (CH_2), 14.0 (CH_3). ATR-FTIR (thin film): 3358, 2926, 1731, 1480, 1429, 1215 cm^{-1} . HRMS (ESI) m/z calculated for $\text{C}_{16}\text{H}_{15}\text{ClN}_2\text{O}_2$ ($\text{M}+\text{H}$) $^+$: 303.0900; found 303.0894.



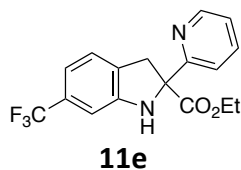
11c

Ethyl 5-fluoro-2-(pyridin-2-yl)indoline-2-carboxylate 11c. The general procedure was followed using 0.0636 g of **10b**, (0.200 mmol), 0.0023 g of Pd(OAc)₂ (0.010 mmol), 0.0036 g of phenanthroline (0.020 mmol) in 1.5 mL of NMP. Purification by MPLC (20:80 EtOAc:hexane) afforded the product as a yellow oil (0.0412 g, 72 %): ¹H NMR (500 MHz, CDCl₃) δ 8.56 (d, *J* = 4.0 Hz, 1H), 7.70 (t, *J* = 7.5 Hz, 1H), 7.58 (d, *J* = 8.0 Hz, 1H), 7.21 (t, *J* = 5.5 Hz, 1H), 6.81 (d, *J* = 8.0 Hz, 1H), 6.74 (t, *J* = 9.0 Hz, 1H), 6.68 – 6.66 (m, 1H), 5.42 (br s, 1H), 4.22 – 4.17 (m, 2H), 4.03 (d, *J* = 16.5 Hz, 1H), 3.51 (d, *J* = 16.5 Hz, 1H), 1.19 (t, *J* = 7.0 Hz, 3H) only visible peaks; ¹³C NMR (125 MHz, CDCl₃) δ 173.6 (C), 160.6 (C), 157.6 (d, *J*_{CF} = 234.5 Hz, C), 149.0 (CH), 145.3 (C), 137.0 (CH), 128.3 (d, *J*_{C-F} = 8.4 Hz, C), 122.8 (CH), 120.6 (CH), 113.8 (d, *J*_{CF} = 23.1, CH), 111.8 (d, *J*_{CF} = 24.0 Hz, CH), 110.3 (d, *J*_{CF} = 8.3 Hz, CH), 75.3 (C), 62.1 (CH₂), 40.3 (CH₂), 14.0 (CH₃); ¹⁹F NMR (376 MHz, CDCl₃) δ –125.9. ATR-FTIR (thin film): 3350, 2981, 1731, 1712, 1364, 1225, 1175 cm⁻¹. HRMS (ESI) *m/z* calculated for C₁₆H₁₅FN₂O₂ (M+H)⁺: 287.1196; found 287.1194.

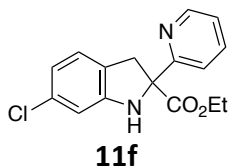


Ethyl 5-methyl-2-(pyridin-2-yl)indoline-2-carboxylate 11d. The general procedure was followed by using 0.0628 g of **10d** (0.200 mmol), 0.0023 g of Pd(OAc)₂ (0.010 mmol), 0.0036 g of phenanthroline (0.020 mmol) in 1.5 mL of NMP. Purification by MPLC (25:75 EtOAc:hexane) afforded the product as a yellow oil (0.0450 g, 80%): ¹H NMR (500 MHz, CDCl₃) δ 8.54 (d, *J* = 4.0 Hz, 1H), 7.68 (t, *J* = 7.0 Hz, 1H), 7.59 (d, *J* = 8.0 Hz, 1H), 7.20 – 7.17 (m, 1H), 6.90 (s, 1H), 6.86 (d, *J*

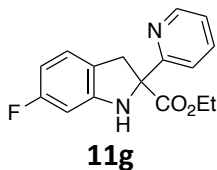
= 8.0 Hz, 1H), 6.67 (d, J = 8.0 Hz, 1H), 4.19 – 4.14 (m, 2H), 4.01 (d, J = 16.0 Hz, 1H), 3.46 (d, J = 16.5 Hz, 1H), 2.22 (s, 3H), 1.18 (t, J = 7.0 Hz, 3H) only visible peaks; ^{13}C NMR (125 MHz, CDCl_3) δ 173.8 (C), 161.1 (C), 148.8 (CH), 146.9 (C), 137.0 (CH), 129.0 (C), 128.1 (CH), 126.8 (C), 125.2 (CH), 122.7 (CH), 120.6 (CH), 109.9 (CH), 74.9 (C), 62.0 (CH_2), 40.3 (CH_3), 20.8 (CH_2), 14.0 (CH_3); ATR-FTIR (thin film): 3280, 2980, 1731, 1618, 1367, 1235 cm^{-1} . HRMS (ESI) m/z calculated for $\text{C}_{17}\text{H}_{18}\text{N}_2\text{O}_2$ ($\text{M}+\text{H}$) $^+$: 283.1447; found 283.1444.



Ethyl 6-trifluoromethyl-2-(pyridin-2-yl)indoline-2-carboxylate 11e. The general procedure was followed using 0.0368 g of **10e** (0.100 mmol), 0.0012 g of $\text{Pd}(\text{OAc})_2$ (0.005 mmol), 0.0018 g of phenanthroline (0.010 mmol) in 0.75 mL of NMP. Purification by MPLC (20:80 EtOAc:hexanes) afforded the product as a yellow oil (0.016 g, 50%): ^1H NMR (500 MHz, CDCl_3) δ 8.57 (dd, J = 4.0, 0.5 Hz, 1H), 7.72 (td, J = 7.5, 1.5 Hz, 1H), 7.58 (d, J = 8.0 Hz, 1H), 7.24 – 7.22 (m, 1H), 7.15 (d, J = 7.5 Hz, 1H), 7.00 (d, J = 8.0 Hz, 1H), 6.96 (s, 1H), 5.61 (br s, 1H), 4.24 – 4.17 (m, 2H), 4.10 (d, J = 16.5 Hz, 1H), 3.54 (d, J = 16.5 Hz, 1H), 1.21 (t, J = 7.0 Hz, 3H); ^{13}C NMR (125 MHz, CDCl_3) δ 173.1 (C), 160.4 (C), 149.5 (CH), 149.0 (CH), 137.0 (C), 130.6 (C), 124.5 (CH), 121.7 (d, J = 313.8 Hz, C), 116.6 (CH), 106.3 (CH), 74.8 (CH_2), 62.2 (C), 39.9 (CH_2), 14.0 (CH_3) only visible peaks; ^{19}F NMR (376 MHz, CDCl_3) δ –62.8. ATR-FTIR (thin film): 3350, 2982, 1732, 1496, 1221, 1043, 1009 cm^{-1} . HRMS (ESI) m/z calculated for $\text{C}_{17}\text{H}_{15}\text{F}_3\text{N}_2\text{O}_2$ ($\text{M}+\text{H}$) $^+$: 337.1164; found 337.1155.

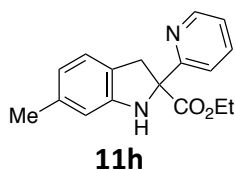


Ethyl 6-chloro-2-(pyridin-2-yl)indoline-2-carboxylate 11f. The general procedure was followed using 0.0668 g of **10f**, (0.200 mmol), 0.0023 g of Pd(OAc)₂ (0.010 mmol), 0.0036 g of phenanthroline (0.020 mmol) in 1.5 mL of NMP. Purification by MPLC (20:80 EtOAc:hexanes) afforded the product as a yellow oil (0.039 g, 65 %): ¹H NMR (500 MHz, CDCl₃) δ 8.55 (d, *J* = 4.5 Hz, 1H), 7.71 (t, *J* = 7.5 Hz, 1H), 7.57 (d, *J* = 8.0 Hz, 1H), 7.22 (t, *J* = 5.5 Hz, 1H), 6.97 (d, *J* = 7.5 Hz, 1H), 6.73 (s, 1H), 6.70 (d, *J* = 7.5 Hz, 1H), 4.22 – 4.16 (m, 2H), 4.00 (d, *J* = 16.5 Hz, 1H), 4.44 (d, *J* = 16.5 Hz, 1H), 1.19 (t, *J* = 7.0 Hz, 3H) only visible peaks; ¹³C NMR (125 MHz, CDCl₃) δ 173.2 (C), 160.5 (C), 150.4 (C), 148.9 (C), 137.1 (CH), 133.3 (CH), 125.2 (C), 125.0 (CH), 122.9 (CH), 120.5 (CH), 119.4 (CH), 110.1 (CH), 75.1 (C), 62.2 (CH₂), 39.6 (CH₂), 14.0 (CH₃). ATR-FTIR (thin film): 3355, 2925, 1730, 1608, 1475, 1230 cm⁻¹. HRMS (ESI) *m/z* calculated for C₁₆H₁₅ClN₂O₂ (M+H)⁺: 303.0900; found 303.0891.



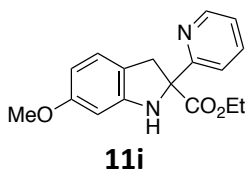
Ethyl 6-fluoro-2-(pyridin-2-yl)indoline-2-carboxylate 11g. The general procedure was followed using 0.0636 g of **10g**, (0.200 mmol), 0.0023 g of Pd(OAc)₂ (0.010 mmol), 0.0036 g of phenanthroline (0.020 mmol) in 1.5 mL of NMP. Purification by MPLC (20:80 EtOAc:hexanes) afforded the product as a yellow oil (0.0458 g, 80 %): ¹H NMR (500 MHz, CDCl₃) δ 8.56 (d, *J* = 3.5

Hz, 1H), 7.72 – 7.69 (m, 1H), 7.57 (d, $J = 8.0$ Hz, 1H), 7.21 (t, $J = 5.0$ Hz, 1H), 6.97 (t, $J = 7.0$ Hz, 1H), 6.60 (d, $J = 9.5$ Hz, 1H), 6.43 – 6.50 (m, 1H), 5.54 (br s, 1H), 4.19 (q, $J = 2.0$ Hz, 2H), 3.99 (d, $J = 16.0$ Hz, 1H), 3.45 (d, $J = 16.0$ Hz, 1H), 1.20 (t, $J = 7.0$ Hz, 3H); ^{13}C NMR (125 MHz, CDCl_3) δ 173.4 (C), 163.3 (d, $J_{\text{CF}} = 240.3$ Hz, C), 160.6 (C), 150.7 (C), 149.0 (CH), 137.0 (CH), 124.9 (d, $J_{\text{CF}} = 10.4$ Hz, CH), 122.8 (C), 121.9 (d, $J_{\text{CF}} = 3.0$ Hz, CH), 120.5 (CH), 105.7 (d, $J_{\text{CF}} = 22.1$ Hz, CH), 97.8 (d, $J_{\text{CF}} = 25.9$ Hz, CH), 75.5 (CH_2), 62.1 (C), 39.4 (CH_2), 14.1 (CH_3); ^{19}F NMR (376 MHz, CDCl_3) δ –115.9. ATR-FTIR (thin film): 3365, 2982, 1731, 1618, 1330, 1236, 1139 cm^{-1} . HRMS (ESI) m/z calculated for $\text{C}_{16}\text{H}_{15}\text{FN}_2\text{O}_2$ ($\text{M}+\text{H}$) $^+$: 287.1196; found 287.1194.

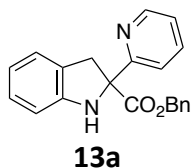


Ethyl 6-methyl-2-(pyridin-2-yl)indoline-2-carboxylate 11h. The general procedure was followed by using 0.0628 g of **10h** (0.200 mmol), 0.0023 g of $\text{Pd}(\text{OAc})_2$ (0.010 mmol), 0.0036 g of phenanthroline (0.020 mmol) in 1.5 mL of NMP. Purification by MPLC (25:75 EtOAc:hexane) afforded the product as a yellow oil (0.0478 g, 85%): ^1H NMR (500 MHz, CDCl_3) δ 8.55 (d, $J = 4.0$ Hz, 1H), 7.68 (dt, $J = 8.0, 1.5$ Hz, 1H), 7.60 (d, $J = 8.0$ Hz, 1H), 7.20 – 7.18 (m, 1H), 6.97 (d, $J = 7.5$ Hz, 1H), 6.61 (s, 1H), 6.57 (d, $J = 7.5$ Hz, 1H), 5.41 (br s, 1H), 4.22 – 4.15 (m, 2H), 4.02 (d, $J = 16.0$ Hz, 1H), 3.46 (d, $J = 16.0$ Hz, 1H), 2.27 (s, 3H), 1.19 (t, $J = 7.0$ Hz, 3H); ^{13}C NMR (125 MHz, CDCl_3) δ 173.8 (C), 161.3 (C), 149.5 (C), 148.9 (CH), 137.6 (C), 136.9 (CH), 124.1 (CH), 123.6 (C), 122.6 (CH), 120.6 (CH), 120.4 (CH), 110.8 (CH), 75.0 (C), 61.9 (CH_2), 39.9 (CH_2), 21.5 (CH_3), 14.0 (CH_3). ATR-

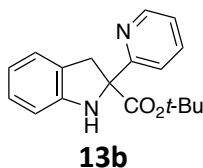
FTIR (thin film): 3374, 2922, 1726, 1585, 1454, 1266 cm^{-1} . HRMS (ESI) m/z calculated for $\text{C}_{17}\text{H}_{18}\text{N}_2\text{O}_2$ ($\text{M}+\text{H}$) $^+$: 283.1447; found 283.1441.



Ethyl 6-methoxy-2-(pyridin-2-yl)indoline-2-carboxylate 11i. The general procedure was followed by using 0.0661 g of **10i** (0.200 mmol), 0.0023 g of $\text{Pd}(\text{OAc})_2$ (0.010 mmol), 0.0036 g of phenanthroline (0.020 mmol) in 1.5 mL of NMP. Purification by MPLC (25:75 EtOAc:hexane) afforded the product as a yellow oil (0.0360 g, 61%): ^1H NMR (500 MHz, CDCl_3) δ 8.56 – 8.55 (m, 1H), 7.69 (td, $J = 7.5, 1.7$ Hz, 1H), 7.59 (d, $J = 8.3$ Hz, 1H), 7.21 – 7.19 (m, 1H), 6.96 (d, $J = 8.1$ Hz, 1H), 6.37 – 6.29 (m, 1H), 6.30 (dd, $J = 8.1, 2.2$ Hz, 1H), 5.47 (br s, 1H), 4.21 – 4.17 (m, 2H), 3.98 (d, $J = 15.8$ Hz, 1H), 3.98 (s, 3H), 3.43 (d, $J = 15.8$ Hz, 1H), 1.20 (t, $J = 7.1$ Hz, 3H); ^{13}C NMR (125 MHz, CDCl_3) δ 173.7 (C), 161.1 (C), 160.2 (C), 150.6 (C), 148.9 (CH), 136.9 (CH), 124.7 (CH), 122.7 (CH), 120.5 (CH), 118.8 (C), 104.7 (CH), 96.8 (CH), 75.5 (C), 62.0 (CH_2), 55.4 (CH_3), 39.5 (CH_2), 14.0 (CH_3). ATR-FTIR (thin film): 3360, 2934, 1727, 1616, 1587, 1500 cm^{-1} . HRMS (ESI) m/z calculated for $\text{C}_{17}\text{H}_{18}\text{N}_2\text{O}_3$ ($\text{M}+\text{H}$) $^+$: 299.1396; found 299.1391.

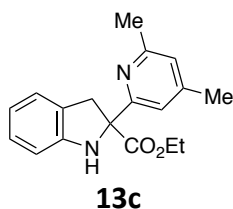


Benzyl 2-(pyridin-2-yl)indoline-2-carboxylate 13a. The general procedure was followed by using 0.0725 g of **12a** (0.200 mmol), 0.0023 g of Pd(OAc)₂ (0.010 mmol), 0.0036 g of phenanthroline (0.020 mmol) in 1.5 mL of NMP. Purification by MPLC (25:75 EtOAc:hexane) afforded the product as a yellow oil (0.0420 g, 64%): ¹H NMR (500 MHz, CDCl₃) δ 8.56 (d, *J* = 4.9 Hz, 1H), 7.67 (td, *J* = 7.7, 1.8 Hz, 1H), 7.58 (d, *J* = 7.7 Hz, 1H), 7.28 – 7.26 (m, 3H), 7.22 – 7.16 (m, 3H), 7.11 – 7.06 (m, 2H), 6.78 – 6.75 (m, 2H), 5.49 (br s, 1H), 5.18 (dd, *J* = 15.2, 12.5 Hz, 2H), 4.10 (d, *J* = 15.8 Hz, 1H), 3.52 (d, *J* = 16.1 Hz, 1H); ¹³C NMR (125 MHz, CDCl₃) δ 173.5 (C), 160.9 (C), 149.2 (C), 148.9 (CH), 136.95 (CH), 136.91 (CH) 135.6 (C), 128.4 (CH), 128.1 (CH), 127.7 (CH), 126.5 (C), 124.5 (CH), 122.8 (CH), 120.6 (CH), 119.7 (CH), 110.0 (CH), 75.0 (C), 67.4 (CH₂), 40.2 (CH₂). ATR-FTIR (thin film): 3366, 3032, 1737, 1588, 1165, 748 cm⁻¹. HRMS (ESI) *m/z* calculated for C₂₁H₁₈N₂O₂ (M+H)⁺: 331.1447; found 331.1446.

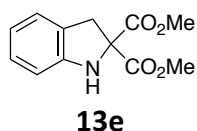


tert-Butyl 2-(pyridin-2-yl)indoline-2-carboxylate 13b. The general procedure was followed using 0.0328 g of **12b**, (0.100 mmol), 0.0011 g of Pd(OAc)₂ (0.010 mmol), 0.0018 g of phenanthroline (0.020 mmol) in 1.5 mL of NMP. Purification by MPLC (10:90 EtOAc:hexanes) afforded the product as a yellow oil (0.0130 g, 44%): ¹H NMR (500 MHz, CDCl₃) δ 8.56 – 8.54 (m, 1H), 7.68 (td, *J* = 7.5, 1.5 Hz, 1H), 7.55 (dd, *J* = 8.0, 1.0 Hz, 1H), 7.20 – 7.17 (m, 1H), 7.08 – 7.04 (m, 2H), 6.77 – 6.72 (m, 2H), 3.99 (d, *J* = 16.0 Hz, 1H), 3.49 (d, *J* = 16.5 Hz, 1H), 1.37 (s, 9H) only peaks visible; ¹³C NMR (125 MHz, CDCl₃) δ 172.6 (C), 161.5 (C), 149.4 (CH), 148.8 (C), 136.7 (CH), 127.6 (CH), 126.8

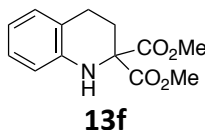
(CH), 124.4 (CH), 122.5 (CH), 120.4 (CH), 119.4 (CH), 109.9 (CH), 73.1 (C), 39.9 (CH₂), 30.9 (C), 27.8 (CH₃). ATR-FTIR (thin film): 3361, 2978, 1731, 1485, 1249, 1150 cm⁻¹. HRMS (ESI) m/z calculated for C₁₈H₂₀N₂O₂ (M+H)⁺: 297.1603; found 297.1597.



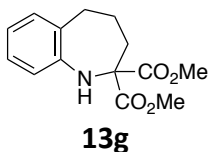
Ethyl 2-(4,6-dimethylpyridin-2-yl)indoline-2-carboxylate 13c. The general procedure was followed using 0.0296 g of **12c**, (0.100 mmol), 0.0011 g of Pd(OAc)₂ (0.010 mmol), 0.0018 g of phenanthroline (0.020 mmol) in 1.5 mL of NMP. Purification by MPLC (10:90 EtOAc:hexanes) afforded the product as a yellow oil (0.0206 g, 70%): ¹H NMR (500 MHz, CDCl₃) δ 7.19 (s, 1H), 7.07 (q, *J* = 8.0 Hz, 2H), 6.87 (s, 1H), 6.77 (q, *J* = 7.5 Hz, 2H), 5.59 (brs, 1H), 4.19 (q, *J* = 7.0 Hz, 2H), 4.01 (d, *J* = 16.5 Hz, 1H), 3.52 (d, *J* = 16.0 Hz, 1H), 2.47 (s, 3H), 2.30 (s, 3H), 1.21 (t, *J* = 7.0 Hz, 3H); ¹³C NMR (125 MHz, CDCl₃) δ 174.0 (C), 160.0 (C), 157.4 (C), 149.5 (C), 127.6 (CH), 126.9 (C), 126.1 (C), 124.4 (CH), 123.2 (CH), 119.4 (CH), 118.3 (CH), 110.0 (CH), 74.5 (CH₂), 61.8 (CH₂), 40.1 (C), 24.3 (CH₃), 21.0 (CH₃), 14.1 (CH₃). ATR-FTIR (thin film): 3356, 2923, 1732, 1607, 1465, 1229 cm⁻¹. HRMS (ESI) m/z calculated for C₁₈H₂₀N₂O₂ (M+H)⁺: 297.1603; found 297.1602.



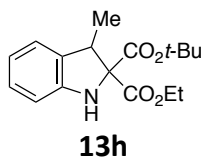
Dimethyl indoline-2,2-dicarboxylate **13e.**⁸¹ The general procedure was followed by using 0.0540 g of **12e** (0.200 mmol), 0.0023 g of Pd(OAc)₂ (0.010 mmol), 0.0036 g of phenanthroline (0.020 mmol) in 1.5 mL of NMP. Purification by MPLC (3:97 to 10:90 EtOAc:hexanes) afforded the product as a yellow oil (0.042 g, 88%). Indoline **13e** was previously reported by Wright and co-workers:⁸¹ ¹H NMR (500 MHz, CDCl₃) δ 7.07 (m, 2H), 6.78 (t, *J* = 7.5 Hz, 1H), 6.73 (d, *J* = 7.5 Hz, 1H), 5.02 (s, 1H), 3.80 (s, 6H), 3.69 (s, 2H); ¹³C NMR (125 MHz, CDCl₃) δ 170.9 (C), 148.3 (C), 127.9 (CH), 125.6 (C), 124.4 (CH), 120.3 (CH), 110.4 (CH), 72.8 (C), 53.4 (CH₃), 18.9 (CH₂). ATR-FTIR (thin film): 3366, 3053, 2949, 2855, 1725, 1609, 1432, 1236, 1163, 1076, 1042 cm⁻¹. HRMS (ESI) *m/z* calculated for C₁₂H₁₄NO₄ (M+H)⁺: 236.0923, found: 236.0917.



Dimethyl 3,4-dihydroquinoline-2,2(1H)-dicarboxylate **13f.** The general procedure was followed by using 0.0560 g of **12f** (0.200 mmol), 0.0023 g of Pd(OAc)₂ (0.010 mmol), 0.0036 g of phenanthroline (0.020 mmol) in 1.5 mL of NMP. Purification by MPLC (3:97 to 10:90 EtOAc:hexanes) afforded the product as a red oil (0.0309 g, 62%): ¹H NMR (500 MHz, CDCl₃) δ 7.02 (t, *J* = 7.5 Hz, 1H), 6.95 (d, *J* = 7.0 Hz, 1H), 6.68 (t, *J* = 7.0 Hz, 1H), 6.65 (d, *J* = 8.5 Hz, 1H), 4.83 (s, 1H), 3.79 (s, 6H), 2.80 (t, *J* = 6.5 Hz, 2H), 2.37 (t, *J* = 6.5 Hz, 2H); ¹³C NMR (125 MHz, CDCl₃) δ 170.5 (C), 141.6 (C), 128.9 (CH), 127.2 (CH), 120.3 (C), 118.5 (CH), 114.8 (CH), 64.8 (C), 53.2 (CH₃), 26.8 (CH₂), 23.8 (CH₂). ATR-FTIR (thin film): 3398, 2949, 2920, 2845, 1739, 1722, 1588, 1488, 1432, 1293, 1220, 1161, 1122, 1053, 749 cm⁻¹. HRMS (ESI) *m/z* calculated for C₁₃H₁₆NO₄ (M+H)⁺: 250.1079, found: 250.1085.

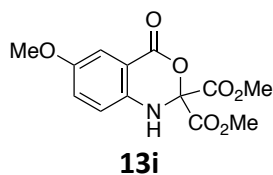


Dimethyl 1,3,4,5-tetrahydro-2H-benzo[*b*]azepine-2,2-dicarboxylate 13g. The general procedure was followed by using 0.0290 g of **12g** (0.100 mmol), 0.0011 g of Pd(OAc)₂ (0.005 mmol), 0.002 g of phenanthroline (0.010 mmol) in 0.75 mL of NMP. Purification by MPLC (3:97 to 10:90 EtOAc:hexanes) afforded the product as a red oil (0.004 g, 14 %): ¹H NMR (500 MHz, CDCl₃) δ 7.06 (m, 2H), 6.89 (dt, *J* = 7.5 Hz, 1H, 1H), 6.85 (d, *J* = 7.5 Hz, 1H), 4.68 (s, 1H), 3.69 (s, 6H), 2.75 (m, 2H), 2.25 (t, *J* = 6.0 Hz, 2H), 1.86 (m, 2H); ¹³C NMR (125 MHz, CDCl₃) δ 170.2 (C), 143.5 (C), 135.0 (C), 129.6 (CH), 126.7 (CH), 122.8 (CH), 122.5 (CH), 68.5 (C), 52.9 (CH₃), 34.8 (CH₂), 33.9 (CH₂), 22.3 (CH₂). ATR-FTIR (thin film): 3381, 2951, 1735, 1613, 1487, 1465, 1431, 1270, 1223, 1098, 906, 730 cm⁻¹. HRMS (ESI) *m/z* calculated for C₁₄H₁₈NO₄ (M+H)⁺: 264.1236, found: 264.1233.

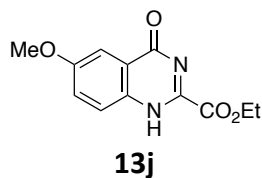


2-(*tert*-Butyl) 2-ethyl 3-methylindoline-2,2-dicarboxylate 13h. The general procedure was followed using 0.067 g of methyl 2-(2-nitrobenzyl)-3-oxobutanoate (0.200 mmol), 0.0023 g of Pd(OAc)₂ (0.010 mmol), 0.0036 g of phenanthroline (0.020 mmol) in 1.5 mL of NMP. Purification by MPLC (1:99 to 5:95 EtOAc:hexanes) afforded the product, a 50:50 mixture of diastereomers, as a yellow liquid (0.027 g, 44%): ¹H NMR (500 MHz, CDCl₃) δ 7.07 – 7.01 (m, 2H), 6.79 – 6.75 (m, 1H), 6.70 (d, *J* = 7.5 Hz, 1H), 4.76 (br s, 1H), 4.38 – 4.23 (m, 1.1H), 4.22 – 4.15 (m, 1.0H), 4.11 (q, *J*

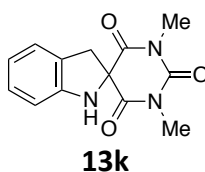
= 7.0 Hz, 0.5H), 4.07 (q, J = 7.5 Hz, 0.5H), 1.47 (d, J = 3.5 Hz, 9H) 1.37 (d, J = 7.0 Hz, 1.7H), 1.33 – 1.28 (m, 4.6H); ^{13}C NMR (125 MHz, CDCl_3) δ 170.2 (C), 169.9 (C), 168.7 (C), 147.9 (C), 131.6 (C), 131.4 (C), 127.9 (CH), 127.9 (CH), 123.2 (CH), 119.9 (CH), 119.8 (CH), 109.8 (C), 109.6 (C), 83.2 (C), 82.5 (C), 61.8 (CH_2), 42.3 (CH_3), 42.2 (CH_3), 28.0 (CH_3), 27.8 (CH_3), 16.1 (CH_3), 16.0 (CH_3), 14.2 (CH), 14.1 (CH), only peaks visible. ATR-FTIR (thin film): 3362, 2978, 1731, 1485, 1610, 1154 cm^{-1} . HRMS (ESI) m/z calculated for $\text{C}_{17}\text{H}_{23}\text{NO}_4$ ($\text{M}+\text{H}$) $^+$: 306.1705; found 306.1698.



Dimethyl 4-oxo-1,4-dihydro-2H-benzo[d][1,3]oxazine-2,2-dicarboxylate 13i. The general procedure was followed by using 0.0600 g of **12i** (0.200 mmol), 0.0022 g of $\text{Pd}(\text{OAc})_2$ (0.0100 mmol), 0.0036 g of phenanthroline (0.020 mmol) in 1.5 mL of NMP. Purification by MPLC (3:97 to 10:90 EtOAc:hexanes) afforded the product as a white solid (0.0295 g, 50%): mp 154 – 156 $^\circ\text{C}$; ^1H NMR (500 MHz, CDCl_3) δ 7.41 (d, J = 3.0 Hz, 1H), 7.10 (dd, J = 9.0 Hz, 3.0 Hz, 1H), 6.87 (d, J = 9.0 Hz, 1H), 5.48 (s, 1H), 3.85 (s, 6H), 3.79 (s, 3H); ^{13}C NMR (125 MHz, CDCl_3) δ 165.4 (C), 155.1 (C), 136.6 (C), 125.1 (CH), 119.3 (CH), 114.5 (C), 111.5 (CH), 87.0 (C), 55.8 (CH_3), 54.3 (CH_3), only visible peaks; ATR-FTIR (thin film): 3366, 3017, 2962, 1772, 1746, 1722, 1626, 1514, 1435, 1354, 1284, 1246, 1215, 1030 cm^{-1} . HRMS (ESI) m/z calculated for $\text{C}_{13}\text{H}_{14}\text{NO}_7$ ($\text{M}+\text{H}$) $^+$: 296.0770, found: 296.0770.

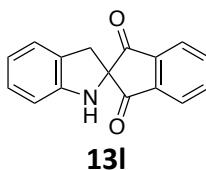


Ethyl 6-methoxy-4-oxo-1,4-dihydroquinazoline-2-carboxylate 13j.⁸² The general procedure was followed using 0.035 g of **12j** (0.100 mmol), 0.001 g of Pd(OAc)₂ (0.0100 mmol), 0.0018 g of phenanthroline (0.020 mmol) in 0.75 mL of NMP. Purification by MPLC (2:98 to 15:85 EtOAc:hexanes) afforded the product as a white solid (0.013 g, 51%). **13j** was previously reported by Nara and co-workers:⁸² mp (dec) 220 – 223 °C; ¹H NMR (500 MHz, CDCl₃) δ 10.1 (br s, 1H), 7.88 (d, *J* = 8.5 Hz, 1H), 7.71 (d, *J* = 3.0 Hz, 1H), 7.41 (dd, *J* = 9.0, 3.0 Hz, 1H), 7.56 (q, *J* = 7.5 Hz, 2H), 3.95 (s, 3H), 1.48 (t, *J* = 7.0 Hz, 3H); ¹³C NMR (125 MHz, CDCl₃) δ 160.6 (C), 160.4 (C), 141.9 (C), 139.4 (C), 131.0 (CH), 125.1 (CH), 124.4 (C), 116.7 (C), 106.6 (CH), 64.0 (CH₂), 56.0 (CH₃), 14.2 (CH₃). ATR-FTIR (thin film): 3250, 2930, 1748, 1723, 1504, 1278 cm⁻¹. HRMS (ESI) *m/z* calculated for C₁₂H₁₂N₂O₄ (M+H)⁺: 249.0875; found 249.0870.

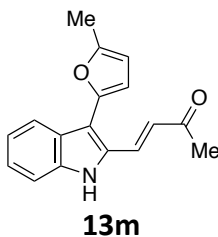


1,3'-Dimethyl-2'*H*-spiro[indoline-2,5'-pyrimidine]-2',4',6'-(1'*H*,3'*H*)-trione 13k. The general procedure was followed by using 0.0580 g of **12k** (0.200 mmol), 0.0023 g of Pd(OAc)₂ (0.010 mmol), 0.0036 g of phenanthroline (0.020 mmol) in 1.5 mL of NMP. Purification by MPLC (3:97 to 10:90 EtOAc:hexanes) afforded the product as a red oil (0.0404 g, 78%): ¹H NMR (500 MHz, CDCl₃) δ 7.13 (t, *J* = 7.5 Hz, 1H), 7.02 (d, *J* = 7.5 Hz, 1H), 6.83 (m, 2H), 4.59 (s, 1H), 3.56 (s, 2H), 3.35

(s, 6H); ^{13}C NMR (125 MHz, CDCl_3) δ 170.6 (C), 150.9 (C), 149.6 (C), 128.6 (CH), 124.2 (CH), 123.8 (C), 121.1 (CH), 111.6 (CH), 69.8 (C), 44.8 (CH_2), 29.5 (CH_3). ATR-FTIR (thin film): 3332, 2958, 2924, 1752, 1682, 1605, 1486, 1445, 1375, 1063, 909, 730 cm^{-1} . HRMS (ESI) m/z calculated for $\text{C}_{13}\text{H}_{14}\text{N}_3\text{O}_3$ ($\text{M}+\text{H}$) $^+$: 260.1035, found: 260.1037.



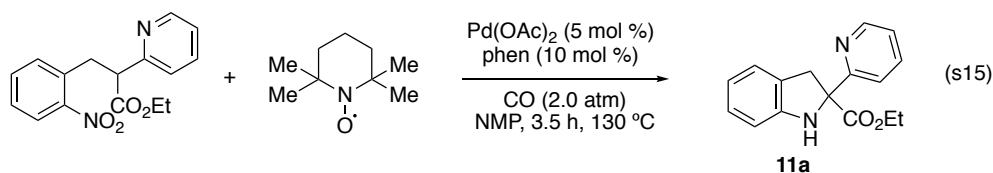
Spiro[cyclopentane-1,2'-indoline]-2,5-dione 13l. The general procedure was followed by using 0.0560 g of **12l** (0.200 mmol), 0.0023 g of $\text{Pd}(\text{OAc})_2$ (0.010 mmol), 0.0036 g of phenanthroline (0.020 mmol) in 1.5 mL of NMP. Purification by MPLC (3:97 to 10:90 EtOAc:hexanes) afforded the product as a brown solid (0.0310 g, 61%): mp 175 – 176 $^\circ\text{C}$; ^1H NMR (500 MHz, CDCl_3) δ 8.05 (m, 2H), 7.92 (m, 2H), 7.11 ($J = 7.5$ Hz, 1H), 7.03 (d, $J = 7.5$ Hz, 1H), 6.82 (t, $J = 7.5$ Hz, 1H), 6.78 (d, $J = 8.0$ Hz, 1H), 4.33 (s, 1H), 3.40 (s, 2H); ^{13}C NMR (125 MHz, CDCl_3) δ 199.6 (C), 150.2 (C), 140.6 (C), 136.5 (CH), 128.3 (CH), 125.3 (C), 124.2 (CH), 124.1 (CH), 120.5 (CH), 110.8 (CH), 71.3 (C), 40.5 (CH_2). ATR-FTIR (thin film): 3351, 2919, 1743, 1698, 1589, 1485, 1466, 1330, 1241, 1050 cm^{-1} . HRMS (ESI) m/z calculated for $\text{C}_{16}\text{H}_{12}\text{NO}_2$ ($\text{M}+\text{H}$) $^+$: 250.0868, found: 250.0876.



(E)-4-(3-(5-Methylfuran-2-yl)-1H-indol-2-yl)but-3-en-2-one 13m.⁸³ The general procedure was followed by using 0.0600 g of **12m** (0.200 mmol), 0.0023 g of Pd(OAc)₂ (0.010 mmol), 0.0036 g of phenanthroline (0.020 mmol) in 1.5 mL of NMP. Purification by MPLC (3:97 to 10:90 EtOAc:hexanes) afforded the product as a brown solid (0.0323 g, 61%). Indole **13m** was previously reported by Butin and co-workers:⁸³ mp 96 – 99 °C; ¹H NMR (500 MHz, MeOD) δ 7.95 (d, *J* = 16.0 Hz, 1H), 7.83 (d, *J* = 7.0 Hz, 1H), 7.39 (d, *J* = 8.5 Hz, 1H), 7.27 (dt, *J* = 8.0 Hz, 1.0 Hz, 1H), 7.10 (dt, *J* = 8.0 Hz, 1.0 Hz, 1H), 6.80 (d, 16.0 Hz, 1H), 6.69 (d, *J* = 3.5 Hz, 1H), 6.26 (dd, *J* = 3.0 Hz, 1.0 Hz, 1H), 2.39 (s, 3H), 2.34 (s, 3H) only visible peaks; ¹³C NMR (125 MHz, MeOD) δ 197.8 (C), 151.8 (C), 147.8 (C), 138.3 (C), 132.2 (CH), 130.0 (C), 126.2 (CH), 125.5 (CH), 125.3 (C), 121.3 (CH), 120.9 (CH), 112.4 (C), 112.1 (CH), 109.3 (CH), 108.4 (CH), 27.7 (CH₃), 13.9 (CH₃). ATR-FTIR (thin film): 3286, 2920, 2851, 1714, 1667, 1639, 1603, 1487, 1443, 1357, 1262, 1234, 1150, 1046, 1029 cm⁻¹. HRMS (ESI) *m/z* calculated for C₁₇H₁₆NO₂ (M+H)⁺: 266.1181, found: 266.1188.

VI. Mechanism Investigations

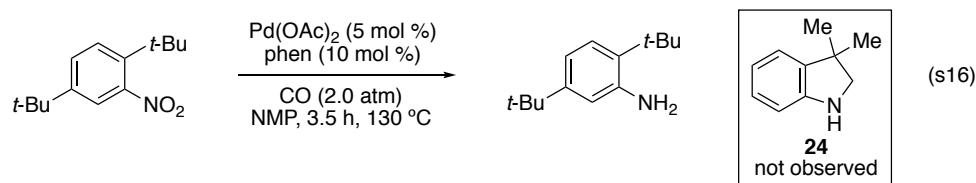
A. Testing for radical intermediates



To a conical vial equipped for magnetic stirring was added 0.060 g of **10a** (0.200 mmol), 0.0022 g of Pd(OAc)₂ (0.010 mmol), 0.0036 g of phenanthroline (0.020 mmol) and 1.5 mL of NMP. To this solution was added 0.031 mg of (2,2,6,6-tetramethylpiperidin-1-yl)oxyl (0.200 mmol). The vial

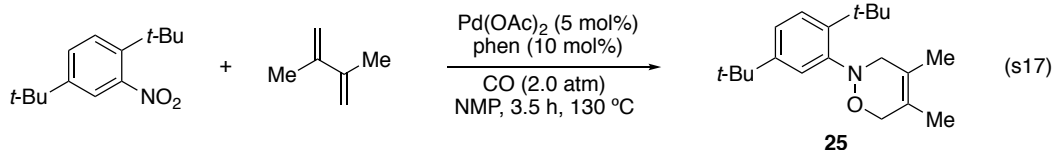
was loosely capped and placed in a Parr reactor. The reactor was sealed, evacuated and charged with CO gas. The Parr reactor was then heated to 130 °C. After 3.5 h, the solution was cooled to room temperature and diluted with 10 mL of saturated NaHCO₃. The mixture was extracted with 3 × 10 mL of ethyl acetate. The organic phase was dried over Na₂SO₄, filtered and the filtrate was concentrated in *vacuo*. Analysis of the reaction mixture using ¹H NMR revealed that indoline **11a** was formed with a 56% yield using CH₂Br₂ as an internal standard.

B. Testing for an *N*-aryl nitrene intermediate



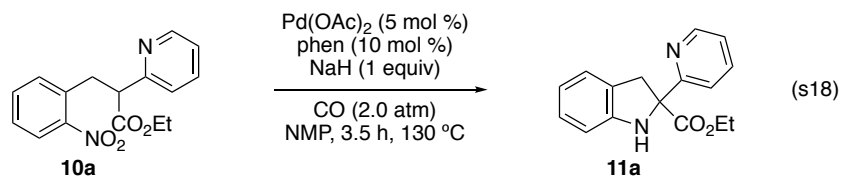
To a conical vial equipped for magnetic stirring was added 0.047 g of 2,5-di-*tert*-butylnitrobenzene (0.200 mmol), 0.0022 g of Pd(OAc)₂ (0.010 mmol), 0.0036 g of phenanthroline (0.020 mmol) and 1.5 mL of NMP. The vial was loosely capped and placed in a Paar reactor. The reactor was sealed, evacuated and charged with CO gas. The Parr reactor was then heated to 130 °C. After 3.5 h, the solution was cooled to room temperature and diluted with 10 mL of saturated NaHCO₃. The mixture was extracted with 3 × 10 mL of ethyl acetate. The organic phase was dried over Na₂SO₄, filtered and the filtrate was concentrated in *vacuo*. Analysis of the reaction mixture using ¹H NMR revealed that no 6-*tert*-butyl-3,3-dimethylindoline was formed.

C. Testing for a nitrosoarene intermediate



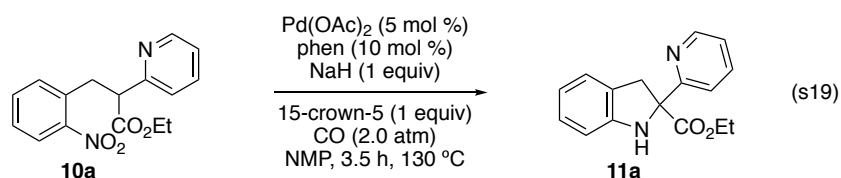
2-(2,5-Di-*tert*-butylphenyl)-4,5-dimethyl-3,6-dihydro-2H-1,2-oxazine (25).⁸⁴ To a conical vial was added 0.047 g of 2,5-di-*tert*-butylnitrobenzene (0.200 mmol), 0.082 g of 2,3-dimethylbutadiene (2.00 mmol), 0.0023 g of Pd(OAc)₂ (0.010 mmol), 0.0036 g of phenanthroline (0.020 mmol) and 1.5 mL of NMP. The vial was loosely capped and placed into a Parr reactor which was then sealed. The Parr reactor was charged with CO gas (2.0 atm) and placed in an oil bath heated to 130 °C. After 3.5 hours, the vial was removed and the reactives were quenched with 10 mL of a saturated aq soln of sodium bicarbonate. The mixture was washed with 3 × 10 mL of ethyl acetate. The organic phase was dried over Na₂SO₄, filtered and the filtrate was concentrated in *vacuo*. Analysis of the reaction mixture using ¹H NMR spectroscopy revealed that oxazine **25** was formed in 39% using CH₂Br₂ as an internal standard.

D. Probing the role of enolization and metal ion coordination on the reaction outcome.

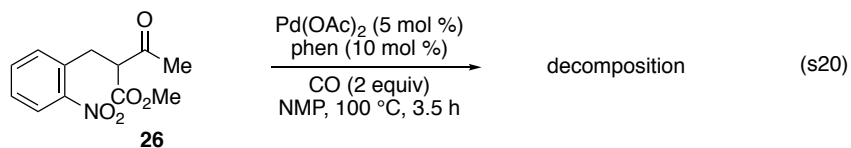


To a conical vial was added 0.060 g of **10a** (0.200 mmol), 0.0022 g of Pd(OAc)₂ (0.010 mmol), 0.0036 g of phenanthroline (0.020 mmol), 0.008 g of NaH (0.200 mmol, 60 wt. % in oil) and 1.5 mL of NMP. The vial was loosely capped and placed into a Parr reactor which was then sealed. The Parr reactor was charged with CO gas (2.0 atm) and placed in an oil bath heated to 130 °C.

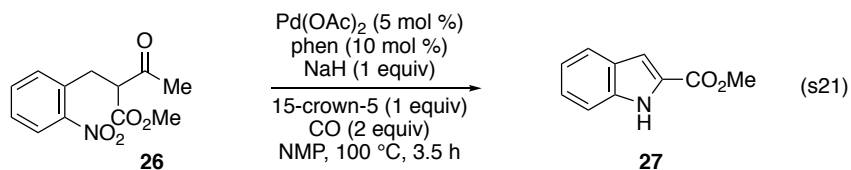
After 3.5 hours, the Parr reactor was allowed to cool to room temperature and the pressure was released. The vial was removed and the reactives were quenched with 10 mL of a saturated aq soln of sodium bicarbonate. The mixture was washed with 3 × 10 mL of ethyl acetate. The organic phase was dried over Na₂SO₄, filtered and the filtrate was concentrated in *vacuo*. Analysis of the reaction mixture using ¹H NMR spectroscopy revealed the formation of indoline **11a** in 72% using CH₂Br₂ as an internal standard.



To a conical vial was added 0.060 g of **10a** (0.200 mmol), 0.0022 g of Pd(OAc)₂ (0.010 mmol), 0.0036 g of phenanthroline (0.020 mmol), 0.008 g of NaH (0.200 mmol, 60 wt. % in oil), 0.044 g (0.200 mmol) of 15-crown-5 and 1.5 mL of NMP. The vial was loosely capped and placed into a Parr reactor which was then sealed. The Parr reactor was charged with CO gas (2.0 atm) and placed in an oil bath heated to 130 °C. After 3.5 hours, the Parr reactor was allowed to cool to room temperature and the pressure was released. The vial was removed and the reactives were quenched with 10 mL of a saturated aq soln of sodium bicarbonate. The mixture was washed with 3 × 10 mL of ethyl acetate. The organic phase was dried over Na₂SO₄, filtered and the filtrate was concentrated in *vacuo*. Analysis of the reaction mixture using ¹H NMR spectroscopy revealed the formation of indoline **11a** in 70% using CH₂Br₂ as an internal standard.



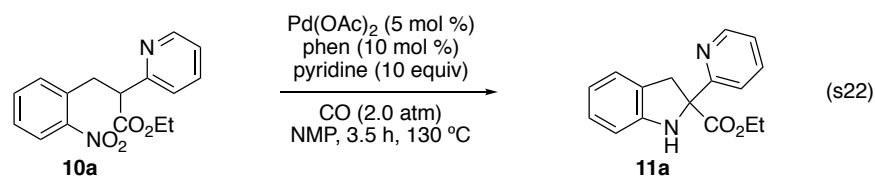
To a conical vial equipped for magnetic stirring was added 0.050 g of methyl 2-(2-nitrobenzyl)-3-oxobutanoate **26** (0.200 mmol), 0.0023 g and 1.5 mL of NMP. This solution was stirred for 15 minutes at RT. To this solution was added Pd(OAc)₂ (0.010 mmol) and 0.0036 g of phenanthroline (0.020 mmol). The vial was loosely capped and placed in a Parr reactor. The reactor was sealed, evacuated and charged with CO gas. The Parr reactor was then heated to 90 °C. After 3.5 h, the solution was cooled to room temperature and diluted with 10 mL of a saturated aq soln of NaHCO₃. The mixture was extracted with 3 × 10 mL of ethyl acetate. The organic phase was dried over Na₂SO₄, filtered and the filtrate was concentrated in *vacuo*. Analysis of the reaction mixture using ¹H NMR spectroscopy revealed complete decomposition of the starting material.



Methyl 1H-indole-2-carboxylate 27. To a conical vial equipped for magnetic stirring was added 0.050 g of methyl 2-(2-nitrobenzyl)-3-oxobutanoate **26** (0.200 mmol), 0.0023 g, 0.008 g of NaH (0.200 mmol, 60 wt. % in oil), 0.044 g of 15-crown-5 (0.200 mmol) and 1.5 mL of NMP. This solution was stirred for 15 minutes at RT. To this solution was added Pd(OAc)₂ (0.010 mmol) and 0.0036 g of phenanthroline (0.020 mmol). The vial was loosely capped and placed in a Parr reactor. The reactor was sealed, evacuated and charged with CO gas. The Parr reactor was then heated to 90 °C. After 16 h, the solution was cooled to room temperature and diluted with 10 mL

of a saturated aq soln of NaHCO₃. The mixture was extracted with 3 × 10 mL of ethyl acetate. The organic phase was dried over Na₂SO₄, filtered and the filtrate was concentrated in *vacuo*. Purification by MPLC (1:99 to 5:99 EtOAc:hexanes afforded the product as a white solid (0.014 g, 40%). The spectral data matched that reported by Driver and co-workers:⁸⁵ ¹H NMR (500 MHz, CDCl₃) δ 9.12 (br s, 1H), 7.71 (d, *J* = 8.0 Hz, 1H), 7.44 (d, *J* = 8.5 Hz, 1H), 7.34 (t, *J* = 7.0 Hz, 1H), 7.24 (s, 1H), 7.17 (t, *J* = 7.0 Hz, 1H), 3.97 (s, 3H); ¹³C NMR (125 MHz, CD₂Cl₂) δ 162.6 (C), 136.9 (C), 127.5 (C), 127.1 (C), 125.5 (CH), 122.7 (CH), 120.9 (CH), 111.9 (CH), 108.8 (CH), 52.1 (CH₃). ATR-FTIR (thin film) 3310, 2950, 1686, 1526, 1440, 1251 cm⁻¹.

E. Effect of superstoichiometric pyridine on the reaction outcome.



To a conical vial was added 0.030 g of **10a** (0.100 mmol), 0.0011 g of Pd(OAc)₂ (0.005 mmol), 0.0018 g of phenanthroline (0.010 mmol), 0.079 g of pyridine (1.000 mmol) and 0.75 mL of NMP. The vial was loosely capped and placed into a Parr reactor which was then sealed. The Parr reactor was charged with CO gas (2.0 atm) and placed in an oil bath heated to 130 °C. After 3.5 hours, the Parr reactor was allowed to cool to room temperature and the pressure was released. The vial was removed and the reactives were quenched with 10 mL of a saturated aq soln of sodium bicarbonate. The mixture was washed with 3 × 10 mL of ethyl acetate. The organic phase was dried over Na₂SO₄, filtered and the filtrate was concentrated in *vacuo*. The crude product was purified by azeotropic distillation using heptane as the entrainer. Analysis of the reaction

mixture using ^1H NMR spectroscopy revealed the formation of indoline **11a** in 42% using CH_2Br_2 as an internal standard.

CITED LITERATURE

1. Du Bois, J. *Org. Process Res. Dev.* **2011**, *15*, 758–762.
2. Collet, F.; Lescot, C.; Dauban, P. *Chem. Soc. Rev.* **2011**, *40*, 1926–1936.
3. Lu, H.; Zhang, X. P. *Chem. Soc. Rev.* **2011**, *40*, 1899–1909.
4. Shin, K.; Kim, H.; Chang, S. *Acc. Chem. Res.* **2015**, *48*, 1040–1052.
5. Jiao, J.; Murakami, K.; Itami, K. *ACS Catal.* **2016**, *6*, 610–633.
6. Park, Y.; Kim, Y.; Chang, S. *Chem. Rev.* **2017**, *117*, 9247–9301.
7. Lebel, H. N.; Huard, K.; Lectard, S. *J. Am. Chem. Soc.* **2005**, *127*, 14198–14199.
8. Huard, K.; Lebel, H. *Chem. - Eur. J.* **2008**, *14*, 6222–6230.
9. Lebel, H.; Trudel, C.; Spitz, C. *Chem. Commun.* **2012**, *48*, 7799–7801.
10. Lu, H.; Subbarayan, V.; Tao, J.; Zhang, X. P. *Organometallics* **2010**, *29*, 389–393.
11. Lu, H.; Jiang, H.; Wojtas, L.; Zhang, X. P. *Angew. Chem., Int. Ed.* **2010**, *49*, 10192–10196.
12. Nguyen, Q.; Sun, K.; Driver, T. G. *J. Am. Chem. Soc.* **2012**, *134*, 7262–7265.
13. Ryu, J.; Kwak, J.; Shin, K.; Lee, D.; Chang, S. *J. Am. Chem. Soc.* **2013**, *135*, 12861–12868.
14. Shin, K.; Baek, Y.; Chang, S. *Angew. Chem., Int. Ed.* **2013**, *52*, 8031–8036.
15. Shin, K.; Ryu, J.; Chang, S. *Org. Lett.* **2014**, *16*, 2022–2025.
16. Jiang, H.; Lang, K.; Lu, H.; Wojtas, L.; Zhang, X. P. *Angew. Chem., Int. Ed.* **2016** *55*, 11604–11608.
17. Lu, H.; Lang, K.; Jiang, H.; Wojtas, L.; Zhang, X. P. *Chem. Sci.* **2016**, *7*, 6934–6939.
18. Kong, C.; Jana, N.; Jones, C.; Driver, T. G. *J. Am. Chem. Soc.* **2016**, *138*, 13271–13280.
19. Adam, W.; Krebs, O. *Chem. Rev.* **2003**, *103*, 4131–4146.
20. Srivastava, R. S.; Tarver, N. R.; Nicholas, K. M. *J. Am. Chem. Soc.* **2007**, *129*, 15250–15258.

21. Penoni, A.; Palmisano, G.; Zhao, Y.-L.; Houk, K. N.; Volkman, J.; Nicholas, K. M. *J. Am. Chem. Soc.* **2009**, *131*, 653–661.
22. Momiyama, N.; Torii, H.; Saito, S.; Yamamoto, H. *Proc. Natl. Acad. Sci. U. S. A.* **2004**, *101*, 5374–5278.
23. Yamamoto, H.; Momiyama, N. *Chem. Commun.* **2005**, 3514–3525.
24. Zuman, P.; Shah, B. *Chem. Rev.* **1994**, *94*, 1621–1641.
25. Beaudoin, D.; Wuest, J. D. *Chem. Rev.* **2016**, *116*, 258–286.
26. Johannsen, M.; Jorgensen, K. A. *J. Org. Chem.* **1995**, *60*, 5979–5982.
27. Srivastava, R. S.; Khan, M. A.; Nicholas, K. M. *J. Am. Chem. Soc.* **1996**, *118*, 3311–3312.
28. Srivastava, R. S.; Nicholas, K. M. *Chem. Commun.* **1996**, 2335–2336.
29. Srivastava, R. S.; Nicholas, K. M. *J. Am. Chem. Soc.* **1997**, *119*, 3302–3310.
30. Murru, S.; Srivastava, R. S. *Eur. J. Org. Chem.* **2014**, *2014*, 2174–2181.
31. Porter, D.; Poon, B. M. L.; Rutledge, P. J. *Beilstein J. Org. Chem.* **2015**, *11*, 2549–2556.
32. Cenini, S.; Ragaini, F.; Tollari, S.; Paone, D. *J. Am. Chem. Soc.* **1996**, *118*, 11964–11965.
33. Srivastava, R. S.; Nicholas, K. M. *Chem. Commun.* **1998**, 2705–2706.
34. Ragaini, F.; Cenini, S.; Borsani, E.; Dompé, M.; Gallo, E.; Moret, M. *Organometallics* **2001**, *20*, 3390–3398.
35. Ragaini, F.; Cenini, S.; Brignoli, D.; Gasperini, M.; Gallo, E. *J. Org. Chem.* **2003**, *68*, 460–466.
36. Formenti, D.; Ferretti, F.; Ragaini, F. *ChemCatChem* **2018**, *10*, 148–152.
37. Jana, N.; Zhou, F.; Driver, T. G. *J. Am. Chem. Soc.* **2015**, *137*, 6738–6741.
38. Shevlin, M.; Guan, X.; Driver, T. G. *ACS Catal.* **2017**, *7*, 5518–5522.
39. Zhou, F.; Wang, D.-S.; Guan, X.; Driver, T. G. *Angew. Chem., Int. Ed.* **2017**, *56*, 4530–4534.
40. Wehman, P.; Borst, L.; Kamer, P. C. J.; Leeuwen, P. W. N. M. V. *Chem. Ber.* **1997**, *130*, 13–21.

41. The scope and limitations of SnCl₂ mediated reductive cyclization of difuryl-substituted nitroarenes is outlined here: Uchuskin, M. G.; Molodtsova, N. V.; Abaev, V. T.; Trushkov, I. V.; Butin, A. V. *Tetrahedron* **2012**, *68*, 4252–4258.
42. Paul, F.; Osborn, J. A.; Fischer, J.; Ochsenbein, P. *Angew. Chem., Int. Ed. Engl.* **1993**, *32*, 1638–1640.
43. Paul, F.; Fischer, J.; Ochsenbein, P.; Osborn, J. A. *Organometallics* **1998**, *17*, 2199–2206.
44. Little, R. G.; Doedens, R. J. *Inorg. Chem.* **1973**, *12*, 537–540.
45. Albéniz, A. C.; Catalina, N. M.; Espinet, P.; Redón, R. *Organometallics* **1999**, *18*, 5571–5576.
46. Sodeoka, M.; Hamashima, Y. *Bull. Chem. Soc. Jpn.* **2005**, *78*, 941–956.
47. Cámpora, J.; Maya, C. M.; Palma, P.; Carmona, E.; Gutiérrez, E.; Ruiz, C.; Graiff, C.; Tiripicchio, A. *Chem. - Eur. J.* **2005**, *11*, 6889–6904.
48. Muñiz, K.; Streuff, J.; Chávez, P.; Hövelmann, C. H. *Chem. - Asian J.* **2008**, *3*, 1248–1255.
49. Kolel-Veetil, M.; Khan, M. A.; Nicholas, K. M. *Organometallics* **2000**, *19*, 3754–3756.
50. Srivastava, R. S.; Nicholas, K. M. *Organometallics* **2005**, *24*, 1563–1568.
51. Penoni, A.; Volkmann, J.; Nicholas, K. M. *Org. Lett.* **2002**, *4*, 699–701.
52. Belley, M.; Sauer, E.; Beaudoin, D.; Duspara, P.; Trimble, L. A.; Dubé, P. *Tetrahedron Lett.* **2006**, *47*, 159–162.
53. Hirschhäuser, C.; Parker, J. S.; Perry, M. W. D.; Haddow, M. F.; Gallagher, T. *Org. Lett.* **2012**, *14*, 4846–4849.
54. Yang, L.; Shi, L.; Xing, Q.; Huang, K.-W.; Xia, C.; Li, F. *ACS Catal.* **2018**, *8*, 10340–10348.
55. Leconte, P.; Metz, F.; Mortreux, A.; Osborn, J. A.; Paul, F.; Petit, F.; Pillot, A. *J. Chem. Soc., Chem. Commun.* **1990**, 1616–1617.
56. Srivastava, R. S.; Khan, M. A.; Nicholas, K. M. *J. Am. Chem. Soc.* **2005**, *127*, 7278–7279.
57. Tollari, S.; Cenini, S.; Crotti, C.; Gianella, E. *J. Mol. Catal.* **1994**, *87*, 203–204.
58. Wehman, P.; Borst, L.; Kamer, P. C. J.; van Leeuwen, P. W. N. M. *J. Mol. Catal. A: Chem.* **1996**, *112*, 23–36.

59. Ragaini, F.; Gasperini, M.; Cenini, S. *Adv. Synth. Catal.* **2004**, *346*, 63–71.
60. Gasperini, M.; Ragaini, F.; Cazzaniga, C.; Cenini, S. *Adv. Synth. Catal.* **2005**, *347*, 105–120.
61. Mooibroek, T. J.; Bouwman, E.; Drent, E. *Organometallics* **2012**, *31*, 4142–4156.
62. Huang, H.; Yang, Y.; Zhang, X.; Zeng, W.; Liang, Y. *Tetrahedron Lett.* **2013**, *54*, 6049–6052.
63. Pangborn, A. B.; Giardello, M. A.; Grubbs, R. H.; Rosen, R. K.; Timmers, F. J. *Organometallics* **1996**, *15*, 1518.
64. Naganawa, A.; Saito, T.; Nagao, Y.; Egashira, H.; Iwahashi, M.; Kambe, T.; Koketsu, M.; Yamamoto, H.; Kobayashi, M.; Maruyama, T.; Ohuchida, S.; Nakai, H.; Kondo, K.; Toda, M. *Biorg. Med. Chem.* **2006**, *14*, 5562.
65. Engler, T. A.; Henry, J. R.; Malhotra, S.; Cunningham, B.; Furness, K.; Brozinick, J.; Burkholder, T. P.; Clay, M. P.; Clayton, J.; Diefenbacher, C.; Hawkins, E.; Iversen, P. W.; Li, Y.; Lindstrom, T. D.; Marquart, A. L.; McLean, J.; Mendel, D.; Misener, E.; Briere, D.; O'Toole, J. C.; Porter, W. J.; Queener, S.; Reel, J. K.; Owens, R. A.; Brier, R. A.; Eessalu, T. E.; Wagner, J. R.; Campbell, R. M.; Vaughn, R. J. *Med. Chem.* **2004**, *47*, 3934.
66. Kong, C.; Jana, N.; Driver, T. G. *Org. Lett.* **2013**, *15*, 824.
67. Bardecker, J. A.; Afzali, A.; Tulevski, G. S.; Graham, T.; Hannon, J. B.; Jen, A. K. Y. *Chem. Mater.* **2012**, *24*, 2017.
68. Blanc, A.; Bochet, C. G. *Org. Lett.* **2007**, *9*, 2649.
69. Nie, H.-J.; Guo, A.-D.; Lin, H.-X.; Chen, X.-H. *RCS Adv.* **2019**, *9*, 13249.
70. Katritzky, A. R.; Xu, Y.-J.; Vakulenko, A. V.; Wilcox, A. L.; Bley, K. R. *J. Org. Chem.* **2003**, *68*, 9100.
71. McAllister, L. A.; Bechle, B. M.; Dounay, A. B.; Evrard, E.; Gan, X.; Ghosh, S.; Kim, J.-Y.; Parikh, V. D.; Tuttle, J. B.; Verhoest, P. R. *J. Org. Chem.* **2011**, *76*, 3484.
72. Rzasa, R. M.; Kaller, M. R.; Liu, G.; Magal, E.; Nguyen, T. T.; Osslund, T. D.; Powers, D.; Santora, V. J.; Viswanadhan, V. N.; Wang, H.-L.; Xiong, X.; Zhong, W.; Norman, M. H. *Biorg. Med. Chem.* **2007**, *15*, 6574.
73. Rudd, A.; Cuevas, J.; Deveraj, M. *J. Am. Chem. Soc.* **2015**, *137*, 4484.
74. Sahoo, B.; Hopkinson, M.; Glorius, F.; *Angew. Chem. Int. Ed.* **2015**, *54*, 15545.

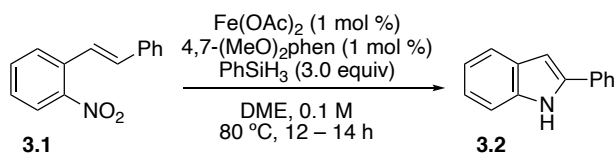
75. Compagnon, P. L.; Gasquez, F.; Kimny, T. *Bull. Soc. Chim. Belg.* **1986**, *95*, 49.
76. Adediran, S. A.; Cabaret, D.; Lohier, J. F.; Wakselman, M.; Pratt, R. F. *Biorg. Med. Chem.* **2010**, *18*, 282.
77. Dale, W. J.; Strobel, C. W. *J. Am. Chem. Soc.* **1954**, *76*, 6172.
78. Bitjukov, O. V.; Vil, V. A.; Sazonov, G. K.; Kirillov, A. S.; Lukashin, N. V.; Nikishin, G. I.; Terent'ev, A. O. *Tetrahedron Lett.* **2019**, *60*, 920.
79. Arens, B.; Dauvarte, M.; Arens, A. *Zh. Org. Khim.* **1969**, *5*, 534.
80. Jones, G.; McKinley, W. H. *Tetrahedron Lett.* **1977**, 2457.
81. Wright, S. W.; Dow, R. L.; McClure, L. D.; Hageman, D. L. *Tetrahedron Lett.* **1996**, *37*, 6965.
82. Nara, H.; Sato, K.; Naito, T.; Mototani, H.; Oki, H.; Yamamoto, Y.; Kuno, H.; Santou, T.; Kanzaki, N.; Terauchi, J.; Uchikawa, O.; Kori, M. *J. Med. Chem.* **2014**, *57*, 8886.
83. Uchuskin, M. G.; Molodtsova, N. V.; Abaev, V. T.; Trushkov, I. V.; Butin, A. V. *Tetrahedron* **2012**, *68*, 4252.
84. Jana, N.; Zhou, F.; Driver, T. G. *J. Am. Chem. Soc.* **2015**, *137*, 6738.
85. Stokes, B. J.; Dong, H.; Leslie, B. E.; Pumphrey, A. L.; Driver, T. G. *J. Am. Chem. Soc.* **2007**, *129*, 7500.

III. Development of Iron-Catalyzed Reductive Nitroso-ene Reaction Towards Synthesis of Six-Membered *N*-Heterocycles

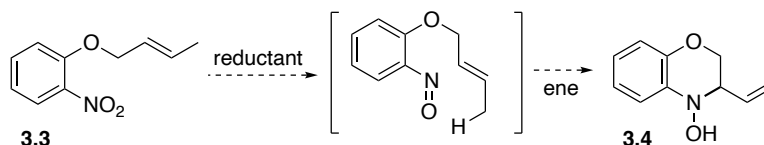
The reduction of bench stable and commercially abundant nitroarenes has the potential to unlock reactive intermediates facilitating the formation of new carbon-nitrogen bonds.^{1–3} The transformation of *ortho*-nitrostyrenes into *N*-heterocycles such as indoles, indolines, or saturated quinolines by way of the nitroso reactive intermediate has caught the interest of the field due to the abundance of *N*-heterocycles commonly found in natural- and synthetic small molecules. These reductive cyclization reactions generally require the implementation of reductants in stoichiometric amounts, such as phosphite^{4–7}, a Grignard reagent^{8–11}, iron^{12–14}, zinc¹², titanium(III)¹⁵, diborane¹⁶. A variety of methods have also been developed allowing facile access to the nitrosoarene reactive intermediate that utilizes a combination of a catalytic amount of a palladium salt and a source of reductive carbon monoxide such as Mo(CO)₆^{17,18} or pressurized CO gas^{19–23}. These methods generally require unforgiving reaction conditions such as high temperatures, pressurized toxic gasses, and strongly acidic or basic reagents. The complexity of setting proper conditions in an autoclave could also lead to irreproducible results. As a result, the library of molecules that can be constructed from these methods remains somewhat restrictive. In order to surmount these limitations, it has been shown that the oxophilic nature of first-row transition metals could be leveraged as oxygen atom acceptors resulting in a mild oxygen-atom transfer catalysis.^{24–26} The greater abundance and decreased cost of these first-row transition metals compared to other precious metal catalysts has garnered substantial attention from the research community.^{27–33} These catalysts have shown

significant usage in a wide range of reductive transformations,^{34–39} including a method developed by Baran and co-workers which allowed the iron-catalyzed reductive hydroamination of alkenes using nitroarenes.⁴⁰ This method did have a number of downsides, however, including a high catalyst loading and a second step in further deoxygenate the N-hydroxylamine into the desired product.

Against this backdrop of precedent, the Driver group hypothesized that a set of conditions could be identified to synthesize indoles from nitroarenes by way of a nitrosoarene intermediate. Using a high throughput experimental method, optimal conditions were rapidly identified to transform a wide series of nitrostilbenes into indoles through a reductive pathway (Scheme 3.1).⁴¹ This method utilized a low catalytic loading of an iron salt, phenanthroline ligand and superstoichiometric phenylsilane to convert nitrostilbene **3.1** into indoles **3.2**. This process synthesizes indoles by triggering a 5-atom-6 π -electron-electrocyclization of the nitrosoarene intermediate. As a result of this mechanistic pathway, this method was limited to the synthesis of 5-membered *N*-heterocycles. Building upon this work, I wanted to explore the synthetic potential of this method by utilizing the hypothesized nitrosoarene reactive intermediate to engage in a nitroso-ene reaction to synthesize 6-membered *N*-heterocycles using mild iron-catalyzed reductive conditions (Scheme 3.2).



Scheme 3.1 Iron-catalyzed reductive cyclization of 2-nitrostilbenes



Scheme 3.2 Intercepting reactive intermediate with nitroso-ene reaction

1,4-Benzoxazines and other 6-membered *N*-heterocycles represent an intriguing synthetic target due to their occurrence in a wide range of biologically active molecules (Figure 3.1). To that end, a number of methods have been developed aimed at not only synthesizing 1,4-benzoxazines, but other 6-membered *N*-heterocycles such as benzothiazines or saturated quinolines (Scheme 3.3). For example, Beifuss and Merisor developed a method to synthesize oxazines and phenazines using a catalytic amount of a palladium metal salt, highly pressurized carbon monoxide gas and superstoichiometric nitrogenous base (Entry 3.3a).⁴² They proposed that the nitroarene is first reduced to a nitrosoarene intermediate followed by further reduction of the nitrogen to form a palladium-nitrene intermediate. Amination followed by β -hydride elimination yielded the target 6-membered *N*-heterocycle. In 2010, Beifuss and co-workers continued their exploration of methods to synthesize *N*-heterocycles by developing a Mo-catalyzed reductive cyclization method to synthesize benzothiazines (Entry 3.3b).⁴³ They proposed that the reductive cyclization of the nitroarene proceeded through an Alder-ene type cyclization. Triphenyl phosphine acted as the reductant and could successfully synthesize the same series of heterocycles without the addition of the molybdenum catalyst, albeit with reduced yields. Malakar and co-workers in 2016 discovered a method to construct *N*-heterocycles similar to the ones synthesized by Beifuss in 2010 (Entry 3.3c).⁴⁴ They proposed that the reductive cyclization occurred first through a palladium-catalyzed deoxygenation of the

nitroarene facilitated by carbon monoxide as the reductant, delivered by the decomposition of cesium formate. A second deoxygenation event forms the reactive palladium nitrene which undergoes [2+2] cycloaddition to form the thiazine. In 2018, Sasai and co-workers developed a method to synthesize *N*-tosylate protected oxazines from tosylate-protected anilines using a palladium catalyst (Entry **3.3d**).⁴⁵ Cyclization proceeded through an aza-wacker type hydroamination. While this method did allow for a much lower reaction temperature than prior methods, it did require a moderate catalytic loading and an extra synthetic step in the form of tosylate protection of the aniline starting material. While these methods are significant in their own right, none of them are hypothesized to accomplish C–N bond formation through a nitroso-ene cyclization. In 2007 however, Beifuss and co-workers developed a method to synthesize benzoxazines from nitroarenes by submitting them to Cadogan-Sundberg type conditions (Entry **3.3e**).⁴⁶ Interestingly, mechanistic studies into sp^3 -C–N bond formation using a phosphorus reductant revealed formation of a nitrosoarene reactive intermediate that is intercepted by the allylic tether in a nitroso-ene type cyclization.

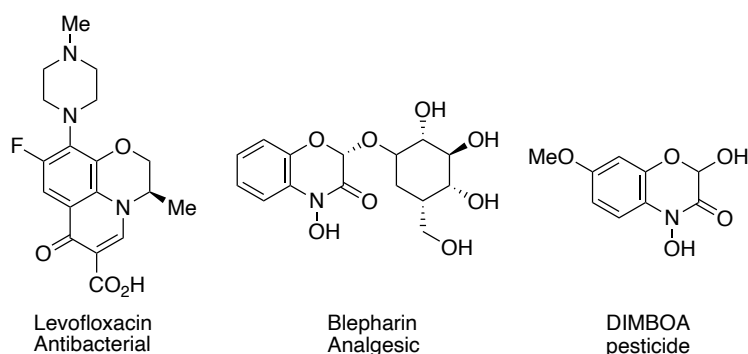
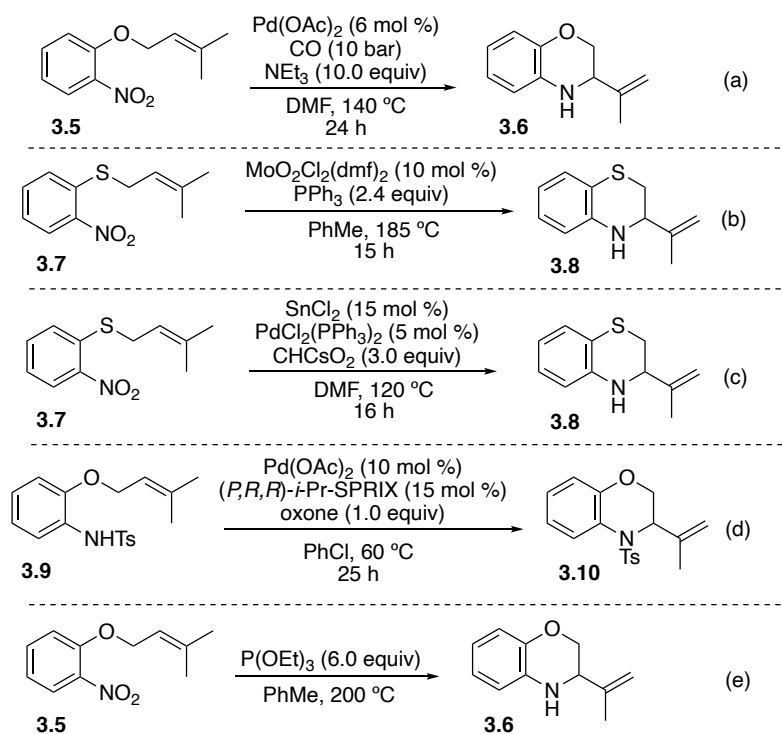
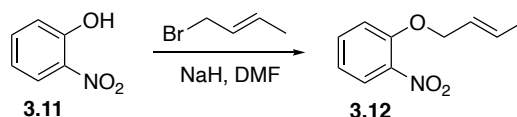


Figure 3.1 Naturally occurring 1,4-benzoxazine molecules

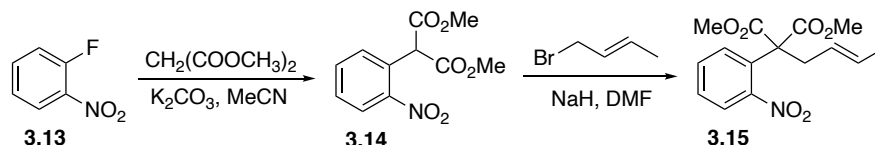


Scheme 3.3 Various methods to access 6-membered *N*-heterocycles

Nitroarenes **3.12** and **3.15** were used as substrates in the search for a transition-metal catalyst and mild deoxygenating reagent that could produce either 1,4-benzoxazine or tetrahydroquinone by way of a reductive nitroso-ene reaction (Scheme **3.4**). Nitroarene **3.12** is readily synthesized by sodium hydride promoted etherification of nitrophenol **3.11** with crotyl bromide. Nitroarene **3.15** is synthesized in a two-step process beginning with potassium carbonate promoted nucleophilic aromatic substitution of nitrobenzene **3.13** with dimethylmalonate, followed by the alkylation of **3.14** with crotyl bromide (Scheme **3.5**).



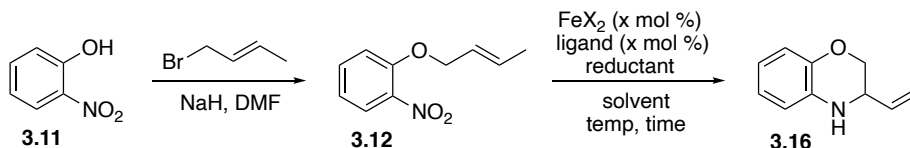
Scheme 3.4 Sodium hydride promoted synthesis of allyl benzyl ethers from nitrophenols



Scheme 3.5 Synthesis of homoallyl nitrobenzenes from fluoronitrobenzenes

To begin, I sought to explore the reactivity of **3.12** when it was exposed to a metal catalyst ligand complex and terminal reductant (Table **3.1**) to gain insight into the hypothesis that the nitroso-ene type cyclization could be triggered by using nitroarenes in reductive conditions. $\text{Fe}(\text{OAc})_2$ and 4,7-(MeO)₂phen was chosen as the initial catalyst, and phenylsilane was selected as a reductant. As these were the conditions found to synthesize indoles from nitrostilbene,⁴¹ I selected them as a starting point for exploration. Initial results provided a promising yield of 50% (Table **3.1**, entry 1). With these results in mind I resubmitted benzoxazine **3.16** to reaction conditions found in entry 1 to determine if the product was being destroyed by the reductive conditions, and I unfortunately was only able to recover 72% of the benzoxazine. In light of this revelation, my efforts were focused on identifying conditions that could afford complete conversion of the nitroarene while simultaneously limiting the destruction of the resultant benzoxazine. Modifying the hydride reductant to a less reactive sodium borohydride (Entry 2) or triethyl silane (Entry 3) saw a complete annunciation of nitroarene reduction. I interpreted this data as the hydride reagents selected were not reactive enough to generate the active iron hydride catalyst. Changing the identity of the counter-ion of the iron salt from acetate to a halogen (Entry 4) also halted nitroarene reduction. Doubling the catalyst loading while simultaneously decreasing the amount of phenylsilane by half afforded partial conversion of the nitroarene to benzoxazine (Entry 5). This partial conversion was completed in five hours, leading to the hypothesis that the reductive cyclization could be

completed in a much shorter amount of time and thereby reducing the amount of time that the benzoxazine would be exposed to destructive conditions. Increasing the phenylsilane loading to 4.0 equivalents or 6.0 equivalents (Entries 6 and 7) saw a complete reduction of the nitroarene but overall attenuated yields. Reduction of the phenylsilane to 2.0 equivalents (Entry 8) afforded complete reduction and conversion of the nitrosoarene to benzoxazine in a good yield of 70 %. Again, changing the counter-ion from acetate to triflate with a small selection of nitrogen containing bidentate ligands yielded a minimum amount of reductive cyclization product (Entries 9 and 10). Optimization concluded with a final screening of other bidentate nitrogen ligands (Entries 11 and 12). The usage of di-*tert*-butyl bipyridine resulted in a modest yield of 55 % with complete conversion of the nitroarene. Interestingly, usage of 2-picolyamine appeared to extend the reaction time as nitroarene reduction was incomplete after five hours while conversion rate remained high. This result suggests that rate of decomposition of the benzoxazine is dependent upon the iron catalyst.



entry	FeX ₂	ligand	mol %	reductant (equiv)	solvent (0.1 M)	time (h)	temp (C)	% yield, pdt : SM
1	Fe(OAc) ₂	4,7-(MeO) ₂ phen	1	PhSiH ₃ (3.0)	DME	18	80	50 : 0
2	Fe(OAc) ₂	4,7-(MeO) ₂ phen	1	NaBH ₄ (3.0)	DME	18	80	n.r.
3	Fe(OAc) ₂	4,7-(MeO) ₂ phen	1	Et ₃ SiH (3.0)	DME	18	80	n.r.
4	FeBr ₂	4,7-(MeO) ₂ phen	3	PhSiH ₃ (3.0)	THF	5	80	0 : 70
5	Fe(OAc) ₂	4,7-(MeO) ₂ phen	2	PhSiH ₃ (1.5)	DME	5	70	49 : 20
6	Fe(OAc) ₂	4,7-(MeO) ₂ phen	1	PhSiH ₃ (4.0)	DME	4	80	42 : 0
7	Fe(OAc) ₂	4,7-(MeO) ₂ phen	1	PhSiH ₃ (6.0)	DME	4	80	34 : 0
8	Fe(OAc) ₂	4,7-(MeO) ₂ phen	2	PhSiH ₃ (2.0)	DME	5	70	70 : 0
9	Fe(OTf) ₂	4,7-(MeO) ₂ phen	2	PhSiH ₃ (2.0)	DME	5	100	8 : 80
10	Fe(OTf) ₂	TMEDA	2	PhSiH ₃ (2.0)	DME	5	100	16 : 0
11	Fe(OAc) ₂	dtbpy	2	PhSiH ₃ (2.0)	DME	5	80	55 : 0
12	Fe(OAc) ₂	2-picolylamine	2	PhSiH ₃ (2.0)	DME	5	80	48 : 32

Table 3.1 Development of optimal conditions

Following conclusion of optimization efforts, I sought to explore the scope and limitations of the reductive sp³-C-N bond formation by first changing the electronic nature of the nitroarene and the identity of the atom that tethers the nitroarene to the allylic functionality (Table 3.2). Initial studies may show that the reductive cyclization is relatively unaffected by the electronic nature of the nitroarene (Entries 3.16b – 3.16d, 3.16f – 3.16i). These results illustrate that this reaction is relatively insensitive to the electronic nature of the nitroarene. Only when a stronger electron-withdrawing CF₃ group was installed did the yield decrease (Entry 3.16d). Installation of a substituent in the *ortho*- position sterically prevented the oxidative addition onto the active iron hydride catalyst and no reduction was observed (Entry 3.16j). This method is not limited to constructing 1,4-benzoxazines (Entries 3.17a, 3.17b). To our delight, rapid construction of 1,4-benzothiazines and tetrahydroquinolines can also

being accomplished using our iron-catalyzed reductive conditions with no significant reduction in overall yield.

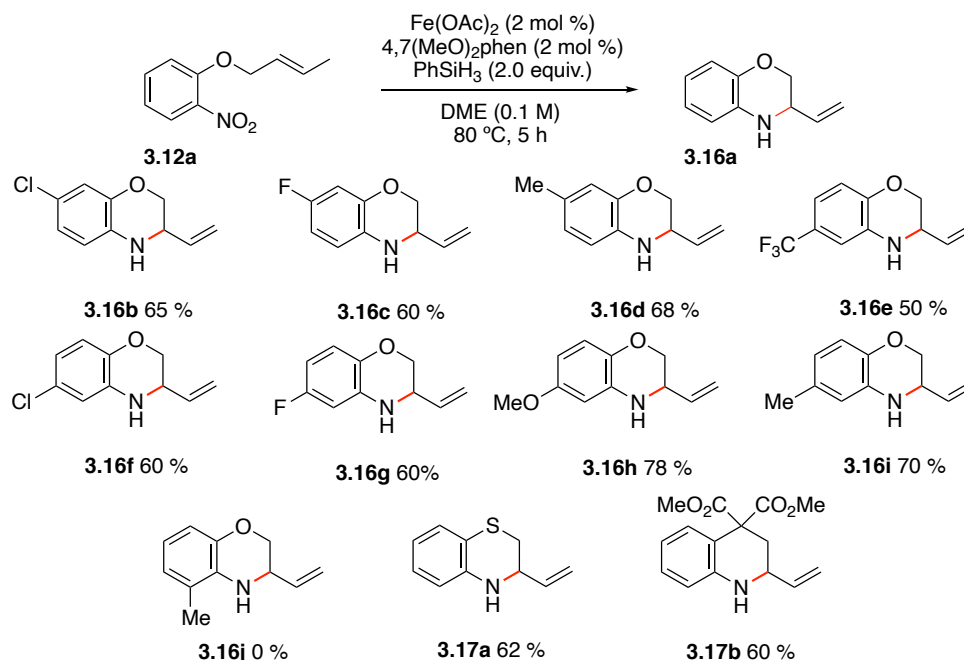
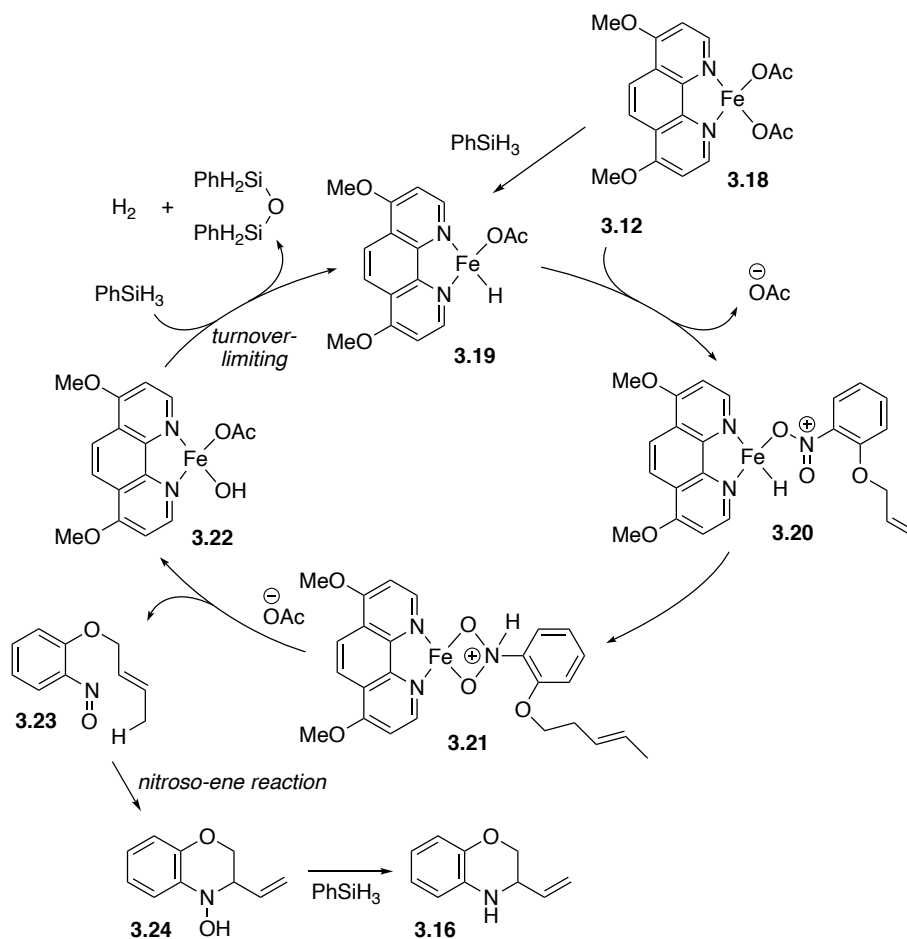


Table 3.2 Initial investigation into scope and limitations of nitroso-ene reaction

Based upon prior studies done by the Driver group into the iron-catalyzed reductive cyclization of nitrostyrenes into indoles, I hypothesize that the nitrosoarene intermediate for the ene reaction is generated through the reduction of the nitroarene with a reactive iron hydride intermediate. (Scheme 3.6). Phenylsilane reduces [4,7-(MeO)₂phen]Fe(OAc)₂ **3.18** to produce **3.19**, the reactive iron hydride intermediate. There was no induction period observed, compared to the iron-boxmi-catalyzed hydrosilylation of ketones using (EtO)₂MeSiH explored by Gade and co-workers.⁴⁷ This lack of the induction period could be attributed to the coordinately less saturated nature of **3.18** affording a more facile σ -bond metathesis with phenylsilane in comparison to the iron-boxmi catalyst that required a less reactive reductant which leads to a slower reduction of iron acetate, yielding the active catalytic species.⁴⁸ Oxidative addition of nitroarene **3.12** with the iron hydride **3.19** displaces the acetate ligand to

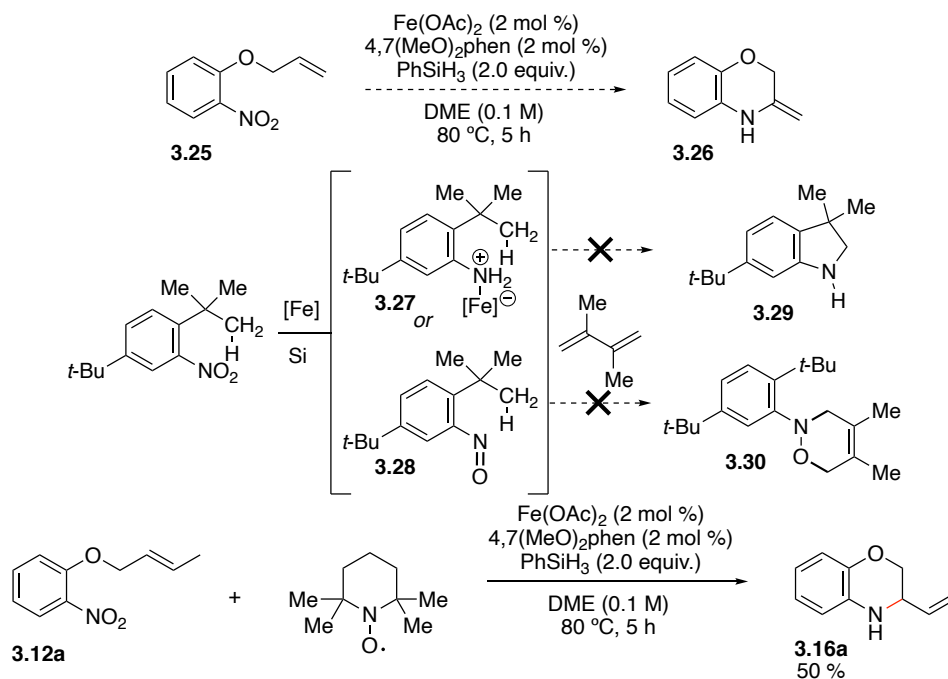
form intermediate **3.20**.⁴⁹ The nitro group then undergoes hydride reduction to form **3.21**, followed by fragmentation to produce iron hydroxide **3.22** and nitrosoarene **3.23**.⁵⁰ The rate-determining step of this catalytic cycle is the reduction of the iron hydroxide **3.22** with phenylsilane which regenerates the reactive iron hydride and produces siloxane (or silanol) and H₂. Nitrosoarene **3.23** undergoes nitroso-ene electrocyclicization to form *N*-hydroxybenzoxazine **3.24**, followed by a second reduction by phenylsilane to yield the desired benzoxazine **3.16**.



Scheme 3.6 Potential mechanism for the Fe-catalyzed reductive nitroso-ene reaction

To probe the mechanism of the iron-catalyzed reductive nitroso-ene reaction, I conducted a series of mechanistic experiments (Scheme **3.7**). First, I sought to provide evidence that the reaction proceeded through a nitroso-ene reaction and not hydroamination. By

removing the allylic hydrogen that is requisite for ene cyclization to carry out (**3.25**), the reductive cyclization was not observed. From this result, it is hypothesized that the reaction does not proceed through an aza-Wacker amination mechanism and provides strong evidence that it instead proceeds through a nitroso-ene pathway. Next, I wanted to probe the possible existence of an *N*-aryl nitrene and its potential role in the reductive cyclization. To do this, I submitted 2,5-di-*tert*-butylnitrobenzene to reductive $\text{sp}^3\text{-C-N}$ bond formation conditions. Since only full reduction to 2,5-di-*tert*-butylaniline was observed and no C-H activation was achieved, it was concluded that the reductive cyclization does not proceed through an *N*-aryl nitrene intermediate. To determine the presence of the nitrosoarene intermediate and to determine if it is bound to palladium, I submitted 2,5-di-*tert*-butylnitrobenzene to reductive $\text{sp}^3\text{-C-N}$ bond formation conditions and added an excess of 2,3-dimethylbutadiene. Unfortunately, the formation of **3.30** was not observed. I also sought to test for radical intermediates through the addition of 1.0 equivalent TEMPO to the optimized reductive cyclization conditions. benzoxazine **3.16a** was formed with a yield of 50%, which suggests one of two things. Either radical intermediates are not formed, or, if radical intermediates do form, they do not leave the solvent shell during the reductive cyclization.



Scheme 3.7 Mechanistic probes

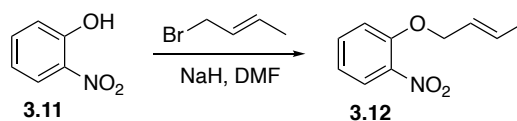
In conclusion, I have developed a method that allows the conversion of an $\text{sp}^3\text{-C-H}$ bond into an $\text{sp}^3\text{-C-N}$ bond by way of iron-catalyzed reductive cyclization. Mechanistic studies suggest that this method of constructing C–N bonds carried out by a nitroso-ene cyclization, representing a mechanistically novel harnessing of the reactive nitrosoarene intermediate from within the Driver group. The turnover limiting step is the reduction of the iron catalyst to the reactive iron hydride intermediate by phenylsilane. Building upon this work, complete exploration of the scope of nitroarenes should be carried out to include other tetrahydroquinolines, benzothiazines, and tetrahydroquinolxalines.

Experimental Section

General. ^1H NMR and ^{13}C NMR spectra were recorded at ambient temperature using 500 MHz or 300 MHz spectrometers. The data are reported as follows: chemical shift in ppm from internal tetramethylsilane on the δ scale, multiplicity (br = broad, s = singlet, d = doublet, t = triplet, q = quartet, m = multiplet), coupling constants (Hz) and integration. High-resolution mass spectra were obtained by peak matching. Melting points are reported uncorrected. Infrared spectroscopy was obtained using a diamond attenuated total reflectance (ATR) accessory. Analytical thin layer chromatography was performed on 0.25 mm extra hard silica gel plates with UV254 fluorescent indicator. Liquid chromatography was performed using forced flow (flash chromatography) of the indicated solvent system on 60Å (40 – 60 μm) mesh silica gel (SiO_2). Medium pressure liquid chromatography (MPLC) was performed to force flow the indicated solvent system down columns that had been packed with 60Å (40 – 60 μm) mesh silica gel (SiO_2). All reactions were carried out under an atmosphere of nitrogen in glassware, which had been oven-dried. Unless otherwise noted, all reagents were commercially obtained and, where appropriate, purified prior to use. Acetonitrile, methanol, toluene, THF, Et_2O , and CH_2Cl_2 were dried by filtration through alumina according to the procedure of Grubbs.⁶³ Metal salts were stored in a nitrogen atmosphere dry box.

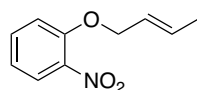
I. Preparation of (*E*)-1-(but-2-en-1-yloxy)-2-nitrobenzenes.

A. General procedure.



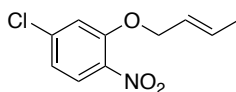
To a solution of 2-nitrophenol (3.60 mmol, 1.0 equiv.) in 6 mL of MeCN was added K_2CO_3 (6.00 mmol, 2.0 equiv.). After 15 minutes, crotyl bromide (4.32 mmol, 1.2 equiv., 85 wt %) was added and the reaction was heated to 70 °C. After 2 hours, the reaction mixture was cooled to room temperature and the reactives were quenched with 10 mL of H_2O . The solution was extracted with 3 × 15 mL of ethyl acetate, and the combined extracts were washed with 2 × 10 mL of brine. The resulting organic phase was dried over Na_2SO_4 , filtered and the filtrate was concentrated *in vacuo*. Purification by MPLC (1:99 to 5:95 EtOAc:hexanes) afforded the product.

B. Characterization Data.



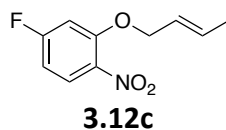
3.12a

(E)-1-(but-2-en-1-yloxy)-2-nitrobenzene 3.12a. The general procedure was followed using 0.500 g of 2-nitrophenol (3.60 mmol), 0.829 g of K_2CO_3 (6.00 mmol), 0.686 g of crotyl bromide (4.32 mmol, 85 % wt.) in 6 mL of MeCN. Purification by MPLC (5:95 EtOAc:hexanes) afforded the product as a light yellow oil (0.510 g, 88%): 1H NMR (500 MHz, $CDCl_3$) δ 7.79 (d, J = 8.0 Hz, 1H), 7.50 – 7.47 (m, 1H), 7.06 (d, J = 8.5 Hz, 1H), 6.99 (t, J = 7.5 Hz, 1H), 5.92 – 5.85 (m, 1H), 5.71 – 5.66 (m, 1H), 4.59 (d, J = 5.5 Hz, 2H), 1.73 (t, J = 5.5 Hz); ^{13}C NMR (125 MHz, $CDCl_3$) δ . ATR-FTIR (thin film): cm^{-1} .

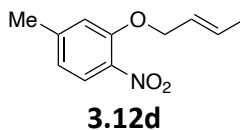


3.12b

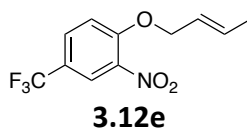
(E)-2-(but-2-en-1-yloxy)-4-chloro-1-nitrobenzene 3.12b. The general procedure was followed using 0.868 g of 5-chloro-2-nitrophenol (5.00 mmol), 1.38 g of K₂CO₃ (10.0 mmol), 0.952 g of crotyl bromide (6.00 mmol, 85 % wt.) in 10 mL of MeCN. Purification by MPLC (5:95 EtOAc:hexanes) afforded the product as a light yellow oil (0.910 g, 80 %)



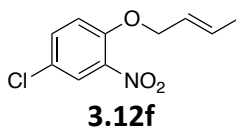
(E)-2-(but-2-en-1-yloxy)-4-fluoro-1-nitrobenzene 3.12c. The general procedure was followed using 0.786 g of 5-fluoro-2-nitrophenol (5.00 mmol), 1.38 g of K₂CO₃ (10.0 mmol), 0.952 g of crotyl bromide (6.00 mmol, 85 % wt.) in 10 mL of MeCN. Purification by MPLC (5:95 EtOAc:hexanes) afforded the product as a light yellow oil (0.929 g, 88 %)



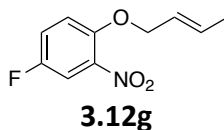
(E)-2-(but-2-en-1-yloxy)-4-methyl-1-nitrobenzene 3.12d. The general procedure was followed using 0.767 g of 5-methyl-2-nitrophenol (5.00 mmol), 1.38 g of K₂CO₃ (10.0 mmol), 0.952 g of crotyl bromide (6.00 mmol, 85 % wt.) in 10 mL of MeCN. Purification by MPLC (5:95 EtOAc:hexanes) afforded the product as a light yellow oil (0.839 g, 81 %)



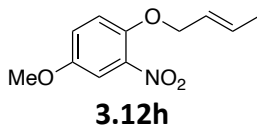
(E)-1-(but-2-en-1-yloxy)-2-nitro-4-(trifluoromethyl)benzene 3.12e. The general procedure was followed using 1.03 g of 5-(trifluoromethyl)-2-nitrophenol (5.00 mmol), 1.38 g of K_2CO_3 (10.0 mmol), 0.952 g of crotyl bromide (6.00 mmol, 85 % wt.) in 10 mL of MeCN. Purification by MPLC (5:95 EtOAc:hexanes) afforded the product as a light yellow oil (0.888 g, 68 %)



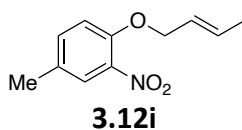
(E)-1-(but-2-en-1-yloxy)-4-chloro-2-nitrobenzene 3.12f. The general procedure was followed using 0.868 g of 4-chloro-2-nitrophenol (5.00 mmol), 1.38 g of K_2CO_3 (10.0 mmol), 0.952 g of crotyl bromide (6.00 mmol, 85 % wt.) in 10 mL of MeCN. Purification by MPLC (5:95 EtOAc:hexanes) afforded the product as a light yellow oil (0.899 g, 79 %)



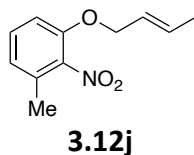
(E)-1-(but-2-en-1-yloxy)-4-fluoro-2-nitrobenzene 3.12g. The general procedure was followed using 0.786 g of 4-fluoro-2-nitrophenol (5.00 mmol), 1.38 g of K_2CO_3 (10.0 mmol), 0.952 g of crotyl bromide (6.00 mmol, 85 % wt.) in 10 mL of MeCN. Purification by MPLC (5:95 EtOAc:hexanes) afforded the product as a yellow solid (0.897 g, 85 %)



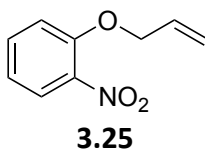
(E)-1-(but-2-en-1-yloxy)-4-methoxy-2-nitrobenzene 3.12h. The general procedure was followed using 0.846 g of 4-methoxy-2-nitrophenol (5.00 mmol), 1.38 g of K₂CO₃ (10.0 mmol), 0.952 g of crotyl bromide (6.00 mmol, 85 % wt.) in 10 mL of MeCN. Purification by MPLC (5:95 EtOAc:hexanes) afforded the product as a light yellow oil (0.837 g, 75 %)



(E)-1-(but-2-en-1-yloxy)-4-methyl-2-nitrobenzene 3.12i. The general procedure was followed using 0.767 g of 4-methyl-2-nitrophenol (5.00 mmol), 1.38 g of K₂CO₃ (10.0 mmol), 0.952 g of crotyl bromide (6.00 mmol, 85 % wt.) in 10 mL of MeCN. Purification by MPLC (5:95 EtOAc:hexanes) afforded the product as a light yellow oil (0.808 g, 78 %)



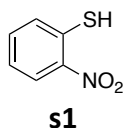
(E)-1-(but-2-en-1-yloxy)-3-methyl-2-nitrobenzene 3.12j. The general procedure was followed using 0.767 g of 3-methyl-2-nitrophenol (5.00 mmol), 1.38 g of K₂CO₃ (10.0 mmol), 0.952 g of crotyl bromide (6.00 mmol, 85 % wt.) in 10 mL of MeCN. Purification by MPLC (5:95 EtOAc:hexanes) afforded the product as a light yellow oil (0.777 g, 75 %)



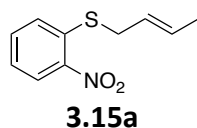
1-(allyloxy)-2-nitrobenzene 3.25.

The general procedure was followed using 0.696 g of 2-nitrophenol (5.00 mmol), 1.38 g of K_2CO_3 (10.0 mmol), 0.725 g of allyl bromide (6.00 mmol) in 10 mL of MeCN. Purification by MPLC (5:95 EtOAc:hexanes) afforded the product as a light yellow oil (0.627 g, 70 %)

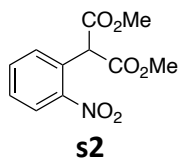
II. Synthesis of substrates 3.15a, 3.15b.



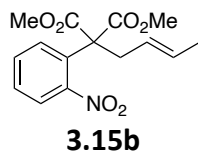
2-nitrobenzenethiol s1. To a suspension of 1.233 g of 2,2'-dinitrophenyl disulfide (4.00 mmol) in 12 mL THF was added 0.378 g of $NaBH_4$ (10.0 mmol) and was heated to 50 °C. To this solution 2.0 mL anhydrous MeOH was added dropwise over 1.5 h. The solution was then cooled to 0 °C and to it was added 1M HCl. The reactives were quenched with 20 mL of H_2O . The mixture was then extracted with 3 × 30 mL of ethyl acetate. The combined organic phases were washed with 10 mL of a saturated aqueous solution of Na_2CO_3 followed by 10 mL of brine. The resulting organic phase was dried over Na_2SO_4 and filtered. The filtrate was concentrated in *vacuo* to afford the product, which was used without further purification.



(E)-but-2-en-1-yl(2-nitrophenyl)sulfane 3.15a. The general procedure was followed using 0.310 g of 2-nitrobenzenethiol **s1** (2.00 mmol), 0.553 g of K_2CO_3 (4.0 mmol), 0.381 g of crotyl bromide (2.40 mmol, 85 % wt.) in 10 mL of MeCN. Purification by MPLC (5:95 EtOAc:hexanes) afforded the product as a dark liquid (0.124 g, 40%)



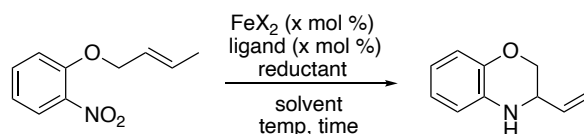
dimethyl 2-(2-nitrophenyl)malonate s2. To a stirring solution of 0.264 g of dimethyl malonate (2.0 mmol) in 5 mL of DMF at r.t. was added 0.100 g NaH (2.50 mmol, 60 wt %), and the resulting suspension was stirred at 90 °C for 10 min. The suspension was then cooled to room temperature followed by addition of 0.142 g of 1-fluoro-2-nitrophenol (1.00 mmol) and the solution was stirred at 90 °C for 16 h. The solution was cooled to room temperature and diluted with 10 mL of H₂O. The mixture was extracted with 3 × 10 mL of ethyl acetate. The organic phase was dried over Na₂SO₄, filtered and the filtrate was concentrated in *vacuo*. The resulting residue was dry loaded onto silica gel and purified by MPLC (2:98 to 10:90 EtOAc:hexanes) to afford the product as a yellow solid (0.157 g, 62 %).



dimethyl (E)-2-(but-2-en-1-yl)-2-(2-nitrophenyl)malonate 3.15b. The general procedure was followed using 0.506 g of **s2** (2.00 mmol), 0.088 g of NaH (2.2 mmol, 60 wt %), 0.413 g of crotyl bromide (2.6 mmol, 85 % wt.) in 5 mL of MeCN. Purification by MPLC (5:95 EtOAc:hexanes) afforded the product as a viscous yellow oil (0.281 g, 46 %).

III. Development of iron-catalyzed reductive nitroso-ene reaction

A. Optimization

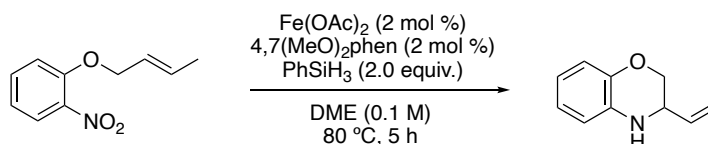


A Schlenk bomb was charged with a stock solution of the iron catalyst and ligand in methanol. The solvent was removed under vacuum. Under an atmosphere of N₂ the Schlenk bomb was charged with 0.019 g of the substrate (0.100 mmol), solvent and reductant. The bomb was heated to the desired temperature. The solution was cooled to room temperature and the reactives were quenched with EtOAc and the resultant mixture was filtered through a plug of celite. The organic phase was dried over Na₂SO₄, filtered and the filtrate was concentrated in *vacuo*. The resulting residue was analyzed by ¹H NMR spectroscopy using CH₂Br₂ as an internal standard to determine the reaction progress.

Table s1. Optimization of Pd-catalyzed reductive amination reaction.

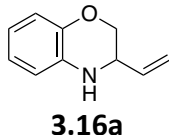
entry	FeX ₂	ligand	mol %	reductant (equiv)	solvent (0.1 M)	time (h)	temp (C)	% yield, pdt : SM
1	Fe(OAc) ₂	4,7-(MeO) ₂ phen	1	PhSiH ₃ (3.0)	DME	18	80	50 : 0
2	Fe(OAc) ₂	4,7-(MeO) ₂ phen	1	NaBH ₄ (3.0)	DME	18	80	n.r.
3	Fe(OAc) ₂	4,7-(MeO) ₂ phen	1	Et ₃ SiH (3.0)	DME	18	80	n.r.
4	FeBr ₂	4,7-(MeO) ₂ phen	3	PhSiH ₃ (3.0)	THF	5	80	0 : 70
5	Fe(OAc) ₂	4,7-(MeO) ₂ phen	2	PhSiH ₃ (1.5)	DME	5	70	49 : 20
6	Fe(OAc) ₂	4,7-(MeO) ₂ phen	1	PhSiH ₃ (4.0)	DME	4	80	42 : 0
7	Fe(OAc) ₂	4,7-(MeO) ₂ phen	1	PhSiH ₃ (6.0)	DME	4	80	34 : 0
8	Fe(OAc) ₂	4,7-(MeO) ₂ phen	2	PhSiH ₃ (2.0)	DME	5	70	70 : 0
9	Fe(OTf) ₂	4,7-(MeO) ₂ phen	2	PhSiH ₃ (2.0)	DME	5	100	8 : 80
10	Fe(OTf) ₂	TMEDA	2	PhSiH ₃ (2.0)	DME	5	100	16 : 0
11	Fe(OAc) ₂	dtbpy	2	PhSiH ₃ (2.0)	DME	5	80	55 : 0
12	Fe(OAc) ₂	2-picolyamine	2	PhSiH ₃ (2.0)	DME	5	80	48 : 32

B. Optimal conditions

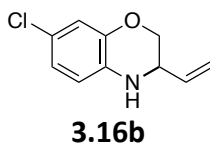


A Schlenk bomb equipped for magnetic stirring was charged with a stock solution of iron (II) acetate (0.002 mmol) and 4,7-dimethoxy phenthroline (0.002 mmol) in methanol. The solvent was removed under vacuum. Under an atmosphere of N₂ the Schlenk bomb was charged with 0.019 g of the substrate (0.100 mmol), 1.0 mL of DME and phenylsilane (0.200 mmol). The bomb was heated to 80 °C. The solution was cooled to room temperature and the reactives were quenched with EtOAc and the resultant mixture was filtered through a plug of celite. The organic phase was dried over Na₂SO₄, filtered and the filtrate was concentrated in *vacuo*. The resulting residue was dry loaded onto celite and purified by MPLC (2:98 to 5:95 EtOAc:hexanes) to afford the product.

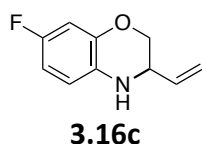
C. Characterization data



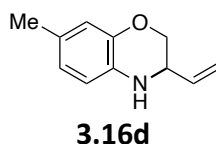
3-vinyl-3,4-dihydro-2H-benzo[*b*][1,4]oxazine 3.16a. The general procedure was followed using a stock solution of iron (II) acetate (0.002 mmol) and 4,7-dimethoxy phenthroline (0.002 mmol) in methanol 0.019 g of **3.12a** (0.100 mmol), 1.0 mL of DME and 0.022g phenylsilane (0.200 mmol). Purification by MPLC (5:95 EtOAc:hexanes) afforded the product as a viscous oil (0.011 g, 70 %).



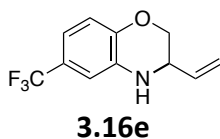
7-chloro-3-vinyl-3,4-dihydro-2H-benzo[*b*][1,4]oxazine 3.16b. The general procedure was followed using a stock solution of iron (II) acetate (0.002 mmol) and 4,7-dimethoxy phenthroline (0.002 mmol) in methanol 0.023 g of **3.12b** (0.100 mmol), 1.0 mL of DME and 0.022g phenylsilane (0.200 mmol). Purification by MPLC (5:95 EtOAc:hexanes) afforded the product as a viscous oil (0.012 g, 65 %).



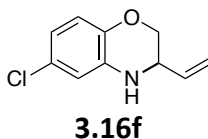
7-fluoro-3-vinyl-3,4-dihydro-2H-benzo[*b*][1,4]oxazine 3.16c. The general procedure was followed using a stock solution of iron (II) acetate (0.002 mmol) and 4,7-dimethoxy phenthroline (0.002 mmol) in methanol 0.021 g of **3.12c** (0.100 mmol), 1.0 mL of DME and 0.022g phenylsilane (0.200 mmol). Purification by MPLC (5:95 EtOAc:hexanes) afforded the product as a viscous oil (0.011 g, 60 %).



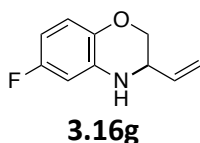
7-methyl-3-vinyl-3,4-dihydro-2H-benzo[*b*][1,4]oxazine 3.16d. The general procedure was followed using a stock solution of iron (II) acetate (0.002 mmol) and 4,7-dimethoxy phenthroline (0.002 mmol) in methanol 0.021 g of **3.12d** (0.100 mmol), 1.0 mL of DME and 0.022g phenylsilane (0.200 mmol). Analysis of the reaction mixture using ^1H NMR with an internal standard revealed formation of **3.16d** in a 68 % yield.



6-(trifluoromethyl)-3-vinyl-3,4-dihydro-2H-benzo[b][1,4]oxazine 3.16e. The general procedure was followed using a stock solution of iron (II) acetate (0.002 mmol) and 4,7-dimethoxy phenthroline (0.002 mmol) in methanol 0.026 g of **3.12e** (0.100 mmol), 1.0 mL of DME and 0.022g phenylsilane (0.200 mmol). Purification by MPLC (5:95 EtOAc:hexanes) afforded the product as a viscous oil (0.011 g, 50 %).

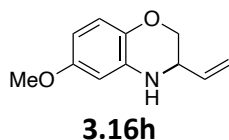


6-chloro-3-vinyl-3,4-dihydro-2H-benzo[b][1,4]oxazine 3.16f. The general procedure was followed using a stock solution of iron (II) acetate (0.002 mmol) and 4,7-dimethoxy phenthroline (0.002 mmol) in methanol 0.023 g of **3.12f** (0.100 mmol), 1.0 mL of DME and 0.022g phenylsilane (0.200 mmol). Purification by MPLC (5:95 EtOAc:hexanes) afforded the product as a viscous oil (0.012 g, 60 %).

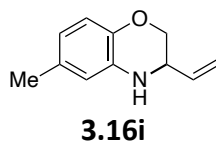


6-fluoro-3-vinyl-3,4-dihydro-2H-benzo[b][1,4]oxazine 3.16g. The general procedure was followed using a stock solution of iron (II) acetate (0.002 mmol) and 4,7-dimethoxy phenthroline (0.002 mmol) in methanol 0.021 g of **3.12g** (0.100 mmol), 1.0 mL of DME and

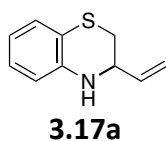
0.022g phenylsilane (0.200 mmol). Purification by MPLC (5:95 EtOAc:hexanes) afforded the product as a viscous oil (0.011 g, 60 %).



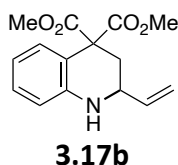
6-methoxy-3-vinyl-3,4-dihydro-2H-benzo[*b*][1,4]oxazine 3.16h. The general procedure was followed using a stock solution of iron (II) acetate (0.002 mmol) and 4,7-dimethoxy phenthroline (0.002 mmol) in methanol 0.022 g of **3.12h** (0.100 mmol), 1.0 mL of DME and 0.022g phenylsilane (0.200 mmol). Purification by MPLC (5:95 EtOAc:hexanes) afforded the product as a viscous oil (0.015 g, 78 %).



6-methyl-3-vinyl-3,4-dihydro-2H-benzo[*b*][1,4]oxazine 3.16i. The general procedure was followed using a stock solution of iron (II) acetate (0.002 mmol) and 4,7-dimethoxy phenthroline (0.002 mmol) in methanol 0.021 g of **3.12i** (0.100 mmol), 1.0 mL of DME and 0.022g phenylsilane (0.200 mmol). Analysis of the reaction mixture using ¹H NMR with an internal standard revealed formation of **3.16i** in a 70 % yield.



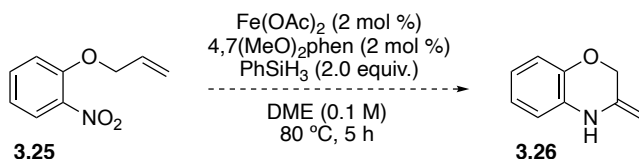
3-vinyl-3,4-dihydro-2H-benzo[*b*][1,4]thiazine 3.17a. The general procedure was followed using a stock solution of iron (II) acetate (0.002 mmol) and 4,7-dimethoxy phenthroline (0.002 mmol) in methanol 0.021 g of **3.15a** (0.100 mmol), 1.0 mL of DME and 0.022g phenylsilane (0.200 mmol). Purification by MPLC (5:95 EtOAc:hexanes) afforded the product as a viscous oil (0.011 g, 62 %).



dimethyl 2-vinyl-2,3-dihydroquinoline-4,4(1H)-dicarboxylate 3.17b. The general procedure was followed using a stock solution of iron (II) acetate (0.002 mmol) and 4,7-dimethoxy phenthroline (0.002 mmol) in methanol 0.031 g of **3.15b** (0.100 mmol), 1.0 mL of DME and 0.022g phenylsilane (0.200 mmol). Purification by MPLC (5:95 EtOAc:hexanes) afforded the product as a viscous oil (0.017 g, 60 %).

IV. Mechanistic investigations

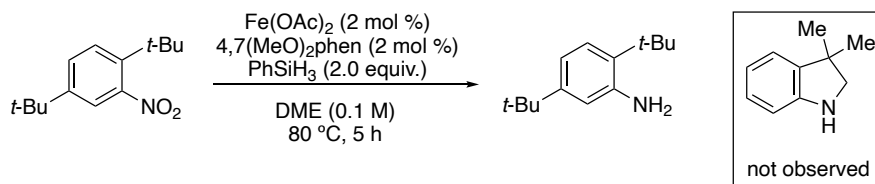
A. Determining a nitroso-ene cyclization versus hydroamination pathway



The general procedure was followed using a stock solution of iron (II) acetate (0.002 mmol) and 4,7-dimethoxy phenthroline (0.002 mmol) in methanol, 0.018 g of **3.25** (0.100 mmol), 1.0 mL of

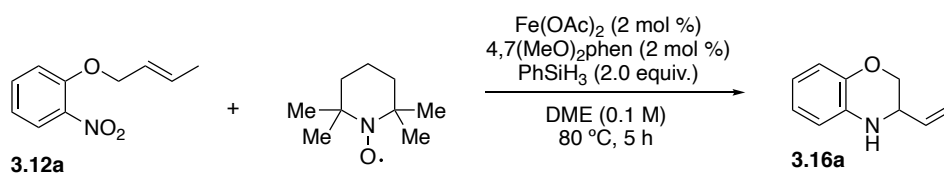
DME and 0.022g phenylsilane (0.200 mmol). The Schlenck bomb was heated to 80 °C. After 5 h, the solution was cooled to room temperature and the reactives were quenched with EtOAc and the resultant mixture was filtered through a plug of celite. The organic phase was dried over Na₂SO₄, filtered and the filtrate was concentrated in *vacuo*. Analysis of the reaction mixture using ¹H NMR revealed that no conversion to oxazine **3.26** was observed.

B. Testing for an *N*-aryl nitrene intermediate



A Schlenck bomb equipped for magnetic stirring was charged with a stock solution of iron (II) acetate (0.002 mmol) and 4,7-dimethoxy phenanthroline (0.002 mmol) in methanol. The solvent was removed under vacuum. Under an atmosphere of N₂ the Schlenck bomb was charged with 0.xxx g of 2,5-di-*tert*-butylnitrobenzene (0.100 mmol), 1.0 mL of DME and phenylsilane (0.200 mmol). The bomb was heated to 80 °C. After 5 h, the solution was cooled to room temperature and the reactives were quenched with EtOAc and the resultant mixture was filtered through a plug of celite. The organic phase was dried over Na₂SO₄, filtered and the filtrate was concentrated in *vacuo*. Analysis of the reaction mixture using ¹H NMR revealed that no 6-*tert*-butyl-3,3-dimethylindoline was formed.

C. Testing for radical intermediates



A Schlenk bomb equipped for magnetic stirring was charged with a stock solution of iron (II) acetate (0.002 mmol) and 4,7-dimethoxy phenanthroline (0.002 mmol) in methanol. The solvent was removed under vacuum. Under an atmosphere of N_2 the Schlenk bomb was charged with 0.019 g of **3.12a** (0.100 mmol), 0.016 g of TEMPO (0.100 mmol), 1.0 mL of DME and phenylsilane (0.200 mmol). The bomb was heated to 80 °C. After 5 h, the solution was cooled to room temperature and the reactives were quenched with EtOAc and the resultant mixture was filtered through a plug of celite. The organic phase was dried over Na_2SO_4 , filtered and the filtrate was concentrated in *vacuo*. Analysis of the reaction mixture using ^1H NMR with an internal standard revealed formation of **3.16a** in a 50 % yield.

CITED LITERATURE

1. Boyer, J. H. In *Nitrenes*; Lwowski, W., Ed.; Wiley: New York, 1970; pp 163–184.
2. Sundberg, R. J. In *Comprehensive Heterocyclic Chemistry*; Vol. 2; Katritzky, A., Rees, C. W., Scriven, E. F. V., Eds.; Pergamon: New York, 1996; pp 119–206.
3. Söderberg, B. C. G. *Curr. Org. Chem.* **2000**, *4*, 727–764
4. Cadogan, J. I. G.; Cameron-Wood, M.; Mackie, R. K.; Searle, R. J. G. *J. Chem. Soc.* **1965**, 4831–4837.
5. Sundberg, R. J.; Yamazaki, T. *J. Org. Chem.* **1967**, *32*, 290–294.
6. Sundberg, R. J.; Kotchmar, G. S. *J. Org. Chem.* **1969**, *34*, 2285–2288.
7. Cadogan, J. I. G. *Acc. Chem. Res.* **1972**, *5*, 303–310.
8. Bartoli, G.; Palmieri, G.; Bosco, M.; Dalpozzo, R. *Tetrahedron Lett.* **1989**, *30*, 2129–2132.
9. Bartoli, G.; Bosco, M.; Dalpozzo, R.; Palmieri, G.; Marcantoni, E. *J. Chem. Soc., Perkin Trans. 1* **1991**, 2757–2761.
10. Dalpozzo, R.; Bartoli, G. *Curr. Org. Chem.* **2005**, *9*, 163–178.
11. Gao, H.; Xu, Q.-L.; Yousufuddin, M.; Ess, D. H.; Kürti, L. *Angew. Chem., Int. Ed.* **2014**, *53*, 2701–2705.
12. Reissert, A. *Ber. Dtsch. Chem. Ges.* **1897**, *30*, 1030–1053.
13. Suh, J. T.; Puma, B. M. *J. Org. Chem.* **1965**, *30*, 2253–2259.
14. Ponticello, G. S.; Baldwin, J. J. *J. Org. Chem.* **1979**, *44*, 4003–4005.
15. Tong, S.; Xu, Z.; Mamboury, M.; Wang, Q.; Zhu, J. *Angew. Chem., Int. Ed.* **2015**, *54*, 11809–11812.
16. Yang, K.; Zhou, F.; Kuang, Z.; Gao, G.; Driver, T. G.; Song, Q. *Org. Lett.* **2016**, *18*, 4088–4091.
17. Zhou, F.; Wang, D.-S.; Driver, T. G. *Adv. Synth. Catal.* **2015**, *357*, 3463–3468.
18. Zhou, F.; Wang, D.-S.; Driver, T. G. *Angew. Chem. Int. Ed.* **2017**, *56*, 4530–4534.

19. Akazome, M.; Kondo, T.; Watanabe, Y. *J. Org. Chem.* **1994**, *59*, 3375–3380.
20. Söderberg, B. C.; Shriver, J. A. *J. Org. Chem.* **1997**, *62*, 5838–5845.
21. Smitrovich, J. H.; Davies, I. W. *Org. Lett.* **2004**, *6*, 533–535.
22. Davies, I. W.; Smitrovich, J. H.; Sidler, R.; Qu, C.; Gresham, V.; Bazaral, C. *Tetrahedron* **2005**, *61*, 6425–6437.
23. Hsieh, T. H. H.; Dong, V. M. *Tetrahedron* **2009**, *65*, 3062–3068.
24. Pearson, R. G. *Inorg. Chem.* **1988**, *27*, 734–740.
25. Pearson, R. G. *Acc. Chem. Res.* **1993**, *26*, 250–255.
26. Kobayashi, S.; Manabe, K. *Acc. Chem. Res.* **2002**, *35*, 209–217.
27. Bolm, C.; Legros, J.; Le Paih, J.; Zani, L. *Chem. Rev.* **2004**, *104*, 6217–6254.
28. Sherry, B. D.; Fürstner, A. *Acc. Chem. Res.* **2008**, *41*, 1500–1511.
29. Fürstner, A. *Angew. Chem., Int. Ed.* **2009**, *48*, 1364–1367.
30. Chirik, P. J. *Acc. Chem. Res.* **2015**, *48*, 1687–1695.
31. Cornil, J.; Gonnard, L.; Bensoussan, C.; Serra-Muns, A.; Gnam, C.; Commandeur, C.; Commandeur, M.; Reymond, S.; Guérinot, A.; Cossy, J. *Acc. Chem. Res.* **2015**, *48*, 761–773.
32. Li, Y.-Y.; Yu, S.-L.; Shen, W.-Y.; Gao, J.-X. *Acc. Chem. Res.* **2015**, *48*, 2587–2598.
33. Shang, R.; Ilies, L.; Nakamura, E. *Chem. Rev.* **2017**, *117*, 9086–9139.
34. Sunada, Y.; Kawakami, H.; Imaoka, T.; Motoyama, Y.; Nagashima, H. *Angew. Chem., Int. Ed.* **2009**, *48*, 9511–9514.
35. Tondreau, A. M.; Atienza, C. C. H.; Weller, K. J.; Nye, S. A.; Lewis, K. M.; Delis, J. G. P.; Chirik, P. J. *Science* **2012**, *335*, 567–570.
36. Zuo, W.; Lough, A. J.; Li, Y. F.; Morris, R. H. *Science* **2013**, *342*, 1080–1083.
37. Ruddy, A. J.; Kelly, C. M.; Crawford, S. M.; Wheaton, C. A.; Sydora, O.; L.; Small, B. L.; Stradiotto, M.; Turculet, L. *Organometallics* **2013**, *32*, 5581–5588.
38. Bleith, T.; Wadepohl, H.; Gade, L. H. *J. Am. Chem. Soc.* **2015**, *137*, 2456–2459.

39. Bleith, T.; Gade, L. H. *J. Am. Chem. Soc.* **2016**, *138*, 4972–4983.
40. Gui, J.; Pan, C.-M.; Jin, Y.; Qin, T.; Lo, J. C.; Lee, B. J.; Spergel, S. H.; Mertzman, M. E.; Pitts, W. J.; La Cruz, T. E.; Schmidt, M. A.; Darvatkar, N.; Natarajan, S. R.; Baran, P. S. *Science* **2015**, *348*, 886–889.
41. Shevlin, M.; Guan, X.; Driver, T. *ACS Catal.* **2017**, *7*, 5518–5522.
42. Merisor, E.; Beifuss, U. *Tet. Lett.* **2007**, *48*, 8383–8387.
43. Malakar, C.; Merisor, E.; Beifuss, U. *Synlett.* **2010**, *12*, 1766–1770.
44. Malakar, C. *et. al. Tet. Lett.* **2016**, *57*, 5695–5699.
45. Sen, A.; Takenaka, K.; Sasai, H. *Org. Lett.* **2018**, *20*, 6827–6831.
46. Merisor, E.; Conrad, J.; Klaiber, I.; Beifuss, U. *Angew. Chem. Int. Ed.* **2007**, *46*, 3353–3355.
47. Bleith, T.; Wadepohl, H.; Gade, L. H. *J. Am. Chem. Soc.* **2015**, *137*, 2456–2459.
48. Bleith, T.; Gade, L. H. *J. Am. Chem. Soc.* **2016**, *138*, 4972–4983.
49. Srivastava, R. S.; Khan, M. A.; Nicholas, K. M. *Inorg. Chim. Acta.* **2003**, *349*, 269–272.
50. Nord, G.; Pedersen, B.; Bjergbakke, E. *J. Am. Chem. Soc.* **1983**, *105*, 1913–1919.

IV. Synthesis of Benzobisoxazole Cruciform Sensors

Spatial separation of the highest occupied and lowest unoccupied molecular orbitals on orthogonal axes on cruciform molecules reveals peculiar electronic and optical properties. Cruciform molecules are easily identifiable by their rigid X-shape and high degrees of symmetry.¹ Through careful selection of electron rich and electron poor substituents to attach to a central aromatic core, spatial separation of the HOMO and LUMO of the molecule could be induced, placing them on perpendicular axes (Figure **4.1**).² DFT calculations were performed on cruciform **4.1** and **4.2**, their respective HOMO is portrayed in red and yellow and their respective LUMO in green and blue. Cruciform **4.1** does not have a significantly electron-withdrawing or electron-releasing groups installed on its axes and as such the frontier molecular orbitals remain even distributed between the two axes. Only when an electron-releasing substituent such as the dimethylaminobenzene on cruciform **4.2** and an electron-withdrawing substituent such as the 4-ethynylpyridine is installed on perpendicular axes is full spatial separation of the frontier molecular orbitals observed.

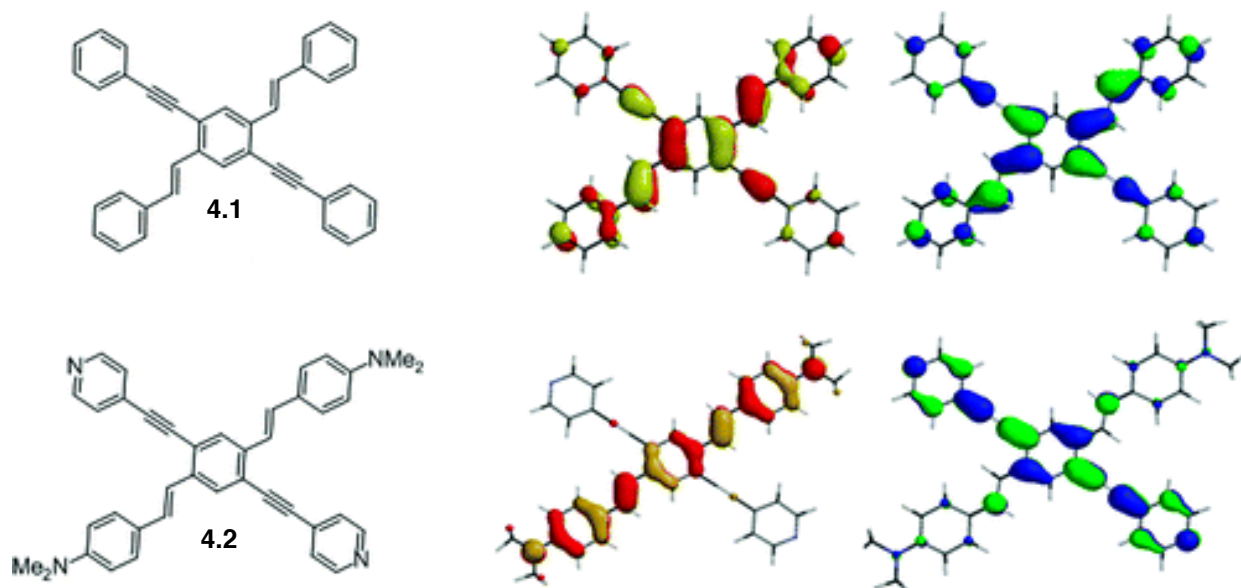


Figure 4.1 Frontier molecular orbitals of cruciforms **4.1** and **4.2**

The rigid geometries afforded by abundant sp^2 hybridization permits organization of these molecules into ordered mono- or poly- layered films, attracting attention in crystal engineering.^{3–6} The properties resultant of their physical structure has seen utility in the fields of organic field effect transistors, photovoltaics, and sensors.^{7–9} Any potential electronic application of these cruciform molecules is dependent upon complete orthogonality of the HOMO and LUMO and the magnitude of this separation is a function of the electronegativity differences of the substituents on the axes.¹⁰ This chapter will contain a brief background on the development and synthesis of cruciform molecules, their properties and structures, and details the contribution that I have made to advance this field.

The substituent pattern on cruciform molecules will also affect the spatial distribution of the HOMO and LUMO, a phenomenon first explored by Bunz and co-workers in their seminal work.¹¹ The frontier orbitals of the cruciform shown in figure **4.2** were calculated using RHF 6-

31G** Spartan, revealing the HOMO was localized on the distyrylbenzene axis and the LUMO localized on the phenylethynyleneaxis. Using a modular 2 step method, they constructed a series of six phenylene-ethnylene cruciform pentamers. This series of highly conjugated systems exhibited a variety of emission patterns based upon the identity of the substituents.

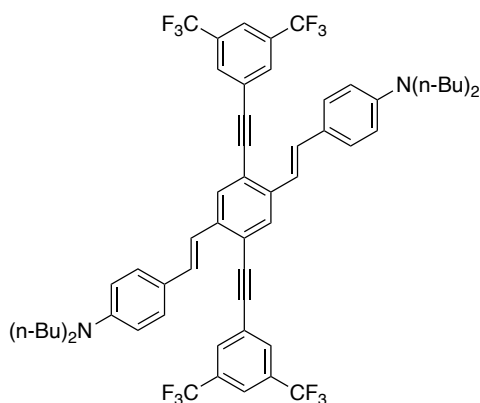
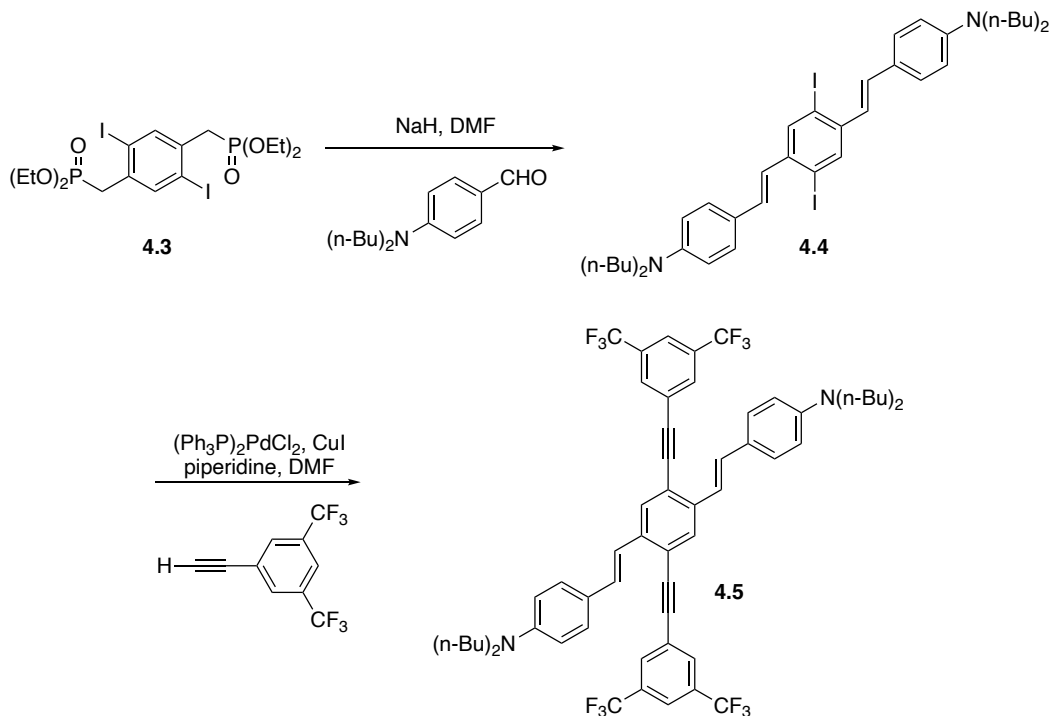


Figure 4.2 Molecule studied for FMO separation

Synthesis of these molecules was accomplished in only two steps (Scheme **4.1**). Starting with bisphosphonate **4.3**, the *N,N*-dibutyl-4-vinylaniline functional groups were installed using Horner-Wadsworth-Emmons reaction to yield distyrylbenzene **4.4**.¹² The trifluoromethyl ethynylbenzene functional groups were installed using a Sonogashira coupling reaction to produce the desired cruciform **4.5**.



Scheme 4.1 Two-step synthesis of cruciform **4.5**

There exists precedent for these cruciform molecules to be used as sensors. In 2005, Bunz and co-workers synthesized a series of cruciform molecules, included the molecule portrayed as **4.6** (Figure 4.3).¹⁴ They observed that, upon addition of a variety of metal ions to a solution of the cruciform molecule in a solution of DCM, the emission patterns were either red or blue shifted. From these observations they proposed that coordination of the metal ions to the dibutylamino groups led to formation of a positive charge, producing an electron withdrawing effect which lowered the energy of the HOMO frontier orbital. This phenomenon is not limited to the sensing of metal ions. In 2014 Miljanić's and co-workers synthesized benzobisoxazole cruciform **4.7**.¹⁵ They noted a significant shift of fluorescence emission when the molecule was exposed as little as 50 equivalents of a fluoride ion source. The desilylation and exposure of the terminal alkynes led to an emission shift that could be observed with the naked eye. This

response was only observed when fluorine was introduced, no shift was observed upon the introduction of a series of other ions. This work was based upon previous syntheses Miljanić and co-workers of cruciform **4.8**.¹⁶ They observed similar photometric phenomenon when the molecule was exposed to a series of carboxylic acids, organoboronic acids or phenols. By measuring the differences in fluorescence response of cruciform **4.8** they could effectively distinguish structural variances of simple acids and phenols. Based upon these works and the observations that these cruciform molecules could be used to identify a wide range of ions, we sought to construct a series of novel benzobisoxazole cruciform molecules that could exhibit similar fluorescence shifts when exposed to Zn^{2+} ions. Since the initial report by Bunz, a broad range of cruciform molecules have been synthesized and studied.^{17–21}

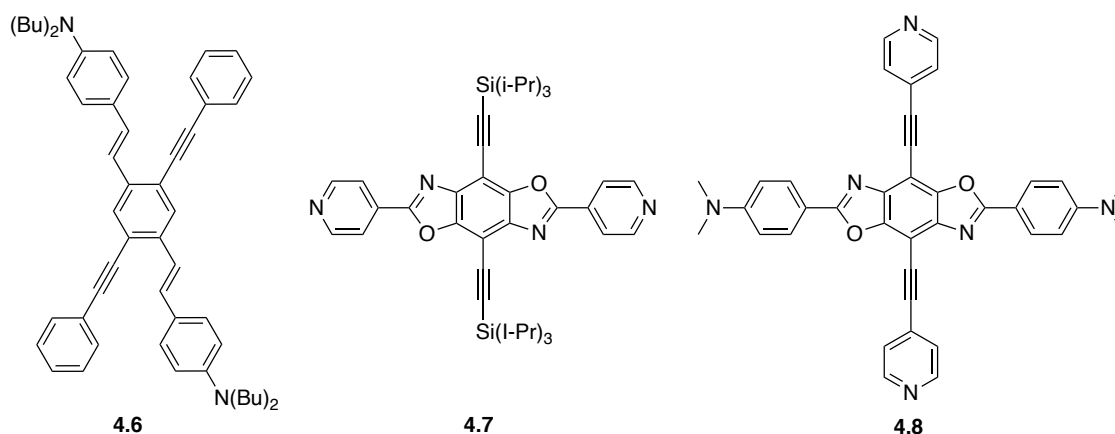
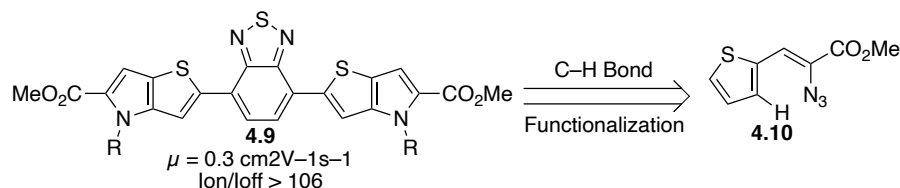


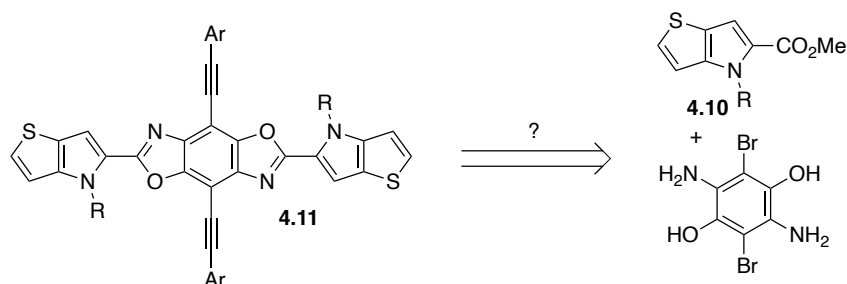
Figure 4.3 Examples of cruciform molecules used as sensors

Previously, the Driver group reported successful synthesis of soluble bispyrrolothiophene **4.10** from vinyl thiophene azide **4.9** by way of rhodium-catalyzed C–H bond functionalization (Scheme **4.2**).^{22,23} While these low molecular weight N-heterocycles form amorphous crystalline structures, they still displayed properties in thin-film organic field effect transistors.²⁴



Scheme 4.2 Retrosynthetic analysis of bispyrrolothiophenes

Following the conclusion of this study, we wanted to explore how the pyrrolothiophene moiety could modify the electronic nature of the benzobisoxazole framework. Specifically, we wanted to synthesize cruciform **4.11** from functionalized azide **4.10** and highly substituted diamino dihydroxybenzene. We believed that with careful manipulation of the HOMO and LUMO of the benzobisoxazole molecule, it could be used as a sensor for identification of metal ions. Herein, I will report a number of synthetic approaches to construct these benzobisoxazole cruciform molecules and initial results for their usage as sensors.



Scheme 4.3 Retrosynthetic approach to form bispyrrolothiophene benzobisoxazole cruciform

Prior to synthesis, low-level DFT calculations were performed in order to provide insight into the spatial separation of the HOMO and LUMO of the envisioned bispyrrolothiophene benzobisoxazole cruciform (Figure **4.4**). These preliminary calculations verified the separation of the HOMO and LUMO and that they exist on opposing axes. Additionally, it was observed that when the pyridine functionalities were protonated, a substantial perturbation of the LUMO occurred. Based upon this observation, we hypothesized that these cruciform molecules could be potential sensors.

(a) HOMO: -5.3 eV

(b) LUMO: -2.3 eV

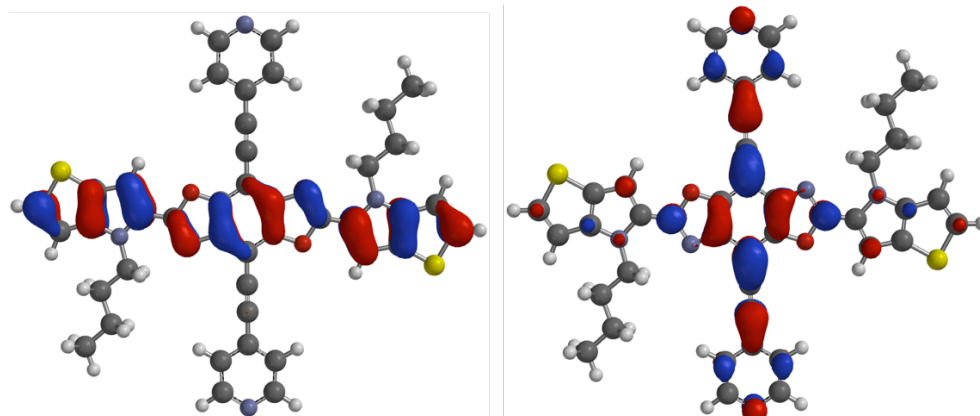
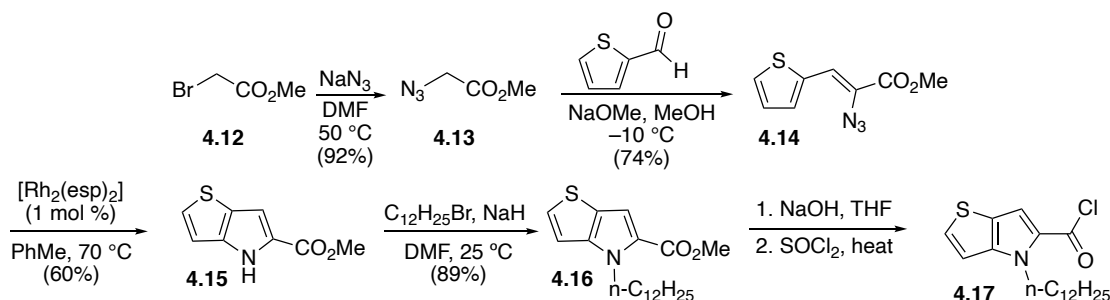


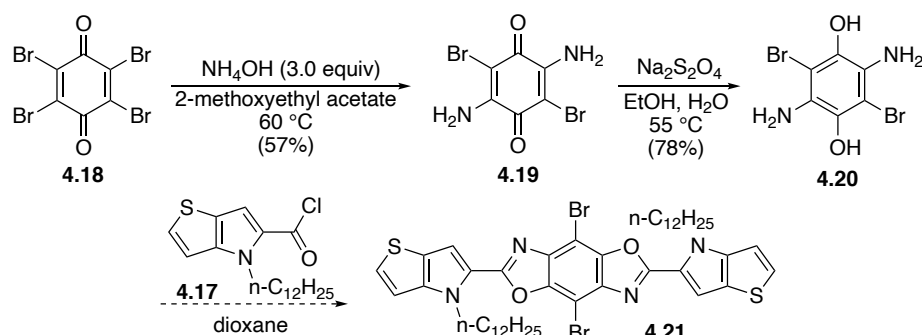
Figure 4.4 DFT calculations of bispyrrolothiophene benzobisoxazole cruciform

The initial synthetic approach utilized a modular method that begins with first constructing the pyrrolothiophene moiety (Scheme 4.4). Bromoacetate **4.12** was converted to azide **4.13** by way of a simple S_N^2 reaction, followed by Knoevenagel condensation with 2-thiophene carboxaldehyde to form **4.14**. Subjection of **4.14** to $Rh_2(II)$ -catalyzed C–H bond amination conditions afforded **4.15**. In order to greatly increase the solubility of the pyrrolothiophene, the pyrrole nitrogen was alkylated using NaH mediated alkylation to form **4.16**. The ester was then hydrolyzed under basic conditions and the resultant acid was converted to the acid chloride **4.17** using thionyl chloride under reflux. Yield was not taken of the acid chloride synthesis; it was used without purification.



Scheme 4.4 Synthesis of pyrrolothiophene functionality

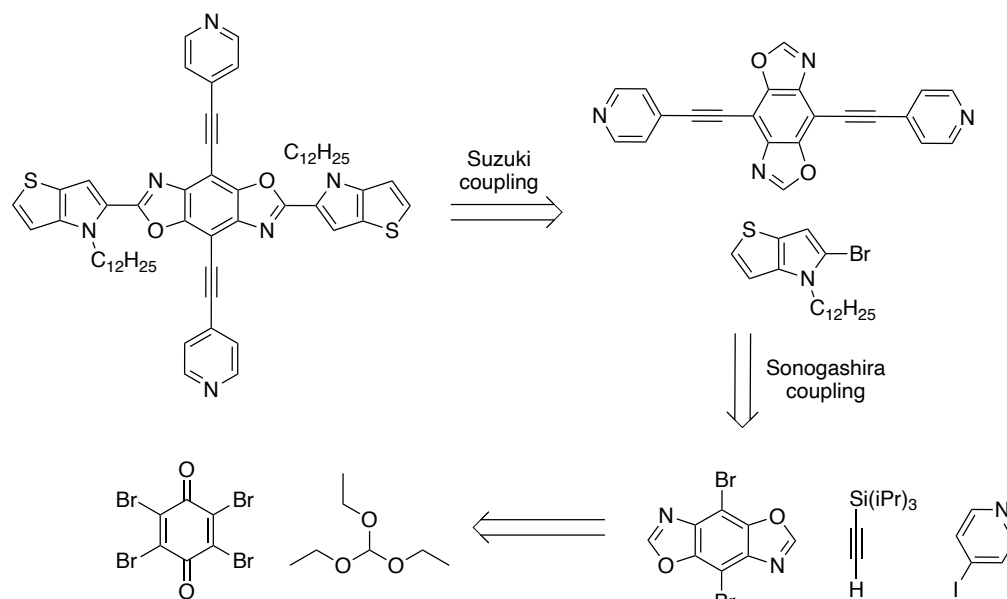
The synthetic route to construct the benzobisoxazole core was postulated using a convergent route to include the electron rich cruciform axis (Scheme 4.5). *P*-bromanil was converted to dione **4.19** by way of nucleophilic aromatic substitution with an excess of ammonium hydroxide, followed by sodium dithionite promoted reduction to produce diamino-diol **4.20**. We were hopeful that simply refluxing acyl chloride **4.17** with the diol would have promoted amide formation followed by condensation to produce the desired benzobisoxazole **4.21**. This synthetic step proved to be unsuccessful.



Scheme 4.5 Synthesis of bispyrrolothiophene axis

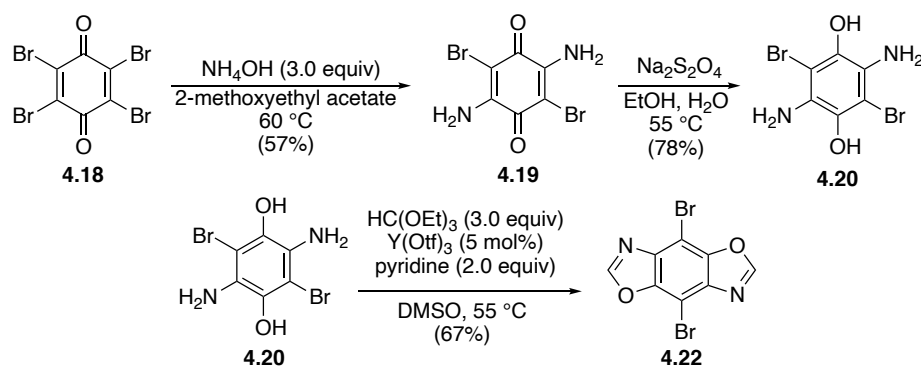
After multiple methods to construct the amide or ester bond were employed to no success, the initial convergent route to synthesize the benzobisoxazole core was abandoned. Instead, I sought to explore a more modular method with regard to both forming the benzobisoxazole and electron rich axis. This approach, in which I envisioned a series of transition metal catalyzed cross-coupling reactions, could afford a facile method to not only construct the target cruciform but would allow a rapid construction of a library of benzobisoxazole cruciform molecules (Scheme 4.6). The electron-rich axis could be installed by way of a Suzuki cross-coupling reaction. The electron-poor axis could be installed in two non-consecutive Sonogashira cross-coupling reactions. This method should allow a library of benzobisoxazole molecules to be

constructed, which could then be used to explore the substituent effect upon fluorophoricity and potential for metal ion sensing.



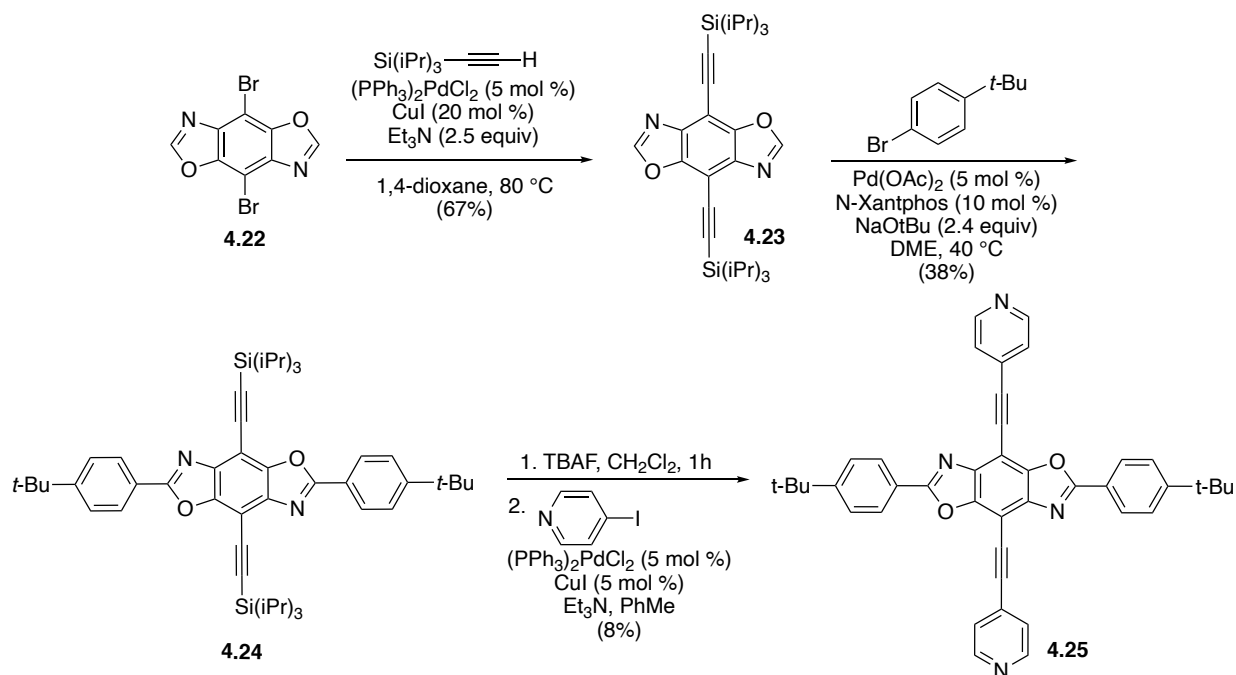
Scheme 4.6 Revised retrosynthetic scheme to synthesize benzobisoxazole cruciforms

Synthesis began by first constructing the unsubstituted benzobisoxazole core (Scheme 4.7). *P*-bromanil was converted to diamino dione **4.19** using electrophilic aromatic substitution. Sodium dithionite mediated reduction afforded the highly substituted benzene core **4.20**. Finally, benzobisoxazole **4.22** was constructed by way of Lewis acid catalyzed cyclocondensation of **4.20** with triethylorthoformate, a method expanded upon by the Jeffries-EL group to synthesize benzobisoxazole molecules.^{25,26}



Scheme 4.7 Construction of benzobisoxazole core

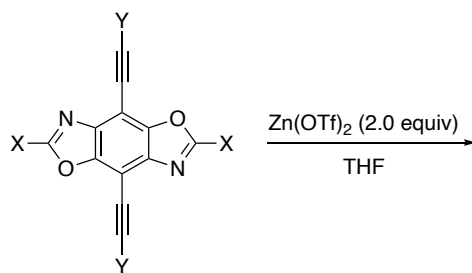
To complete the synthesis, benzobisoxazole **4.22** was further functionalized firstly by way of Sonogashira cross coupling to install triisopropylsilyl acetylene on the 4,8- positions to afford **4.23** (Scheme 4.8). After exploring a number of methods to install boronic acid moieties onto the 2,6- positions of benzobisoxazole **4.22**, it was revealed that the C–H bond in the 2,6-positions were weakly acidic and therefore could be functionalized by way of a deprotonative cross-coupling process developed by Walsh and co-workers to form **4.24**.²⁷ The molecule was then desilylated with TBAF followed by a second Sonogashira reaction with the resultant terminal acetylene and 4-iodopyridine to produce the desired benzobisoxazole **4.25**.



Scheme 4.8 Construction of benzobisoxazole cruciform axes

Following the synthesis of benzobisoxazole cruciform **4.25** I sought to test its metal ion sensing capabilities (Table 4.1). Unfortunately, none of the cruciform molecules exhibited a shift in their UV-Vis spectra after the addition of 2.0 equivalents of zinc salt. From this data, I believe the following can be interpreted. Firstly, I propose that the nitrogen of the pyridine is required

for the desired Lewis acid interaction that leads to the perturbation of the LUMO (Entries 1,2). Second, sole inclusion of the Lewis basic pyridine moiety and formation of the zinc–nitrogen Lewis adduct is not sufficient to produce an observable emission shift. Additionally, pyridine alone does not exhibit a substantial influence over the electronic nature of the cruciform in order to properly spatially separate the frontier molecular orbitals that is requisite of cruciform ion sensors (Entry 3). Inclusion of an electron releasing functionality on the opposite axis is also required. Furthermore, I believe that if the metal ion is interacting with the highly conjugated pi-system of the benzobisoxazole then the zinc-pi adduct does not sufficiently perturb the frontier orbitals to elicit an emission shift.



Entry	X	Y	initial abs. (nm)	abs. after Zn(II) addition
1	H	Si(<i>i</i> -Pr) ₃	320	320
2	4- <i>t</i> -Bu	Si(<i>i</i> -Pr) ₃	320	320
3	4- <i>t</i> -Bu	4-pyridyl	420	420

Table 4.1 Initial spectrophotometric data

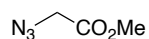
In conclusion, the method developed to access benzobisoxazole cruciform molecules holds promise in their ability to act as metal ion sensors. This could be due in part to the electronically-neutral 4-*tert*-butylbenzene installed on the x-axis leading to incomplete separation of the frontier molecular orbitals. DFT calculations of cruciform molecules tested in Table 4.1 should be performed to fully determine if this is the case. While the preceding molecules did not exhibit any red- or blue- shifting in UV absorbance when exposed to zinc (II)

ions, the ability to install electron-withdrawing or electron-releasing functional groups onto the benzobisoxazole core in a rapid, step-wise manner will allow for an efficient exploration of the metal ion sensing propensity of a wide range of molecules.

Experimental Section

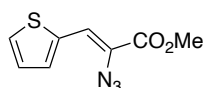
General. ^1H NMR and ^{13}C NMR spectra were recorded at ambient temperature using 500 MHz or 300 MHz spectrometers. The data are reported as follows: chemical shift in ppm from internal tetramethylsilane on the δ scale, multiplicity (br = broad, s = singlet, d = doublet, t = triplet, q = quartet, m = multiplet), coupling constants (Hz) and integration. High-resolution mass spectra were obtained by peak matching. Melting points are reported uncorrected. Infrared spectroscopy was obtained using a diamond attenuated total reflectance (ATR) accessory. Analytical thin layer chromatography was performed on 0.25 mm extra hard silica gel plates with UV254 fluorescent indicator. Liquid chromatography was performed using forced flow (flash chromatography) of the indicated solvent system on 60Å (40 – 60 μm) mesh silica gel (SiO_2). Medium pressure liquid chromatography (MPLC) was performed to force flow the indicated solvent system down columns that had been packed with 60Å (40 – 60 μm) mesh silica gel (SiO_2). All reactions were carried out under an atmosphere of nitrogen in glassware, which had been oven-dried. Unless otherwise noted, all reagents were commercially obtained and, where appropriate, purified prior to use. Acetonitrile, methanol, toluene, THF, Et_2O , and CH_2Cl_2 were dried by filtration through alumina according to the procedure of Grubbs.²⁸ Metal salts were stored in a nitrogen atmosphere dry box.

I. Preparation of Pyrrolothiophenes.



4.13

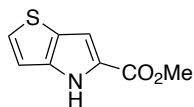
Methyl 2-azidoacetate 4.13. To a stirring solution of 0.152g methyl 2-bromoacetate (1.00 mmol) in 5 mL DMF was added 0.065g sodium azide (1.00 mmol) The resulting solution was heated to 50 °C. After 1 hour, the reactives were quenched with the addition of 10 mL of H₂O. The mixture was then extracted with 3 × 20 mL of diethyl ether. The combined organic phases were washed with 10 mL of a saturated aqueous solution of Na₂CO₃ followed by 10 mL of brine. The resulting organic phase was dried over Na₂SO₄ and filtered. The filtrate was concentrated in *vacuo* to afford the product as a clear liquid (0.085g, 74%).



4.14

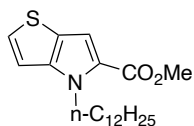
Methyl (Z)-2-azido-3-(thiophen-2-yl)acrylate 4.14. 5.00g of 2-thiophene carboxaldehyde (44.6 mmol) and 21.0g of methyl azidoacetate **4.13** (178 mmol) were added dropwise to a solution of 6.00g of NaOMe (112 mmol) cooled to –20 °C over a period of 20 minutes. The reaction mixture was then warmed to –10 °C and stirred for 16 hours. The reactives were quenched with the addition of 150 mL of H₂O. The mixture was then extracted with 3 × 50 mL of Et₂O. The combined organic phases were washed with 2 × 50 mL of distilled water and 1 × 50 mL of brine. The organic phase was dried over MgSO₄, and the heterogeneous mixture was filtered. The filtrate was concentrated *in vacuo* yielding a reddish orange oil. The product was purified by flash chromatography (1:99 EtOAc:hexanes) affording the product (6.85 g, 74 %). The spectral data for the product matched that reported by Driver and co-workers:²³ ¹H NMR (CDCl₃, 500 MHz) δ 7.49 (d, *J* = 4.9 Hz, 1H), 7.31 (d, *J* = 3.5 Hz, 1H), 7.16 (t, *J* = 0.7 Hz, 1H), 7.08-7.04 (m, 1H), 3.88 (s, 3H);

^{13}C NMR (CDCl_3 , 125 MHz) δ 163.6 @, 136.5 @, 132.1 (CH), 130.6 (CH), 127.1 (CH), 122.3 @, 119.5 (CH), 52.8 (CH_3); IR (thin film): 2951, 2120, 1706, 1075, 1210, 706 cm^{-1} ; HRMS EI m/z calcd for $\text{C}_8\text{H}_7\text{N}_3\text{O}_2\text{S}$ (M) $^+$: 209.0259, found: 209.0304.



4.15

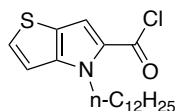
Methyl 4H-thieno[3,2-*b*]pyrrole-5-carboxylate 4.15. A solution of vinyl azide **4.14** (23.9 mmol, 5.00 g) and rhodium(II) 150heptafluorobutyrate (0.120 mmol, 0.130 g) in 16 mL of toluene was heated to 75 °C. After 16 hours, the reaction mixture was cooled to room temperature and was purified by flash column chromatography (10:90 EtOAc:hexanes) to yield the product as a yellow solid (3.40 g, 60 %). The characterization data matched that reported by Driver and co-workers:²³ ^1H NMR (CDCl_3 , 500 MHz) δ 9.52 (s, 1H), 7.33 (d, J = 5.3 Hz, 1H), 7.15 (s, 1H), 6.96 (d, J = 5.3 Hz, 1H), 3.92 (s, 3H); ^{13}C NMR (CDCl_3 , 125 MHz) δ 161.9 @, 138.5 @, 129.6 (CH), 126.7 @, 124.8 @, 111.1 (CH), 107.7 (CH) only signals visible; IR (thin film): 3291, 3131, 2942, 1665, 1307, 1198 cm^{-1} ; HRMS EI m/z calcd for $\text{C}_8\text{H}_7\text{NO}_2\text{S}$ (M) $^+$: 181.0197, found: 181.0197.



4.16

Pyrrolothiophene 4.16. 0.500 g of pyrrolothiophene **4.15** (2.76 mmol) was suspended in a solution of 2.8 mL potassium *tert*-butoxide (2.76 mmol) and 11 mL of THF in the presence of

0.070 g of 18-crown-6 (0.28 mmol). This was followed by the addition of 0.80 mL of 1-bromododecane (3.45 mmol). The reaction mixture was stirred at room temperature for 16 hours. The reactives were quenched with 100 mL of water and the product was extracted with 3 × 50 mL of Et₂O. The combined organic phases were washed with 2 × 50 mL of distilled water and 1 × 50 mL of brine. The organic phase was dried over MgSO₄ and the heterogeneous mixture was filtered. The filtrate was concentrated *in vacuo* yielding an orange solid. The product was purified by flash chromatography (1:99 EtOAc:hexanes) affording the product as a yellow oil (0.88 g, 91 %): ¹H NMR (CDCl₃, 500 MHz) δ 7.32 (d, *J* = 5.4 Hz, 1H), 7.17 (d, *J* = 0.6 Hz, 1H), 6.93 (dd, *J* = 5.4, 0.7 Hz, 1H), 4.47 (t, *J* = 7.4 Hz, 2H), 3.86 (s, 3H), 1.79 (q, *J* = 7.2 Hz, 2H), 1.26 (d, *J* = 27.3 Hz, 18H), 0.88 (t, *J* = 7.0 Hz, 3H); ¹³C NMR (CDCl₃, 125 MHz) δ 161.9 ©, 145.2 ©, 129.0 (CH), 125.8 ©, 121.8 ©, 110.3 (CH), 109.3 (CH), 51.2 (CH₃), 47.6 (CH₂), 31.9 (CH₂), 31.1 (CH₂), 29.67 (CH₂), 29.65 (CH₂), 29.61 (CH₂), 29.5 (CH₂), 29.3 (CH₂), 26.9 (CH), 22.7 (CH), 14.1 (CH) only signals visible; IR (thin film): 2919, 2852, 1700, 1463, 1226, 1171, 712 cm⁻¹; HRMS EI *m/z* calcd for C₂₀H₃₁NO₂S (M)⁺: 349.2075, found: 349.2081.

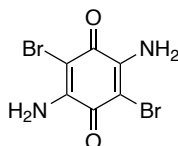


4.17

Acid Chloride 4.17. 0.180 g of Pyrrolothiophene **4.16** (1.00 mmol) was suspended in a solution 0.200 g of NaOH (5.00 mmol) of 15 mL of THF and was heated to 40 °C. After 48 hours, the reactives were quenched with the addition of 30 mL of H₂O. The mixture was then extracted with 3 × 10 mL of Et₂O. The combined organic phases were washed with 2 × 20 mL of distilled water

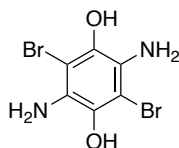
and 1 × 30 mL of brine. The organic phase was dried over MgSO₄, and the heterogeneous mixture was filtered. The filtrate was concentrated *in vacuo* and the resultant soft, white crystal was dissolved in 5 mL of CH₂Cl₂. To this solution was added 0.238g of thionyl chloride (2.00 mmol). The reaction mixture was stirred at room temperature. After 1.5 h, the reaction mixture was concentrated *in vacuo* to yield acid chloride **4.17** as a dark liquid. **4.17** was used immediately without further purification.

II. Preparation of Benzobisoxazole Cruciforms.



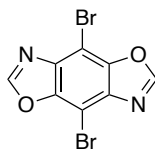
4.19

2,5-Diamino-3,6-dibromocyclohexa-2,5-diene-1,4-dione 4.19. To a round bottom flask was added 4.24 g of *p*-bromanil (10.00 mmol) and the flask was sealed, evacuated and backfilled with N₂ gas. To the flask 20.0 mL of 2-ethoxyethyl acetate was added and the mixture was heated to 60 °C. After 15 minutes, the reaction was cooled to room temperature and 2 mL of a 15 M solution of NH₄OH (30.0 mmol) was added dropwise over 10 minutes. The mixture was then heated to 80 °C. After 3 h, the mixture was cooled to room temperature. After 12 h, the reaction mixture was vacuum filtered, and the precipitate was washed with 3 × 50 mL of H₂O followed by 3 × 20 mL of acetone. The precipitate was concentrated *in vacuo* to yield **4.19** as a dark red powder (1.68 g, 57 %). The product was used without further purification or analysis.



4.20

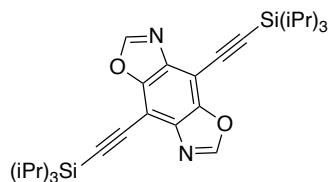
3,6-Diamino-2,5-dibromo-1,4-hydroquinone 4.20. To a 25 mL round bottom flask was added 0.296 g of **4.19** (1.00 mmol), followed by 3.0 mL of 95% EtOH and 0.5 mL of H₂O. The flask was then degassed, backfilled with Ar gas and heated to 55 °C. To this solution was added a 1 M solution of Na₂S₂O₄ in H₂O (1.00 mmol) dropwise. After 1 hour, the precipitate was vacuum filtered and washed with cold water and ethanol. The solid was collected, dried *in vacuo* to afford **4.20** as a pink solid (0.232 g, 78 %). The air sensitivity of **4.20** required its immediate use without further purification or analysis.



4.22

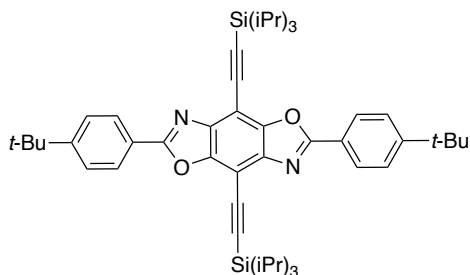
4,8-Dibromobenzo[1,2-*d*:4,5-*d'*]bis(oxazole) 4.22. 0.297 g of hydroquinone **4.20** (1.00 mmol) was added to a round bottom flask followed by 5 mL of DMSO. To the mixture was added 0.031 g of Y(Otf)₃ (0.05 mmol) followed by 0.160 g of pyridine. The flask was sealed, degassed, filled with Ar gas and heated to 55 °C. To the flask 0.55 mL of triethyl orthoformate (3.00 mmol) was added dropwise. After 16 hours, the reactives were quenched with 20 mL of H₂O. The mixture was then extracted with 3 × 20 mL of diethyl ether. The combined organic phases were washed with 10 mL of a saturated aqueous solution of Na₂CO₃ followed by 10 mL of brine. The resulting

organic phase was dried over Na₂SO₄ and filtered. Purification by flash column chromatography (10:90 EtOAc:hexanes) afforded the product as a white solid (0.213 g, 67 %).



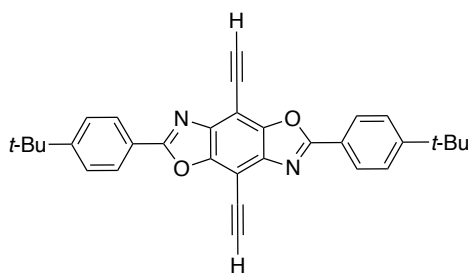
4.23

Benzobisoxazole 4.23. To a round bottom flask was added 0.318 g of benzobisoxazole **4.22** (1.00 mmol), 0.035 g of (PPh₃)₂PdCl₂ (0.050 mmol), 0.038 g of CuI (0.200 mmol), 0.350 mL of triethylamine (2.50 mmol) and 5.0 mL of 1,4-dioxane. The flask was sealed, degassed, backfilled with Ar gas and heated to 80 °C. To the flask, 0.547 g of (triisopropylsilyl)acetylene (3.00 mmol) was added. After 16 hours, the reactives were quenched with 20 mL of H₂O. The mixture was then extracted with 3 × 20 mL of ethyl acetate. The combined organic phases were washed with 10 mL of a saturated aqueous solution of Na₂CO₃ followed by 10 mL of brine. The resulting organic phase was dried over Na₂SO₄ and filtered. Purification by flash column chromatography (2:98 EtOAc:hexanes) afforded the product as a yellow crystal (0.349 g, 67 %).



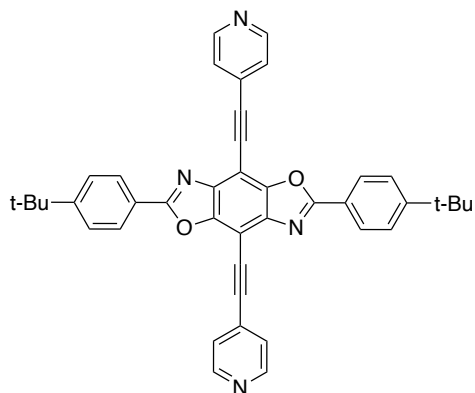
4.24

Benzobisoxazole 4.24. To a round bottom flask under an N₂ atmosphere was added 0.052 g of benzobisoxazole **4.23** (0.100 mmol), 0.001 g of Pd(OAc)₂ (0.005 mmol), 0.005 g of *N*-XantPhos (0.010 mmol), 0.023 g of sodium *tert*-butoxide (0.240 mmol), 0.051 g of 4-bromo-1-(*tert*-butyl)benzene (0.240 mmol), and 1.0 mL of DME. The flask was heated to 40 °C. After 16 hours, the reactives were quenched with 10 mL of H₂O. The mixture was then extracted with 3 × 10 mL of ethyl acetate. The combined organic phases were washed with 10 mL of a saturated aqueous solution of Na₂CO₃ followed by 10 mL of brine. The resulting organic phase was dried over Na₂SO₄ and filtered. Purification by flash column chromatography (2:98 EtOAc:hexanes) afforded the product as a yellow crystal (0.030 g, 38 %).



s1

Benzobisoxazole s1. To a round bottom flask was added 0.078 g of benzobisoxazole **4.24** (0.100 mmol) and 1.0 mL of CH₂Cl₂. To the mixture was added 0.066 g of tetrabutylammonium fluoride (0.250 mmol). The reaction was stirred at room temperature. After 1 hour, the reactives were quenched with 10 mL of H₂O. The mixture was then extracted with 3 × 10 mL of ethyl acetate. The combined organic phases were washed with 10 mL of a saturated aqueous solution of Na₂CO₃ followed by 10 mL of brine. The resulting organic phase was dried over Na₂SO₄ and filtered. Purification by flash column chromatography (5:95 EtOAc:hexanes) afforded the product as a yellow crystal (0.038 g, 80 %).



4.25

Benzobisoxazole 4.25. To a round bottom flask under an N₂ atmosphere was added 0.047 g of benzobisoxazole **s1** (0.100 mmol), 0.004 g of (PPh₃)₂PdCl₂ (0.005 mmol), 0.001 g of CuI (0.005 mmol), 0.350 mL of triethylamine (0.250 mmol), 0.051 g of 4-iodopyridine (0.250 mmol) and 1.0 mL of toluene. The flask was sealed and heated to 60 °C. After 16 hours, the reactives were quenched with 10 mL of H₂O. The mixture was then extracted with 3 × 10 mL of ethyl acetate. The combined organic phases were washed with 10 mL of a saturated aqueous solution of Na₂CO₃ followed by 10 mL of brine. The resulting organic phase was dried over Na₂SO₄ and filtered. Purification by flash column chromatography (10:90 EtOAc:hexanes) afforded the product as a yellow crystal (0.003 g, 8 %).

CITED LITERATURE

1. Nuckolls, C.; Klare, J. E.; Tulevski, G. S.; Sugo, K.; de Picciotto, A.; White, K. A. *J. Am. Chem. Soc.* **2003**, *125*, 6030–6031.
2. Zuccherro, A.; McGrier, P.; Bunz, U. *Acc. Chem. Res.* **2010**, *43*, 397–408.
3. Arroyave, F.; Reynolds, R. *Org. Lett.* **2010**, *12*, 1328–1331.
4. Lee, L.; Liu, R.; Cho, S.; Xiao, R. *J. Am. Chem. Soc.* **2007**, *129*, 4483–4489.
5. Schottland, P.; Zong, K.; Thomas, C.; Reynolds, J. *Adv. Mater.* **2000**, *12*, 222–225.
6. Gaupp, C.; Zong, K.; Thompson, B.; Thomas, C.; Reynolds, J. *Macromolecules* **2000**, *33*, 1132–1133.
7. Katz, H. *Chem. Mater.* **2004**, *16*, 4748–4756.
8. Boisselier, E.; Ornelas, C.; Astruc, D. *Chem. Rev.* **2010**, *110*, 1857–1959.
9. McCollough, R. *Adv. Mater.* **1998**, *10*, 93–116.
10. Ogawa, K.; Rasmussen, S. *Macromolecules* **2006**, *39*, 1771–1778.
11. Wilson, J.; Josowicz, M.; Wang, Y.; Bunz, U. *Chem. Commun.* **2003**, 2962.
12. H. Hoffmann, H.; Wippel, H.; Horner, L. *Chem. Ber.*, **1958**, *91*, 61.
13. Sonogashira, K. *Organomet. Chem.* **2002**, *653*, 46–49.
14. Wilson, J.; Bunz, U. *J. Am. Chem. Soc.* **2005**, *127*, 4124.
15. Saeed, M.; Le, H.; Miljanić, O.; *Acc. Chem. Res.* **2014**, *47*, 2074–2083.
16. Lim, J.; Nam, D.; Miljanić, O. *Chem. Sci.* **2012**, *3*, 559.
17. Spitler, E.; Shirtcliff, L.; Haley, M. *J. Org. Chem.* **2007**, *72*, 86–96.
18. Kivala, M.; Diedrich, F.; *Acc. Chem. Res.* **2009**, *42*, 235–248.
19. Kang, H.; Evmenenko, G.; Dutta, P.; Clays, P.; Song, K.; Marks, T. *J. Am. Chem. Soc.* **2006**, *128*, 6194–6205.
20. Pålsson, L. *et. al. J. Phys. Chem.* **2010**, *114*, 12765–12776.

21. Pina, J.; de Melo, S.; Burrows, H. D.; Galbrecht, B.; Bilge, A.; Kudla, C.; Scherf, U. *J. Phys. Chem.* **2008**, *112*, 1104–1111.
22. Dong, H.; Shen, M.; Redford, J.; Pumphrey, A.; Driver, T. *Org. Lett.* **2007**, *9*, 5191–5194.
23. Dong, H.; Leslie, B.; Pumphrey, A.; Driver, T. *J. Am. Chem. Soc.* **2007**, *129*, 7500–7501.
24. Jones, C.; Boudinet, D.; Xia, Y.; Denti, M.; Das, A.; Facchetti, A.; Driver, T. *Chem. Eur. J.* **2014**, *20*, 5938–5945.
25. Kobayashi, S.; Sugiura, M.; Kitagawa, H.; Lam, W. *Chem. Rev.* **2002**, *102*, 2227–2302.
26. Mike, J.; Makowski, A.; Jeffries-EL, M. *Org. Lett.* **2008**, *10*, 4915–4918.
27. Gao, F.; Kim, B.; Walsh, P., *Chem. Commun.* **2014**, *50*, 10661–10664.
28. Pangborn, A. B.; Giardello, M. A.; Grubbs, R. H.; Rosen, R. K.; Timmers, F. J. *Organometallics* **1996**, *15*, 1518.

VITA

NAME: Russell Lawrence Ford

EDUCATION: B.Sc., Chemistry, University of Illinois at Chicago, Chicago, IL, 2010–2014

Ph.D, Organic Chemistry, University of Illinois at Chicago, Chicago, IL, 2014–2020

TEACHING: Department of Chemistry, University of Illinois at Chicago, Chicago, IL, 2015 – 2020

PUBLICATIONS: “Intramolecular Pd-Catalyzed Reductive Amination of Enolizable sp³-C–H Bonds.” Ford, R.; Alt, I.; Jana, N.; Driver, T. G. *Org. Lett.* **2019**, *21*, 8827-8831.

“Oxidation of Non-Activated Anilines to Generate N-Aryl Nitrenoids.” Deng, T.; Mazumdar, W.; Ford, R. L.; Jana, N.; Izar, R.; Wink, D. J.; Driver, T. G. *J. Am. Chem. Soc.* **2020**, *142*, 4456–4463.

APPENDIX

University of Illinois at Chicago Mail - Regarding Incident 3546073 AC... <https://mail.google.com/mail/u/1?ik=c748da4b21&view=pt&search=all...>



Russell Ford <rford8@uic.edu>

Regarding Incident 3546073 ACS AuthorsChoice Rights

1 message

support@services.acs.org <support@services.acs.org>
To: rford8@uic.edu

Tue, May 26, 2020 at 8:06 PM



Dear Dr. Ford,

Your permission requested is granted and there is no fee for this reuse. In your planned reuse, you must cite the ACS article as the source, add this direct link <https://pubs.acs.org/doi/10.1021/ar500099z> and include a notice to readers that further permissions related to the material excerpted should be directed to the ACS.

If you need further assistance, please let me know.

Sincerely,
Simran Mehra
ACS Publications Support
Customer Services & Information
Website: <https://help.acs.org/>

Incident Information:

Incident #:	3546073
Date Created:	2020-05-26T21:52:34
Priority:	3
Customer:	Russell Ford
Title:	ACS AuthorsChoice Rights
Description:	Good afternoon,

My name is Russell Ford and I am currently a graduate student at the University of Illinois at Chicago. I am reaching out to request access to reprint two figures found in the following article:

Acc. Chem. Res. 2014, 47, 2074–2083